POLITECNICO DI TORINO

Master's Degree in Energy and Nuclear Engineering

Master's Degree Thesis

Performance analysis of a DC converter developed for LIFE SAVE project

Supervisors

Prof. Filippo SPERTINO

Ing. Alessandro CIOCIA

Candidate

Stefano SCHUBERT

Dec 2021

Summary

In order to succeed in the ecological transition, a change in the automotive sector is mandatory. Automotive sector is pushing the new electric and hybrid vehicles in the market, but many problems arise in the process.

The world is still populated for the most by Internal Combustion Vehicles and getting rid of all of them would be a huge waste. An European project, LIFE SAVE, is trying to connect the two worlds developing an all-in-one kit to turn any vehicle into a hybrid plug-in solar vehicle.

This Master Thesis focuses on the solar charge of the kit, analysing the performances of the DC boost converter needed to connect the PV to the high voltage battery.

An analysis of the components of a PV system is performed and the major characteristics are illustrated, an explanation of the theory behind the precision circuit used to measure the efficiency of the converter and the practical aspects of the development are described in detail.

Finally an analysis of the performances of the newly developed converter is illustrated with it's characteristic load curve.

Acknowledgements

Dear Luca,

Thank you for the great help you have provided me in drafting the thesis, for the availability, the accuracy in giving me the best advice and for the ability to stimulate my interest in the subject matter. Without your help, my work would not have been so complete and I would not have reached this level of knowledge.

Dear prof. Filippo Spertino and ing. Alessandro Ciocia,

thanks for the great availability shown. This work would have been less exciting without your input. You have opened the way for me in this fantastic world that is new to me, which I can't wait to deepen. I will always carry with me the cultural baggage you passed on to me.

Dear mom, dad and Emanuele,

I thank you for the sweet and tireless support that has allowed me to get here before you today, contributing to my formation and personal growth. You are my source of support and courage, you have transmitted to me the passion for studying and the desire to reach this goal more than anything else.

Dear friends,

In my life I have been lucky enough to have you next to me as a second family.

Simone S., Federico S., Matteo G., Enrico UB, Giulia UB, Myriam R., Luca M., Francesca KI, Lucia C., Marco S. (Giaveno), Matteo M., Andrea E., Cecilia B ., Alessandro C., Francesca V., Marta C., Sarah R., Grazia P., Tatiana D., Marco S. (Giaglione), Chiara L., Yasmine C., Boris G., Francesca M., Chiara G., Carolina B., Federico M., Nicholas M., Roberto R., Samuele B., Giovanni C., Milena M., Filippo I., Alessandro M., Alessandro C., Lorenzo G., Anne Marie B. It does not matter if we grew up together, or we have known each other for a short time because each of you in your own way has had a decisive role in my growth. And if I was able to get here, I also owe it to all the experiences we shared. So the least I can do is say thank you, I love you.

Dear Marta,

they have been indescribable years since I met you, you have been a point of reference in this course of study and you have always encouraged me to give my best. You know how much you have helped me in this very demanding job and every time I felt myself falling you pulled me back up. We are a very close-knit team and every day I feel more and more fortunate to have met you.

Sincerly yours,

Stefano

Ringraziamenti

Caro Luca,

Grazie del grande aiuto che mi hai fornito per la stesura della tesi, per la disponibilità, la precisione nel consigliarmi al meglio e per la capacità di stimolare il mio interesse per l'argomento trattato. Senza il tuo aiuto, il mio lavoro non sarebbe stato così completo e non avrei raggiunto questo livello di conoscenza.

Cari prof. Filippo Spertino e ing. Alessandro Ciocia,

grazie per la grande disponibilità dimostrata. Questo lavoro sarebbe stato meno entusiasmante senza il vostro contributo. Mi avete aperto la strada in questo fantastico mondo a me nuovo, che non vedo l'ora di approfondire. Porterò sempre con me il bagaglio culturale che mi avete trasmesso.

Cari mamma, papà ed Emanuele,

vi ringrazio per il dolce e instancabile appoggio che mi ha permesso di arrivare fin qui davanti a voi oggi, contribuendo alla mia formazione e crescita personale. Siete la mia fonte di sostegno e di coraggio, mi avete trasmesso la passione per lo studio e la voglia di raggiungere questo traguardo più di qualsiasi altra cosa.

Cari amici,

Nella mia vita ho avuto la fortuna di avervi accanto come una seconda famiglia.

Simone S., Federico S., Matteo G., Enrico UB, Giulia UB, Myriam R., Luca M., Francesca KI, Lucia C., Marco S. (Giaveno), Matteo M., Andrea E., Cecilia B., Alessandro C., Francesca V., Marta C., Sarah R., Grazia P., Tatiana D., Marco S. (Giaglione), Chiara L., Yasmine C., Boris G., Francesca M., Chiara G., Carolina B., Federico M., Nicholas M., Roberto R., Samuele B., Giovanni C., Milena M., Filippo I., Alessandro M., Alessandro C., Lorenzo G., Anne Marie B. Non importa se siamo cresciuti insieme, o ci conosciamo da poco tempo perché ognuno di voi a modo suo ha avuto un peso determinante nella mia crescita. E se sono potuto arrivare fin qui, lo devo anche a tutte le esperienze che abbiamo condiviso. Dunque il minimo che posso fare è dire grazie, vi voglio bene.

Cara Marta,

sono stati anni indescrivibili da quando ti ho conosciuta, sei stata un punto di riferimento in questo percorso di studi e mi hai sempre spronato a dare il massimo. Sai bene quanto mi hai aiutato in questo lavoro molto impegnativo e ogni volta che mi sono sentito cadere mi hai ritirato su. Siamo un'affiatatissima squadra e ogni giorno mi sento sempre più fortunato di averti incontrata.

Il vostro Stefano

Table of Contents

List of Tables

List of Figures

Acronyms

PV
Photovoltaic

eV
Electronvolt

m-Si
monocrystalline silicon

p-Si
polycrystalline silicon

a-Si
amorphous silicon

CIS
Indium and Copper diselenide

CdTe
Cadmium telluride

GaAs
Gallium arsenide

CZ
Czochralski Technique

FZ
Float Zone

WICP

Wacher Ingot Facturing Process

CdS

Cadmium Sulfide

TCO

Transparent Conductive Oxide as SnO_2

EVA

ethylene-vinyl acetate

NOCT

Nominal Operating Cell Temperature

STC

Standard Test Conditions

MPPT

Maximum Power Point Tracker

PWM

pulse width modulation

AC

Alternating current

DC

Direct current

ESR

Equivalent Series Resistance

MPP

Maximum Power Point

SEPIC

Single-ended Primary-inductor Converter

VLA

Vented Lead Acid

VRLA

Valve Regulated Lead Acid

BMI

Battery Management Interface

$LiPF_6$

Lithium Hexafluorophosphate

SEI

Solid-Electrolyte Interface

$LiCoO_2$

lithiated cobalt oxide

$LiFePO_4$

lithiated iron phosphate

$Li_4Ti_5O_{12}$

lithium titanate anode

BMS

Battery Management System

HVD

High Voltage Disconnection

LVD

Low Voltage Disconnection

LVR

Low Voltage Reconnection

NPRS

Non Programmable Renewable Sources

CAES

Compressed Air Energy Storage

SMES

Superconducting Magnetic Energy Storage

SAVE

Solar Aided Vehicle Electrification

TRL

Technology Readiness Level

NO_x

Nitric Oxide

CO_2

Carbon Dioxide

LCA

Life Cycle Assessment

SDG

Sustainable Development Goals

UN

United Nations

AESME

Executive Agency for Small and Medium-sized Enterprises

DG

Directorate General of the European Commission

OBD

On-board diagnostics

ZTL

Zona a Traffico Limitato

CNG

Compressed Natural Gas

LPG

Liquefied Petroleum Gas

NREL

National Renewable Energy Laboratory

US

United States

IDE

Integrated Development Environment

USB

Universal Serial Bus

LED

Light Emitting Diode

FSR

Full Scale Range

Op Amp

Operational Amplifier

ADC

Analog-to-Digital Converter

PGA

Programmable Gain Amplifier

PCB

Printed Circuit Board

i^2c

Inter-Integrated Circuit

CHP

Combined Heat and Power

Chapter 1

Introduction

1.1 Master Thesis goals

This Master Thesis has been developed in collaboration with Solbian Energie Alternative S.R.L., a company based in Avigliana, province of Turin; which deals with the design and production of flexible solar panels used mainly in automotive and marine applications. Solbian is the leading company in its sector even though it is fairly young (founded in 2010).

The aim of this project is to analyze the performances of a DC converter employed in the design of a European project in order to convert standard cars into solar hybrid plug-in vehicles. This analysis is performed by an electronic sensor designed and developed in the process.

The converter under analysis is used to boost the voltage generated by the solar panels on the roof and bonnet of the car. This voltage charges the high voltage battery that fuels the power-train of the rear electric driving wheels.

The Master Thesis is structured in five macro sections. The first one is entirely descriptive and regards the explanation and classification of photovoltaic systems. The second treats about power conversion and the electronic devices suitable for off-grid PV system, essential for the connection of the battery to the panels. The third one focuses on the description energy storage, in the specific electrochemical storage, the technology and working principle. The fourth part and more important one regards the case study, description of the LIFE SAVE project and in general solar hybrid vehicles; then a detailed depiction of the development of the sensor, the final prototype and the data analysed. The last section is a comment regarding the data measured and analysed, as well as the final result and characterisation of the converter.

Observing the results, it is possible to declare that the converter worked properly with voltage ranges coherent with the design values. The efficiency is not yet comparable to the solutions available in the market, so some tuning to the circuit are still required; still it

could drive the project without any significant issue.

1.2 Energy Transition

Nowadays 'Energy Transition' resounds everywhere. All the newspapers, magazines, TV channels, TV shows talk about this topic. In particular it is a pathway toward transformation of the global energy sector from fossil-based to zero-carbon by the second half of this century [1].

It consists in a continuous mutation of production processes and use of energy from human being. Energy system must manage different problems, from the traditional ones such as the population growth and develop, to the recent ones such as the fight against climate change. Sustainable energy must be the guideline to the current and future decisions, and it must be able to accomplish all the prefixed targets.

Energy transition is a complex and long process, it involves significantly different sectors, such as the economic development, the life quality, the social organization and the environment. It depends on various transitions which interact and combine together, and they regard the main elements of an energy system: the sources of primary energy, machines and technologies for the energy conversions, energy vectors (which are forms of energy derived by the primary sources) and the energy services (users' demands). The mechanisms which modify these elements and therefore initiate the new transition phase, can be summarized in these following categories:

1. Availability and competitivity about new primary sources or energy vectors
2. Availability and competitivity about new machines for energy conversion (prime movers or primary motive forces)
3. Adoption of new energy and environmental policies
4. Changing of level and typology of energetic services requested by users

All these mechanisms are concentrated mainly on the competitivity of energy sources, in economic, qualitative and environment points of view. The research and technology development are and will be always more important to identify all the competitivity levels regarding the power sources and motive forces.

To explain how they are developed, it is useful to describe the past energy transitions. A famous researcher Vaclav Smil identifies four energy transitions. The first one is dated in the primitive era. At the beginning human being was able to survive due to only the muscular strength, picking vegetables or hunting animals; successively, due to discovery of fire, heat source, he ate in a batter way, and he managed to heat up, so his longevity increased. The second transition consists in the agricultural revolution in Neolithic era. From a nomadic life, human being started sedentary life; in this way the alimentary energy was more reliable, safe and constant. The third change happened with the prime mover's

fabrication, activating with water or wind. Due to these machines, human was able to make less efforts and so live longer. Finally, the fourth one, the more recent, consists in the substitution of biomass as an energy source with the fossil fuels, coal, oil and natural gas, the introduction of electricity as energy vector and the introduction of devices more powerful and sophisticated [2].

The third one triggered the fourth one because the aim was to augment the workforce productivity and to satisfy a growing demand due to population growth. In addition, the last transition was characterized by an exponential trend of energy demand due to economic progress and population development.

Observing superficially the diagram of the energy sources evolution, figure 1.1, a new energy transition would not seem to appear; however, looking more carefully, on the bottom right side the renewable sources are growing and developing. Some researchers declare that it is the signal of a new transition, because there are facts which demonstrate this.

The first one consists in the cost's reduction of electric generation. If they decrease, it means that the source is become competitive, and it can substitute another one with more lacks. In addition, also the storage costs are lower, but they are not sufficient. For this reason, other technology progresses are necessary to reach the set targets. The third evidence which demonstrates a fifth energy transition is the growing adoption of measurement against the climate change from politicians and international governments. Finally, the last evidence is linked to the users' preferences. During last years the knowledge regarding these arguments is increased and the desire to move towards sustainability persuades more people to modify their habits, to adopt low carbon solutions and to make wise decisions.

Megatrends are groups of tendencies which push the system in the direction of new energy sources or technological process, they are big forces of changes which model the entire social organization, the production systems and the collective consciousness. These guide mechanisms direct:

- The political decisions, by inducing the legislator to compile environment rules and standards more or less stringent or to promote the usage of specific energy sources.
- Technology innovation, by inducing the industry and the research to give a boost to development activities and to commercialization of new technologies and energy sources having characteristics that respond to emerging needs.
- The consumers' preferences, transforming the technologies and the energy sources available in the market more or less attractive and competitive and modifying definitely the demand composition and the offer mixture.

The equilibrium is the final result.

The megatrends are seven and they are the following:

1. Industrial development → due to the third energy transition, the production processes

are changed in favor of a greater number of goods and services supplied in less time and so more coal, oil and natural gas are used.

2. Energy security → guarantee to have available enough energy to provide the growing demand and to satisfy the welfare level reached. For this megatrend, the renewable energy resources are favored than fossil fuels because they are present everywhere, while the second ones are depended on some countries.

3. Reduction of pollutant emissions → it has led to the introduction of important technological processes regarding mainly the industrial and transport sectors.

4. Mitigation of climate change → some human activities produce a constant earth's temperature increment due to the use of fossil fuels that emit in the atmosphere pollutant agents. The first is the carbon dioxide which generates an atmospheric barrier that is able to trap the energy received by the sun, causing a temperature variation and a modification of global earth's climate.

5. Universal energy access → everyone must to have the possibility to access to energy sources to grow in economical and energetic points of view and to develop socially

6. Fight against energy poverty → it has the same aims of the fifth megatrend, only the matter of survival is added. In 2019 International Energy Agency estimated that around 10% of world's population has not access to electric energy [3] and around 2,6 billion of people – 35% of world's population and 45% of developing countries' population – lack access to clean cooking [4]. This target is added to the '17 Sustainable Development Goals', a list aimed to sustainable evolution to terminate the poverty, to reduce the inequalities and to favor the social and economic growing.

7. Population growth → considering only the elimination of life inequalities, a growing of economy and energy availability is unavoidable and this process must be compatible with environment, climate and social goals.

However, some megatrends are in contrast between other ones, it means that the direction chosen could reveals contrary respect to other one. For this reason, the energy transition developed in these years must be respond to all the requirements, solving all the conflict problems under all aspects.

The timelines regarding the changes are not known with certainty, different points of view exist. Some researchers think that the main character will be the renewable energy resources growth, exponentially and unavoidable; other scientists declare that RES (Renewable Energy Sources) diffusion will be progressive and to reach the prefixed targets different wide-ranging solutions will need, in particular for decarbonization. Two reasons affect principally the first current of thought.

The first relates to technological development regarding the photovoltaic and wind power systems that are more and more comparable with electronic devices; they follow the exponential Moore's law. Features are short time costs reduction, good competitive, usage flexibility and diffusion velocity on commercial markets. The second reason consists in

standard aspects. In the future obligations and incentives will be more and more present and they could accelerate the diffusion time of renewable resources uses.

Nevertheless, the diffusion needs to transition plurality, because non only a single aspect must change, but also the other ones must modify in cascade. For example, knowing that RES generate principally electric energy, not only sectors that use them directly are advantaged, but also the other ones should benefit. For this reason, an electrification process should be necessary in all fields. Network problems are born, because RES are not programmable and constant sources. Storage systems are essential [2].

To reach decarbonization and improve energy efficiency, Europe has drawn up a list of targets to accomplish. In 2020 the goals were:

- 20% increase of energy efficiency
- 20% reduction of CO_2 emissions
- 20% increase of renewable energies employed

Italy has reached these purposes and it is ready to attain already the ones for the 2030 so -40% greenhouse gases emissions, + 32% RES and +32,5% of energy efficiency [5].

Currently the country has the following trend regarding the total energy supply classified by groups [6]:

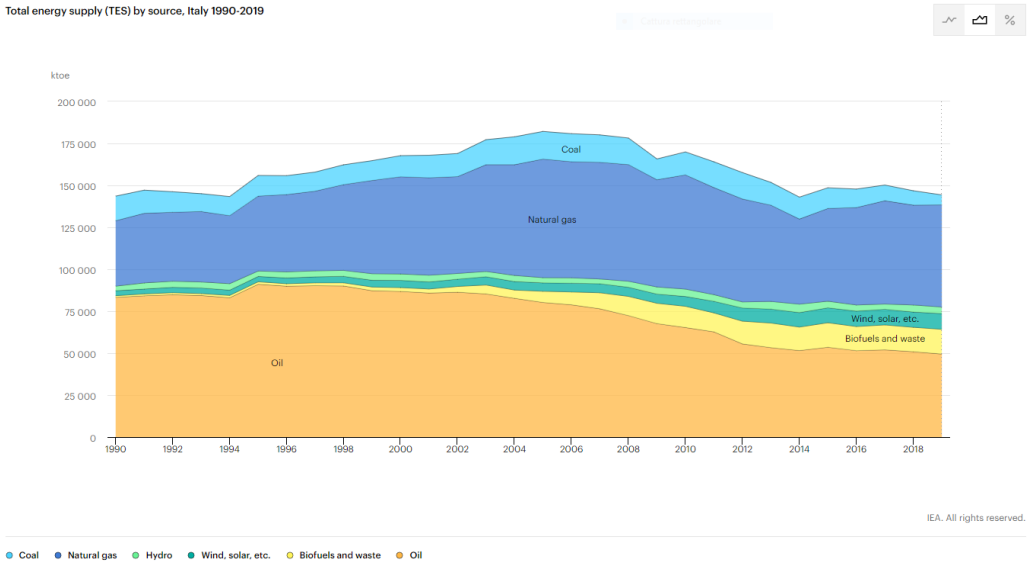

Figure 1.1: Total Energy supply by source

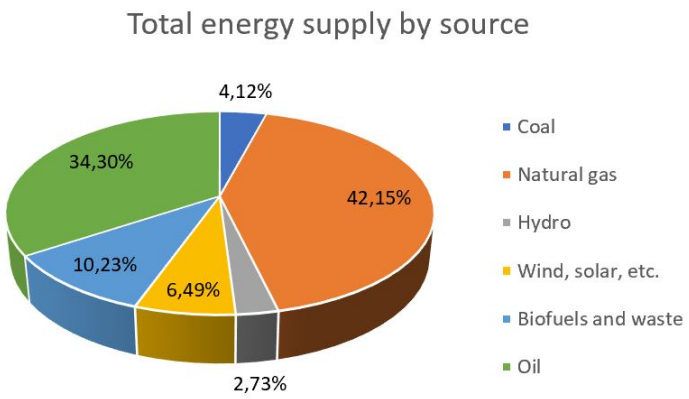

Figure 1.2: Total Energy Supply by source- pie chart

In figure 1.1, the decrease of coal and oil is visible, and these portions has been occupied by bio-fuels and waste, wind, solar and hydro power during the last decades. To enhance this trend in July 2020 the Legislative Decree n° 73 came into force and the main topics discussed concern the energy efficiency. The amendments are the following:

- Energy savings for which no energy efficiency qualifications or other incentives have been recognized, will be counted for the calculation of the savings achieved for the achievement of targets at national level. In this way, not only the savings offered, but also those made independently by individual companies, will be counted.
- Thermal account extended in the period 2021-2030. In addition to small efficiency interventions and the thermal heat production from RES, it encourages the connection to the district heating, district cooling and micro-CHP. It could include also the requalification of buildings and the recharge columns for the electric vehicles.
- Relief from energy audit is enlarged to the company with an annual energy consumption smaller than 50 toe.
- The companies which do not implement efficiency measures detected by the diagnosis, they incur in a penalty from 2000 to 40000€ [7].

Chapter 2

Photovoltaic energy

Solar energy is the energy associated to the solar radiation and represents the primary energy source of Earth.

Solar energy [8] , in fact is the one normally used by autotrophs organisms, namely those that live by photosynthesis, commonly called "vegetables" (from which fossil fuels are derived); other living organisms exploit instead the chemical energy derived from vegetables or other organisms which feed on vegetables, so indirectly exploit solar energy themselves.

Figure 2.1: Photovoltaic solar energy.

From this energy derive more or less directly almost all the other energy sources available to humans such as: fossil fuels, eolic energy, wave energy, hydroelectric energy and solid waste; with the only exception of nuclear, geothermal and tidal energy. It can be used directly for energetic purposes, to generate heat or electric energy with different plant configurations.

PV plants, composed of one or more PV modules, allow to transform , directly and instantly, solar energy (or **photovoltaic PV**, "photo" derives from Greek "*phos*"which means "*light*" and "*Volt*" from the Italian scientist Alessandro Volta inventor of the battery) in electric energy without use of fuels. [9]

The main advantages [10] of a PV plant can be summarized in:

- It exploits free energy, available in all the world and inexhaustible (estimated solar

lifespan is another 5 billion years);

- Production directly in place of use: transmission losses are avoided;
- Saving of fossil fuels;
- Total absence of noise and air pollution: only form of pollution regards the process of production and decommission of the silicon which composes PV modules;
- Plant reliability due to the absence of moving parts: plant lifespan is usually longer than 20 years;
- Reduced operation costs and maintenance: constituted essentially by cleaning of the PV modules costs to avoid a decrease in system efficiency;
- possibility to recycle up to 80% of the weight oh the PV module: silicon, glass, copper and aluminium once disassembled are easily recyclable and useful to make new panels or different objects.

The main disadvantages, instead are [10]:

- Production of electric energy is intermittent, not programmable: it depends on the solar radiation, which is zero during the dark hours and varies based on meteorologic conditions, which alter the transparency of the atmosphere to solar rays and the astronomical motions of Earth that cause the alternation of seasons;
- Low efficiency $\eta \approx 20\%$;
- Low power density, which translates in the need to have large working surfaces;
- Non standard design: having different conditions of irradiance with latitude, optimization of plant characteristics change from place to place;
- CapEx still high for the realization of a plant.

2.1 Solar radiation

The energy source that a PV plant uses is the **Sun**, the star at the center of the Solar System. [11] It has a diameter of about 1392000 km (about 109 times bigger than Earth's) and a mass of about $2 \cdot 10^{30} kg$ (about 330000 times bigger than Earth).

The Sun is composed by about 75% of hydrogen, 23% of helium and other gases (2%) and it is characterised by a layer structure. The inner layer is at a temperature of $1.5 \cdot 10^{6} °C$ while the outer layer is at a temperature of 6000 °C.

The energy released by the Sun is generated by nuclear fusion processes where hydrogen is converted in helium. The fusion reaction, called p-p chain (proton-proton) is the following:

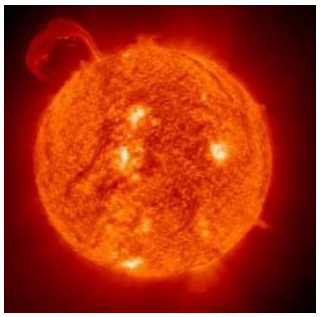

Figure 2.2: The Sun

$$4p^{+} \rightarrow^{4} He^{2+} + 2v + \Delta mc^{2} \tag{2.1}$$

Protons melt making helium, releasing positrons and neutrinos. This process, is poor of mass, so the energy of 26.7 Mev is released for every reaction. It is calculated that, in every second, a lack of $4.3 \cdot 10^{9}$ kg is generated. So for the mass-energy correlation $E = m \cdot c^{2}$ (where E is the produced energy, m is the mass and c is the speed of light), the obteined power emitted by the Sun in the form of electromagnetic waves is about $3.85 \cdot 10^{26} W$.

The Sun can be approximated as an ideal radiation emitter (*black body*)with a surface temperature of about 5800 K. The electromagnetic radiation $g(\lambda)[Wm^{-2}\mu m^{-1}]$, out of the atmosphere has a spectral distribution from ultraviolet to infrared with a maximum in the field of visible for a wave width λ around 0.5 μm: the correspondent power density, on the unit of area perpendicular to the ray, is known as the **solar constant** G_{SC}= $\int G(\lambda)d\lambda \approx 1367 w/m^{2}$.

$$G_{SC} = \frac{P_s}{4\pi r_{SE}^{2}} = \frac{3.85 \cdot 10^{26}}{4\pi \cdot (1496 \cdot 10^{11}} \approx 1367 \frac{W}{m^{2}} \tag{2.2}$$

where P_S is the power emitted by the Sun and r_{SE} is the average distance from the Earth.

The solar constant G_{SC} can vary during the year up to $\pm 3\%$ caused mainly by the Earth orbit being elliptic. In fact it is possible to write the equation of the extraterrestrial radiation as:

$$G_{o,n} = G_{SC} \cdot \left(1 + 0.033 \cdot \cos \frac{360 \cdot DoY}{365}\right) \tag{2.3}$$

where DoY is the day of the year.

Generally, the total power is generated by a radiation source that covers a unit of area is called **irradiance G** $[W/m^{2}]$.

When the solar radiation enters the atmosphere of the Earth, part of the energy gets refracted and dispersed by the external space, or absorbed.

The **absorption** is a *discreet* phenomenon (it happens only for certain wave lengths λ) and it's due mainly on the presence of the molecules of ozone, water and carbon dioxide.

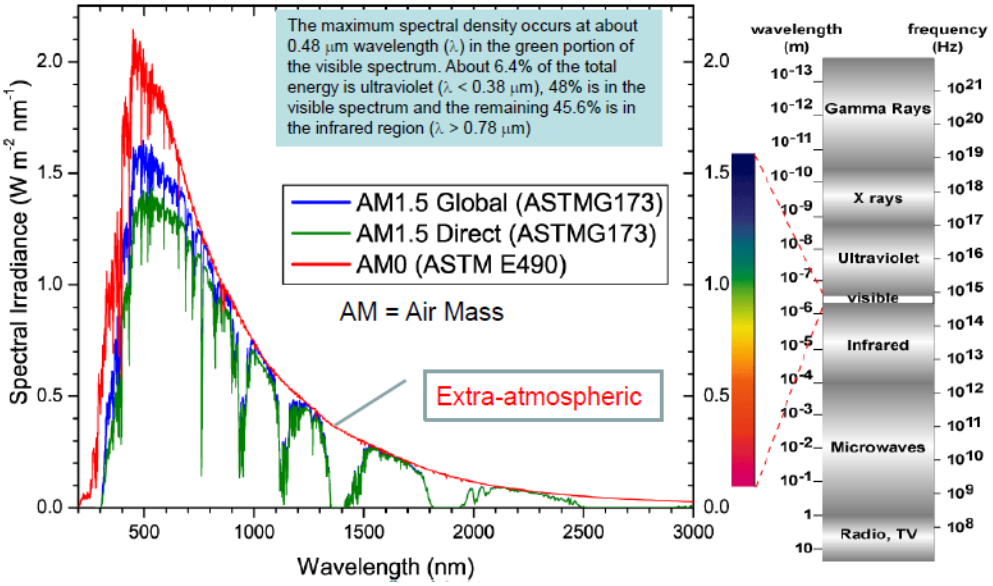

Figure 2.3: Spectral distribution of solar radiation.

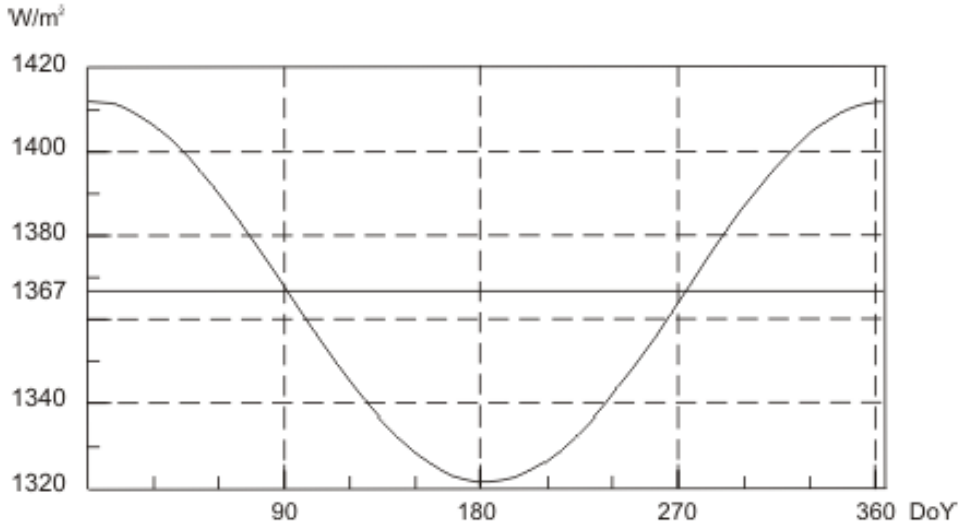

Figure 2.4: Annual variation of extraterrestrial radiation over a unit of surface normal to the direction of the ray.

The **dispersion** and **reflection**, instead, are *continuous* phenomena due to the presence of nitrogen and oxygen, dust and drops of water. The radiations characterised by shorter band width, tend to suffer more reflection. It is important to note that phenomena like dispersion depend strongly by the location of the site and assume maximum values in the

industrialized or urban areas (high concentration of aerosol).

These phenomena cause the majority of the radiation that impact Earth surface to be in the wave length range of 0.29 and 2.5 μm.

The global solar radiation is so divided in:

- Direct G_b (b stands for "beam") constituted by the rays of Sun that don't suffer angular deviations on the surface.
- Diffuse G_d that considers the part of solar rays that encounter atmospheric gases or dust and from these they get reflected, varying the angle of incidence. It represents an important fraction of the radiation variable based on the meteorologic conditions (in a cloudy sky the radiation is almost all diffused while in a clear day it isn't more than 20%), beside altitude, latitude and location.
- Albedo G_a that considers a small part of the radiation that, after being reflected by the Earth, can reach a receiver. It is called **coefficient of reflection** ρ the light flux reflected in all directions over the flux parallel in a direction. The coefficient ρ varies with the color of light and the type of surface that reflects.

SURFACE	ρ
Fresh snow	0.7-0.95
Sand	0.1-0.25
Asphalt	0.15
Arid terrain	0.17
Grass	0.18-0.23
Wood	0.05-0.18

Table 2.1: Typical values of albedo

The total solar radiation that hits a receiver on the surface of the Earth is constituted by the sum of these three components.

$$G = G_b + G_d + G_a \tag{2.4}$$

2.2 Air mass

The influence of the solar radiation on a location on Earth surface in an instant is determined by the **Air Mass AM** parameter. This index in given by the mass of air crossed by the light over the mass that would behave been crossed if the Sun was at the Zenit (perpendicular to the Earth surface in the same location where it is observed). [12]

In a clear day of summer, at sea level, with the radiation coming from the Zenit corresponds an Air Mass equal to 1 (AM=1).

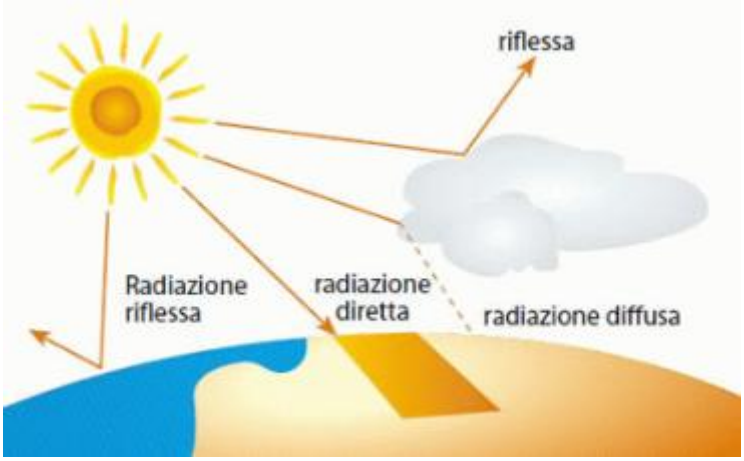

Figure 2.5: Behavior of solar radiation in the atmosphere.

In other climatic conditions, the Air Mass can be approximated with the formula:

$$AM = \frac{1}{cos\Theta_z} \quad or \quad AM = \frac{1}{P_0 \cdot sin\Theta_z} \tag{2.5}$$

where:

- P = atmospheric pressure in the point and time of consideration [Pa];
- P_0 = reference pressure, equal to $1.013 \cdot 10^5[Pa]$;
- Θ_z = angle of the sun with respect of the Zenit direction.

The extra-atmospheric spectrum, depicted as AM=0, is important for applications of solar cells on satellites.

An average value of AM on the Earth surface is 1.5. That spectrum, with global irradiance of $1000W/m^2$ (obtainable in a sunny day at noon from March to September) is used for tests on cells and PV modules.

Lastly, the irradiance integrated in an interval of time is defined as **radiation H**, whose unit measurement is kWh/m^2.

$$H = \int_{t_1}^{t_2} G(t)dt \tag{2.6}$$

where G(t) is the solar irradiance that arrives to a receiver on Earth surface and t_1 and t_2 are the extreme in the considered interval of time. In the design of PV systems it is important the daily, monthly and yearly radiation.

As it is possible to observe in 2.7 the mean yearly value of radiation is influenced by latitude. Moreover, during the year, the solar radiation varies with the season, due to the revolution of Earth around the Sun.

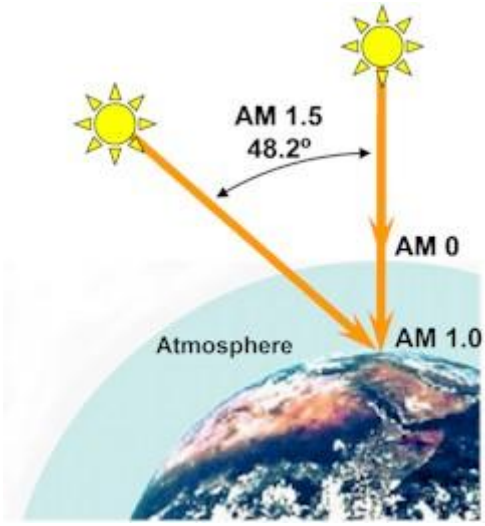

Figure 2.6: Correlation between the AM index and the Zenith angle.

2.3 Measurement of solar radiation

The instruments used to detect the solar radiation are **solarimeters** or **pyranometers**. [12] [13] [14] There are different typologies, categorized by the their working principle:

- thermopile solarimeter (pyranometer)
- PV solarimeter

Pyranometer is an instrument for the measure of global radiation that impacts on the surface. The working principle is based on the measure of the difference of temperature from a dark and a light surface. The dark surface absorbs the most solar radiation, while the light surface reflect, absorbing less radiation. The consequent difference in temperature is measured using a thermopile.

The voltage that generates in the thermopile due to the temperature gradient between the two surfaces, allows to measure the value of global incident solar radiation. A thermopile is composed by thermocouples connected in series. A thermocouple is a junction between two different metals used to measure the difference of temperature in two points. a thermocouple produces a voltage that depends by the temperature gradient.

The response of a pyranometer of this type can cover all the range of wave lengths of the solar spectrum: from 300 to 2800 nm.

Solarimeter is an instrument based on the PV effect, it has the same working principle of a solar cell: produces an electrical signal based on the incident solar radiation, it is more responsive to the visible light and its response depends by the temperature of

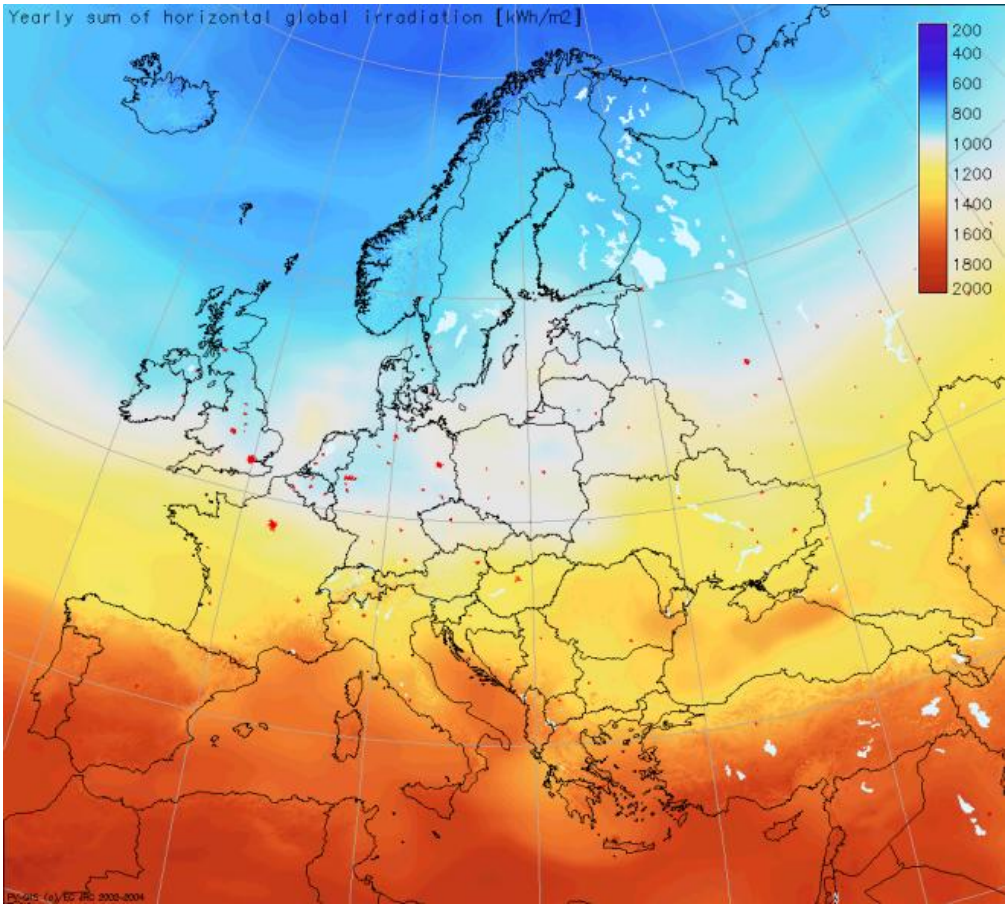

Figure 2.7: European average annual irradiation $[\frac{kWh}{m^2}]$ on a horizontal surface. Source: PVGIS.

the cell. Values measured by a solarimeter need to be corrected taking into account the operating temperature, measured by a thermocouple.

2.4 Solar cell: structure and operation

To understand the PV energy conversion process it is appropriate to recall some notions of physics: the energy bands and the PV effect. Then we will move on to analyze in detail the basic element of a PV generator, that is the PV cell.[10] [15]

2.4.1 Energy bands

The physical model of the atom used is the one proposed by Bohr. In this model the interaction between electron and nucleus is seen as a balance of electrostatic (Coulombian)

Figure 2.8: Pyranometer and solarimeter.

forces of attraction and centrifugal forces. The latter due to the speed of rotation of the electron. This balance of forces can occur, according to Planck, only on some orbits, characterized by a specific energy level. The energy bands, therefore, are the set of energy levels that an electron can take which orbits the nucleus of an atom. The energy bands can take on three different values and states:

Valence band : composed of the set of electrons used in the chemical bonds of the atom with other atoms;

Conduction band : characterized by electrons with an energy level higher than that of valence which allows them to leave the atom they belong to and to move within the crystal lattice, giving rise to an electrical conduction;

Band jump : represents the energy value needed to make an electron pass from the valence band to the conduction band.

The energy jump E_g size is a very important because it quantifies the amount of energy it takes to move the electron from the valence band to the conduction band. The value of E_g varies according to the type of material. Therefore, based on the ability that a material has to conduct electrons it is possible to define the following distinction:

Insulating materials : high E_g

Semiconductors : limited E_g

Conductors : most of the electrons already have the energy needed to pass through the conduction band and give rise to a flow of electrons

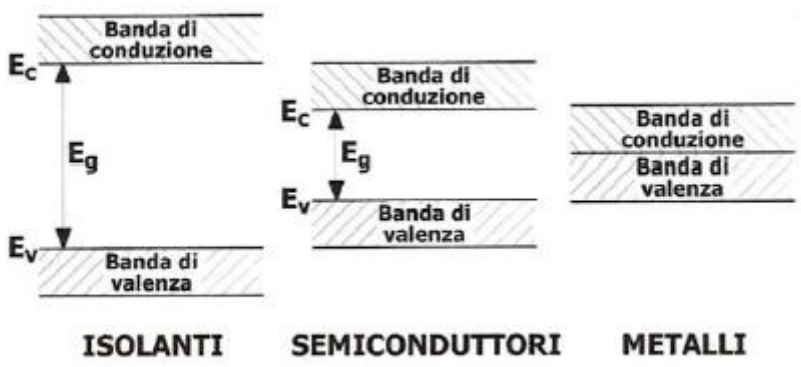

Figure 2.9: E_g values depending on the type of material.

Table 2.2 shows the energy gap values of the main semiconductors expressed in electron volts: The energy can be expressed in Joules or in eV, with a conversion factor equal to:

Semiconductor	E_g **[eV]**
Crystalline silicon (c-Si)	1.12
Amorphous silicon (a-Si)	1.75
Germanium (Ge)	0.67
Gallium arsenide (GaAs)	1.42
Indium phosphide (InP)	1.34
Indium copper diselenide (CuInSe)	1.05
Cadmium telluride (CdTe)	1.45
Cadmium Sulfide (CdS)	2.40

Table 2.2: E_g values of the main semiconductors.

$$1eV = 1.60218 \cdot 10^{-19} j \tag{2.7}$$

2.4.2 Photovoltaic (or photoelectric) effect

The physical phenomenon characterized by the emission of electrons from a surface, when this is hit by electromagnetic radiation, i.e. by photons having a certain wavelength, is called PV (or photoelectric) effect.

As Einstein understood, taking up Planck's theory, the photoelectric effect highlights the quantum nature of light. In electromagnetic radiation, the energy is not uniformly

distributed over the entire wave front but is concentrated in single quanta (discrete packets) of energy, the photons, and each photon interacts individually with an electron, to which it yields its energy.

In order for the PV effect to occur, the photon must have sufficient energy to break the electrical bond that holds the electron bound to the atom. This "minimum threshold" of photon energy is determined on the basis of Einstein's relation:

$$E_{ph} = h \cdot f = h \cdot \frac{c}{\lambda} \geq E_g \tag{2.8}$$

where:

- E_{ph} = photon energy [J]
- E_g = energy gap [J]
- h = Planck's constant (6.625 10-34 J $\cdot$ s)
- ν = frequency [Hz]
- c = speed of light ($\approx$ 300,000 $\frac{km}{s}$)
- λ = wavelength [m]

Therefore, only if $E_{ph} \geq E_g$, the electron of the valence band jumps to the conduction band.

As a hole forms in the valence band, the absorption process generates electron-hole pairs.

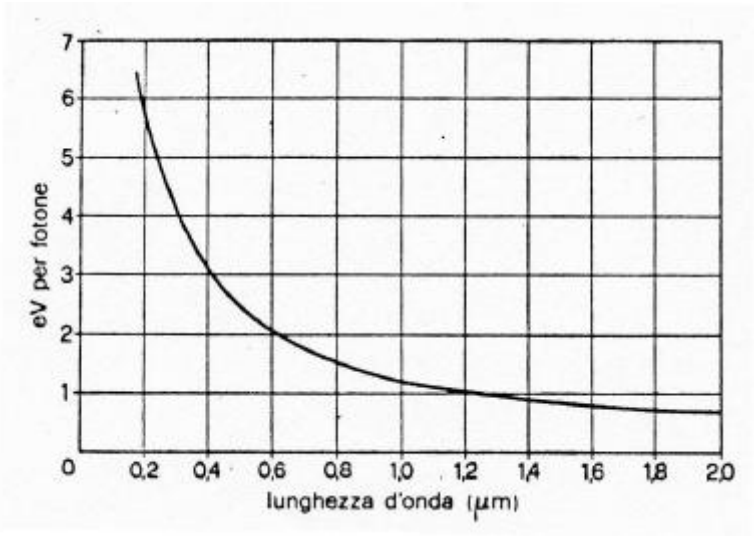

Figure 2.10: Photon energy as a function of wavelength.

2.4.3 Constitution and functioning of the solar cell

The basic element of a PV generator is the "*PV cell*". The types of cells currently most widespread for terrestrial use are those of **m-Si**, p-Si and thin film cells (amorphous silicon a-Si and other semiconductors such as CIS or CdTe).

A PV cell is basically a large cross-section semiconductor diode, with a square (m-Si), pseudo-square and circular (m-Si) or rectangular shape (a-Si and CIS) placed between two electrodes, one massive front, if transparent to light, or in the shape of a grid, to allow the passage of solar radiation, and the other flat-shaped rear.

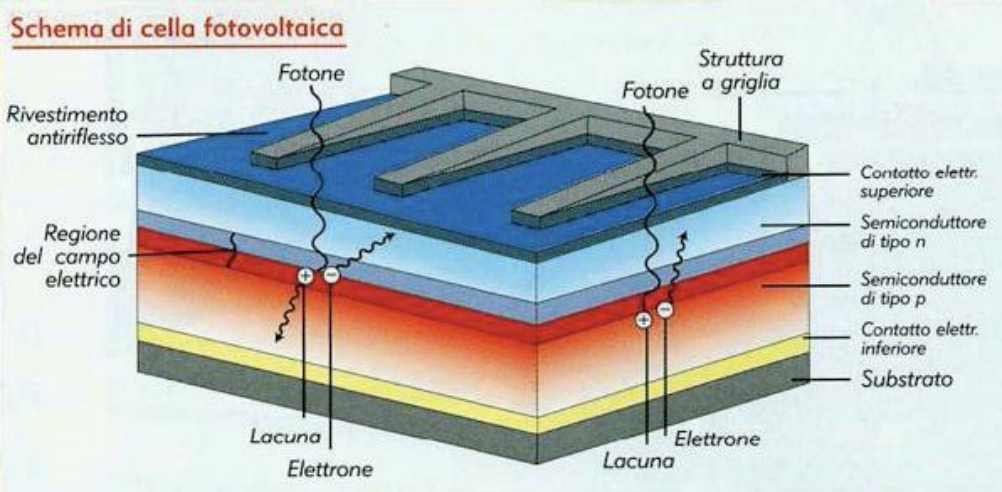

Figure 2.11: Section of a photovoltaic cell.

The total thickness of the cell is between the micrometer for thin films and a few hundred micrometers for crystalline silicon.

In a single crystal of Silicon (semiconductor belonging to the IV group) each atom is covalently bonded to four other atoms: two atoms side by side of a crystal have in common a pair of electrons, one of which belongs to an atom and the other to the neighboring one (figure 2.21). This very strong electrostatic bond can be broken with an amount of energy of **1.08 eV** which allows the electron to free itself from the covalent bond with the atom, to overcome the energy gap and therefore to pass through the valence band. to the conduction band where it is free to move thus contributing to the flow of electricity.

When it passes into the conduction band, the electron leaves behind a hole called a **hole**, which is easily occupied by a nearby electron.

When it passes into the conduction band, the electron leaves behind a hole, which is easily occupied by a nearby electron.

A luminous flux of photons that invests the crystalline lattice of Silicon has the ability to release a certain number of electrons to which an equal number of holes corresponds; in the recombination process each free electron near a hole can occupy it, returning a part of

the kinetic energy it possessed in the form of heat.

To exploit electricity, it is necessary to create a coherent motion of electrons (and holes), or a current, by means of an electric field inside the cell.

The field is achieved with particular physical and chemical treatments by creating a layer of positively charged fixed atoms in one part of the semiconductor and a layer of negatively charged atoms in the other.

To do this, it is necessary to introduce a small amount of atoms belonging to the III or V group of the periodic system into the Silicon in order to obtain two different structures, one with an insufficient number of electrons, the other with an excessive number of electrons.

This treatment is called doping and the amount of impurities introduced is of the order of one part per million.

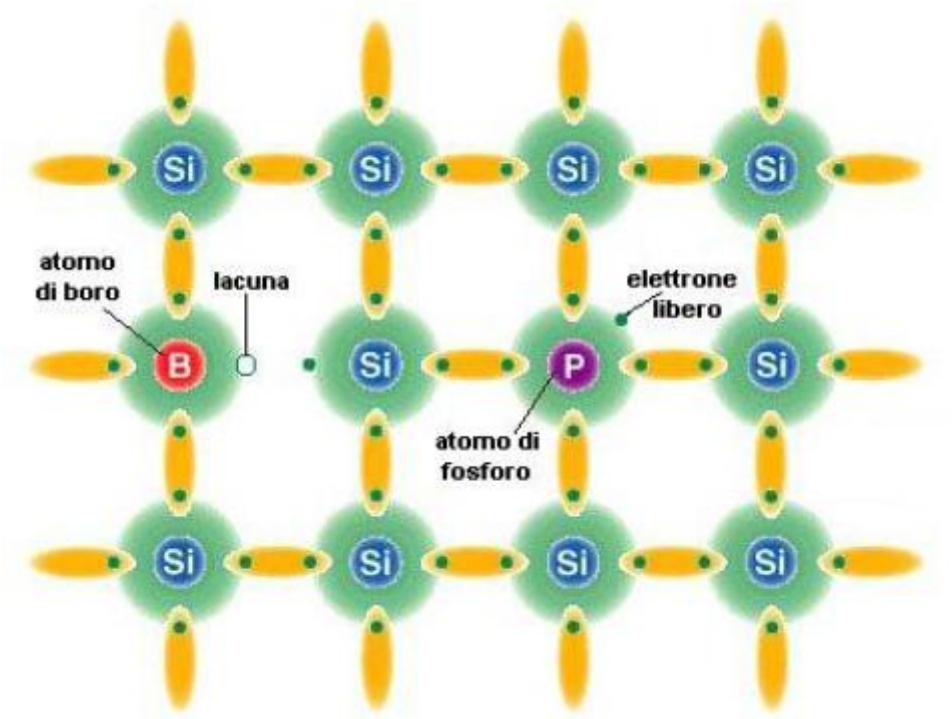

Figure 2.12: Representation of silicon doped with phosphorus and boron.

Generally, Boron (third group) and Phosphorus (fifth group) are used as impurities to obtain respectively a p-type structure (with an excess of holes) and an n-type structure (with a excess electrons). See figure 2.12 .

By placing the two types of structures in contact, whose separation zone is called the p-n junction, an electronic flux from zone n to zone p is activated between the two layers by means of a diffusion process, due to the different concentration of the two types of free charges (electrons and holes); the holes, which cross the junction from the p-type zone,

recombine with some electrons in the n zone and, conversely, some electrons crossing the junction from the n-type zone, recombine with some holes in the p zone.

These recombinations result in the formation, immediately astride the junction, of two layers of fixed charges and of opposite sign with an absence of free charges, hence the name of the depletion zone or depletion layer (2.13).

Illuminating the p-n junction generates **electron-hole pairs** in both the n and p zones. The electric field separates the excess electrons generated by the absorption of light from respective holes pushing them in opposite directions (the electrons towards the n zone and the holes towards the p zone). Once they cross the field, the free electrons never go back, because the field, acting like a diode, prevents them from reversing.

If you connect the p-n junction with a conductor, in the external circuit you will get a flow of electrons starting from the n layer, at higher potential, towards the p layer, at lower potential. As long as the cell is exposed to light, electricity flows regularly in the form of direct current. It is important that the layer exposed to light, generally the n layer, is such as to guarantee the maximum absorption of photons incident in the vicinity of the junction: for Silicon this thickness must be 0.5 mm, while the total thickness of the cell must not exceed 250 mm.

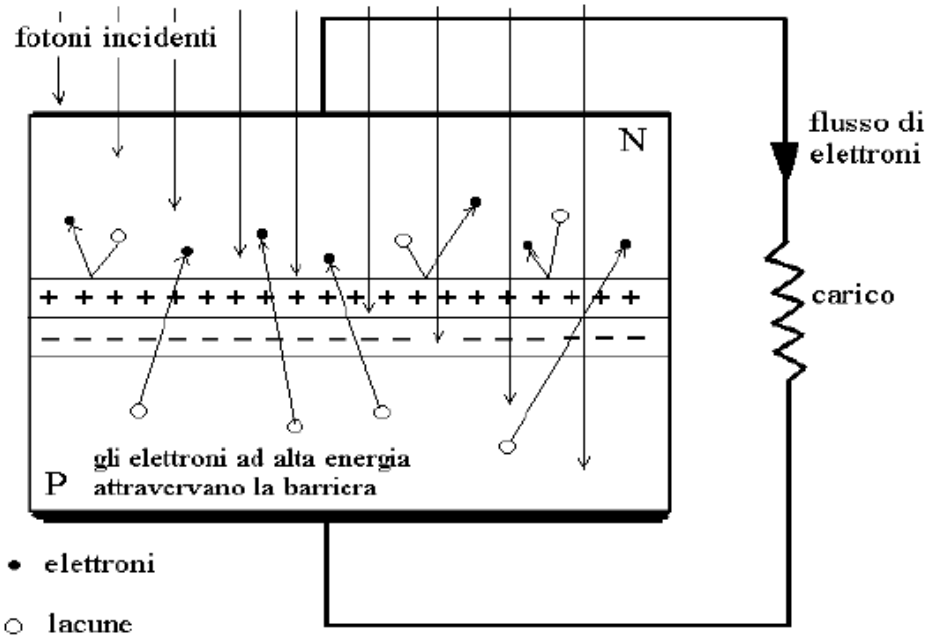

Figure 2.13: Principle of operation of a typical monocrystalline silicon photovoltaic cell with an external load applied.

If, through two leads, the cell is connected to an electric circuit, a current proportional to the incident photons will flow in it. Therefore, in the solar cell illuminated by sunlight,

a current I_{ph} will be produced proportional to the irradiance G:

$$I_{ph}[A] \propto G\left[\frac{W}{m^2}\right] \tag{2.9}$$

Therefore, the continuous presence of solar radiation is indispensable, without which the formation process of the electron-hole pairs would cease in a few μs.

Of all the energy that invests the solar cell in the form of light radiation, only a part is converted into electricity available at its terminals.

The conversion efficiency for monocrystalline silicon PV cells is generally between 13 and 20%, while special applications in the laboratory have reached values over 30%.

The reasons for this low efficiency are many and can be grouped into four categories:

Reflection and masking of the cell surface (≈10%) : not all the photons that affect a cell penetrate inside it, since they are partly reflected by the cell surface and partly affect the metal grid of the contacts. To minimize these negative effects, anti-reflective treatments are used and the screen surface is minimized;

Too much or too little energetic photons (≈50%) : a certain amount of energy is required to break the bond between the electron and the nucleus, and not all incident photons have sufficient energy. On the other hand, some photons that are too energetic generate electron-hole pairs, dissipating in heat the energy in excess of that necessary to detach the electron from the nucleus. In both cases there is a generation of heat;

Recombination (≈2%) : not all the electron-hole pairs generated are collected by the junction electric field and sent to the external load, since in the path from the generation point towards the junction they can meet charges of opposite sign and therefore recombine. The extent of this loss depends on the impurities and defects of the material;

Parasitic resistances (≈20%) : the charges generated and collected in the emptying area must be sent outside. The collection operation is carried out by the metal contacts, located on the front and back of the cell. Even if an alloy process is carried out between Silicon and Aluminum of the contacts during the drying, a certain resistance remains at the interface, which causes a dissipation that reduces the power transferred to the load [1]. In the case of polycrystalline silicon cells, the efficiency is further decreased due to the resistance that electrons encounter at the boundaries between one grain and another and, even more so in the case of amorphous silicon cells, due to the resistance by orientation randomness of individual atoms. This phenomenon, as will be seen later, determines the typical deformation of the characteristic curve of the cell with respect to the rectangular trend.

[1] The main source of loss of metal contacts is given by the Joule effect, which is proportional to the

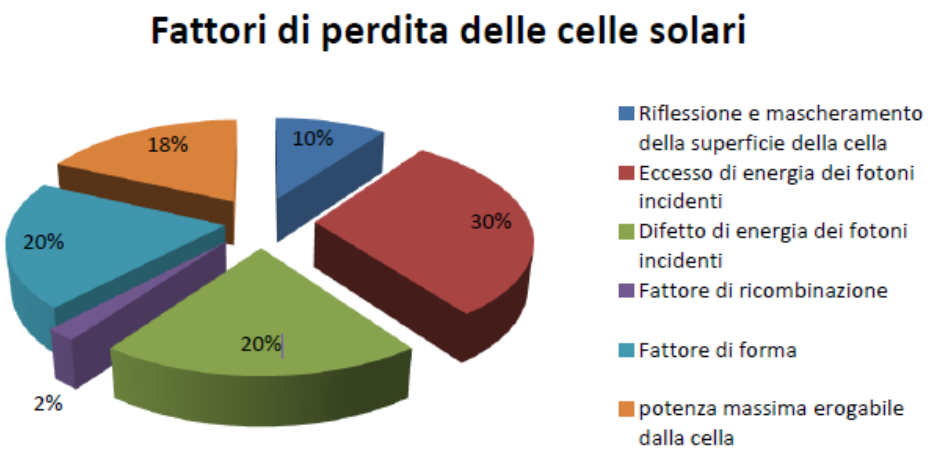

Figure 2.14: Loss factors of solar cells.

2.4.4 The technologies of PV cells

The objectives that the manufacturers of PV cells try to achieve in the rather delicate and complicated production processes are essentially two: increasingly performing PV cells (high efficiency values) and cost containment.

To achieve the second objective, the most used material is silicon, a material easily available and present in large quantities on the earth's surface (after oxygen it is the second most abundant element in the earth's crust, making up 27.7% of its weight). This element is found in the form of silicates, silica and quartz. To separate it from the other elements, it is reduced by adding charcoal, in an electric oven at a temperature above the melting point (1420 °C) and between 1800 °C and 2000 °C. The reaction that is created is the following:

$$SiO_2 + 2C \rightarrow Si + 2CO \tag{2.11}$$

This reaction produces the so-called metallurgical grade silicon, with a purity of 98-99%. The cost is around 2 $\frac{e}{kg}$. Furthermore, the degree of purity of silicon required for solar cells is lower than that required by the electronic sector (another sector that uses silicon a lot), which is why the waste materials of the latter can be used for the construction of PV cells. That said, as mentioned in the previous paragraph, there are essentially three types of PV cells on the market, distinguished on the basis of the crystalline structure of the semiconductor material:

---

circulating current and resistance, according to the formula:

$$P_j = R \cdot I^2 \tag{2.10}$$

where P_J is the power dissipated by the Joule effect [W], R is the resistance of the conductor [Ω] and I is the current flowing through the conductor [A].

- Monocrystalline silicon cells
- Polycrystalline silicon cells
- Thin film cells, i.e. amorphous silicon or materials such as CIS, CdTe and GaAs

In recent years, the increasing use of PV technology has encouraged research in this sector. There are, therefore, different technologies of PV cells and different methods to realize them. The main ones will be listed below [10] [13] [14] .

MONOCRYSTALLINE SILICON CELLS

The first and still the most common semiconductor material used for PV cells is monocrystalline silicon (m-Si).

High purity monocrystalline silicon cells are the highest efficiency cells: they convert more than 23% of solar energy into electricity and are also very durable over time.

However, the main problem with monocrystalline silicon is its high production cost. In fact, the crystallographic growth and then the cutting into thin films (0.1 - 0.3mm) of the piece produced is a slow and expensive process.

The most commonly used technique for the growth of single silicon crystals from molten material is the CZ. The apparatus involved in implementing this technique consists of:

- A furnace, which includes a crucible of molten silica, a graphite susceptor, a rotation mechanism, a heating element and the power supply.
- A mechanism for crystal growth that includes a crystalline seed support and a rotation mechanism.
- An environmental control apparatus.

In the process of growth, a crystallographic seed, appropriately oriented and positioned on a special support, is placed in contact with the molten mixture present in the crucible of the furnace, subsequently the seed, which is subjected to a rotary movement, is slowly lifted (see figure 2.15).

Progressive solidification at the interface between solid and liquid generates a large single crystal. At the end of the process, the material has the shape of a cylinder with a diameter of 10-12.5 cm and a length of one meter and appears gray in color.

The crystal is then cut to obtain wafers with a thickness of 200 μm. Finally, the surface of the wafer on which the chips are to be made is polished until it is mirrored.

The main electrical and mechanical properties of the wafer depend on the direction along which the silicon crystal is grown and on the type and number of impurities

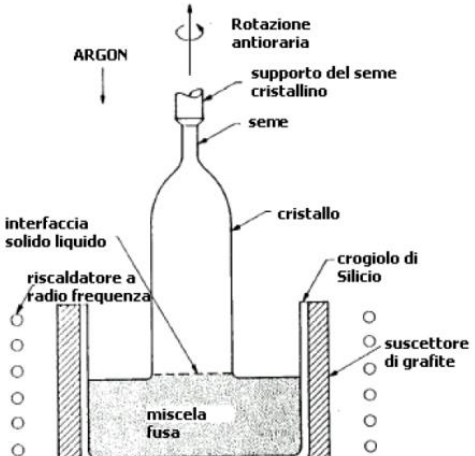

present. Both of these variables are strictly controlled during crystal growth.

The conversion of wafers into finished PV cells takes place in three stages:

1. A chemical texture of the surface to produce pyramids that reduce the loss of energy by reflection.
2. Formation of a p-n junction by exposing the cells to the desired impurities at high temperature: the impurities will diffuse for a thin layer on the surface.
3. The last and most important step is the metallization of the cell, that is, the application on the front and back of metal contacts.

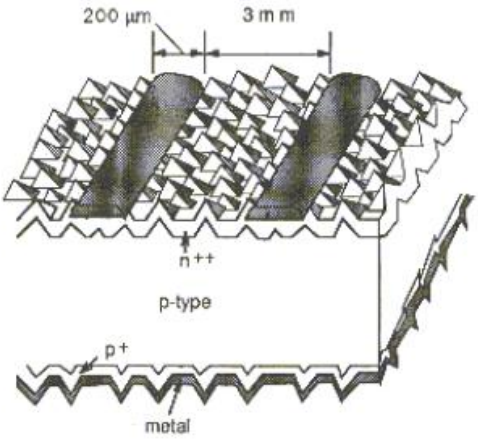

Figure 2.16: Section of a monocrystalline silicon cell.

After the cells are produced individually, they are interconnected using metal strips as interconnectors.

Monocrystalline silicon with the highest degree of purity in absolute can be obtained through a second method, the **FZ** process, which leads to the production of more efficient PV cells than the CZ process (+1-2%) but with higher costs.

Figure 2.17: Monocrystalline silicon single crystal and respective PV cell.

For obvious cost problems, researchers are developing some alternative materials to monocrystalline silicon. An alternative material is polycrystalline silicon.

POLYCRYSTALLINE SILICON CELLS

The polycrystalline silicon (m-Si) production technique is, instead of the CZ method, the WICP method. WICP uses two different containers for fusion and recrystallization. The process consists in melting the previously purified silicon in a quartz crucible, placing the molten silicon in a preheated mold, and then making a one-way solidification; the mold is built with graphite elements. The solidification process is performed with a controlled vertical temperature gradient in the mold to obtain a block with horizontal layers of crystalline silicon from the bottom to the top of the solidified block.

The division of the solidified block into large-sized blocks (eg 10x10, 15x15 cm) is done with sawing slabs. The single bread is then cut into wafers with a thickness of about 300 μm.

This method is cheaper than the CZ method but has disadvantages: the wafers produced contain internal stresses, impurities and grain boundaries; all factors that increase the resistance of the material to electronic flow.

Polycrystalline silicon cells are essentially cheaper but always have a lower efficiency: 15-17%

AMORPHOUS SILICON CELL (or thin film)

Another inexpensive but low-efficiency alternative material is amorphous silicon (a-Si) which represents the latest technology.

In amorphous silicon each atom is not bonded to the other four adjacent ones, as in crystalline silicon, but free bonds are present. By bridging the bonds with hydrogen atoms, a compound is obtained which has all the characteristics of crystalline silicon.

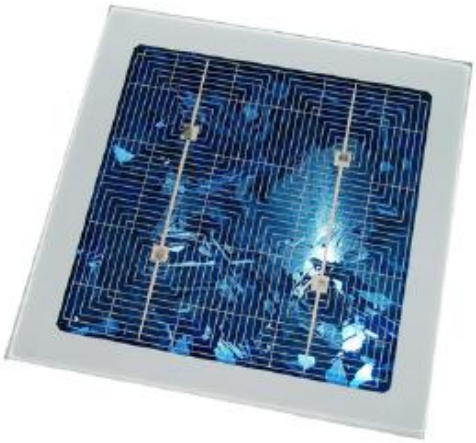

Figure 2.18: Polycrystalline Silicon PV Cell.

Figure 2.19: Amorphous silicon PV module.

The PV transformation yields, however, are considerably lower due to the crystallographic disorder introduced by Hydrogen: 12% in the laboratory and 7% for commercial PV cells (they also degrade over time, losing about 50% of their efficiency with exposure to light).

Amorphous silicon is very sensitive to light compared to crystalline silicon, in fact very thin layers are sufficient, with an order of magnitude of thickness equal to the micrometer to capture photons, with an enormous saving of material. In addition, there is also an

energy saving in the construction phase, since, unlike other techniques in which silicon must be melted, the temperatures involved for this technology are of the order of a hundred degrees and are kept for a few minutes. The section of a typical a-Si cell is shown in the figure below. It is immediately evident that the greater thickness is given by the support material.

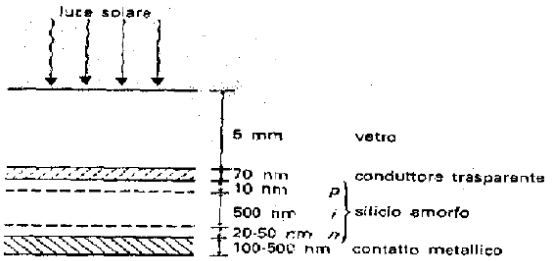

Figure 2.20: Section of an amorphous silicon PV module.

Starting from the top, the following layers are presented:

- High transmittance glass plate;
- Transparent conductor (e.g. Tin oxide, 70 nm);
- p-type doped a-Si (10 nm);
- a-Si of intrinsic type (500 nm);
- n-type doped a-Si (20-50 nm);
- Sheet of metallic material (e.g. aluminum, 100-500 nm);

With amorphous silicon it is possible to create monolithic panels without having to build a mosaic of cells. Furthermore, the module has the advantage of being light and flexible.

Thin-film cells built with materials other than silicon have been developed in an effort to overcome the inefficiency and degradation of amorphous silicon thin-film cells while maintaining a low cost.

Among these, the **CdTe thin-film solar cell** is currently the most promising for its high efficiency and low cost. CdTe is a compound semiconductor with an ideal bandgap (or energy gap) of 1.45 eV. Its absorption coefficient is high enough to allow a $1\mu m$ thick layer of material to absorb 99% of visible light.

A disadvantage of this technology is the toxicity of the Cd. For this reason the device is encapsulated, to protect it from the environment and the environment from it. Also, after their useful life period, the panels need to be recycled and this expense is an additional cost to the technology cost. The CdTe cell is generally based on a *CdS / CdTe heterojunction.*

The first layer on glass, with which the devices are encapsulated, is a transparent **TCO** electrode. The second layer is the doped thin films of CdS and CdTe, then an electrode typically made of carbon paste or a thin metal film.

OTHER INNOVATIVE MATERIALS AND TECHNOLOGIES (hints)

Finally, there are PV cells consisting of techniques based on thin film spreading with the use of compounds, in addition to the CdTe previously analyzed, such as indium and copper dishelenurium ($CuInSe_2$) also called CIS. The support used can be flexible and allow the creation of very light cells suitable for mobile uses (e.g. boats). The values obtained for the conversion efficiency are of the order of 10-12%.

Still under development are the polycrystalline films of GaAs and gallium aluminum arsenide (GaAlAs). They are characterized by a high theoretical efficiency with values around 30% but penalized by very high production costs and justified for now only by space applications.

An interesting evolution of thin film cells is the possibility of making multilayer cells called **multiple junction** cells. Made up of different semiconductor materials, each with its own value of E_g (energy gap), arranged in overlapping layers. The layers individually exploit the spectrum of solar radiation that belongs to them and overall maximize the PV energy obtained, with the effect of increasing the total conversion efficiency. The most common type consists of two superimposed single junction cells called a tandem. On a theoretical level it is calculated that they can reach a value for conversion efficiency equal to 30%.

Another innovative technique being developed is the use of concentration systems (mirrors) combined with (very expensive) monocrystalline GaAs, which allows to replace a part of the surface occupied by the PV cells with a reflective surface with a cost advantage on the latter.

Figure 2.21: World production of PV cells by type [%]. ENEA

2.4.5 The equivalent circuit of the PV cell

At the external terminals the electrical behavior of the solar cell is described, as a first approximation, by an ideal current generator, proportional to the irradiance, and by a real diode connected together in anti-parallel. An equivalent circuit, closer to reality (Figure 2.22), also includes two dissipative elements: a resistance connected in parallel R_{sh} and one in series R_s to the previous circuit.

The resistance R_{sh} corresponds to the surface leakage current between the plate and

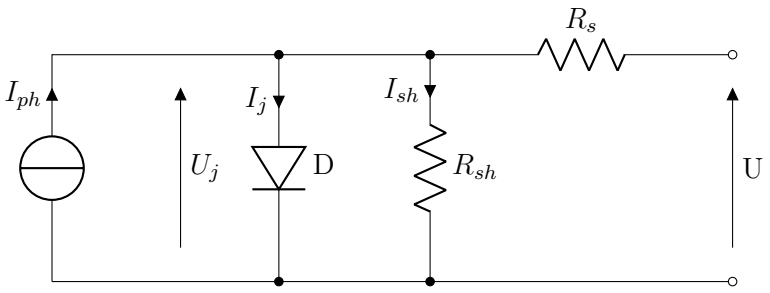

Figure 2.22: Equivalent circuit of the PV cell.

the grid. The resistance R_s is the sum of the volumic resistance of the semiconductor, the contact resistances and those of the electrodes.

The movement of electrons induced by solar radiation across the interdicted band is interpreted as a current of electrons, called the *"generation current"*.

Ideally, without considering the losses, each electron contributes to the formation of the PV current according to the following equation:

$$I_{ph} = q \cdot N \cdot S \tag{2.12}$$

where:

- q = charge of the electron ($1.6 \cdot 10^1 9$ eV);
- N = number of photons;
- S = area of the semiconductor surface exposed to solar radiation [cm_2];

Diode D represents the rectifying effect of the p-n junction. By indicating with I_0 the inverse saturation current of the diode, which is strongly dependent on the temperature and with U_j the voltage [V] that occurs at its ends, it is possible to give a quantitative description of the current that passes through it:

$$I_j = I_0 \cdot \left(e^{\frac{q \cdot U_j}{n \cdot K \cdot T}} - 1 \right) \tag{2.13}$$

where:

- K = Boltzmann constant ($1.38 \cdot 10^2 3 \ \frac{j}{k}$);
- T = absolute temperature, measured at the junction surface between the zone p and n [K];
- m = coefficient of non-ideality of the junction (also defined as emission coefficient depending on the manufacturing process or quality factor of the junction);

Indicating with U the voltage across the load and with I the current flowing in it, the equations at the node and at the mesh of the equivalent circuit are:

$$I = I_{ph} - I_j - \frac{U_j}{R_{sh}} \tag{2.14}$$

The current is therefore expressible by inserting the equation 2.13 in 2.14. We thus obtain the expression:

$$I = I_{ph} - I_0 \cdot \left(e^{\frac{q \cdot U_j}{n \cdot K \cdot T}} - 1 \right) - \frac{U_j}{R_{sh}} \tag{2.15}$$

As regards the voltage U instead:

$$U = U_j - R_s \cdot I \tag{2.16}$$

Substituting equation 2.15 into 2.16 we obtain:

$$U = \frac{m \cdot K \cdot T}{q} \ln \left[\frac{I_{ph} - \left(1 - \frac{R_s}{R_{sh}}\right) I - \frac{U}{R_{sh}} + I_0}{I_0} \right] - R_s I \tag{2.17}$$

Equation 2.17 can be simplified by taking into account the fact that ${}_Rs \ll R_{sh}$ and that, therefore, the ratio $\frac{U_j}{R_{sh}}$ is negligible.

$$U = \frac{m \cdot K \cdot T}{q} \ln \left(\frac{I_{ph} - I + I_0}{I_0} \right) - R_s I \tag{2.18}$$

where:

- I = current applied to the external load [A]
- I_{ph} = generation current of the PV generator [A]
- I_0 = reverse saturation current of the diode [A]
- U_j = potential difference across the diode [V]
- U = potential difference on the external load [V]
- I_j = current flowing through the diode [A]
- R_s = resistance in series due to the particular construction of the upper electrode of the cell
- R_{sh} = resistance in parallel due to the leakage current between the two electrodes

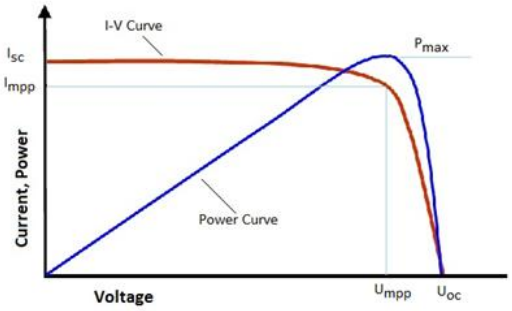

Figure 2.23: Operating characteristic curve and power curve of a PV cell.

Equation 2.18 describes the trend of the voltage as a function of the current generated by the PV cell and transferred to the load. The operating characteristic is described by a current - voltage curve.

Once irradiance and temperature are fixed, an I (U) curve is identified: the coordinates of the points that constitute it provide the deliverable power P:

$$P = U \cdot I \tag{2.19}$$

By observing figure 2.23 it is possible to notice the point f maximum power P_{max} that can be supplied by the PV cell. It is identified by the coordinates (U_{mpp}, I_{mpp}). The point is included within two points that represent the limits of the characteristic curve: the **short circuit**, in which the current delivered is maximum and the voltage is zero ($U = 0$; $I = I_{sc}$) and the **open circuit**, in which the voltage is maximum and current is zero ($U = U_{oc}$; $I = 0$). By canceling the value of the current I, the **no-load voltage** of the circuit is obtained:

$$U = \frac{m \cdot K \cdot T}{q} \ln\left(\frac{I_{ph} + I_0}{I_0}\right) = \frac{m \cdot K \cdot T}{q} \ln\left(\frac{I_{ph}}{I_0} + 1\right) \tag{2.20}$$

On the other hand, by canceling the voltage U, the equation of the **short-circuit current** is obtained:

$$I_{SC} = I_{ph} - I_0 \left[e^{\frac{q}{mKT} \cdot (R_s i)} - 1\right] \tag{2.21}$$

Assuming that Rs is negligible, it would result that $I_{SC} \approx I_{ph}$ and consequently that the short-circuit current is directly proportional to the irradiance according to the equation:

$$I_{SC} \approxeq I_{ph} = \epsilon \cdot S \cdot G \tag{2.22}$$

where:

- ϵ is a coefficient that depends on the type of PV cell;
- S is the surface area of the PV cell exposed to solar radiation;
- G is the irradiance.

A very important parameter of PV cells is the **FILL FACTOR**, or form factor. It is defined by the ratio:

$$K_f = \frac{U_{mpp} \cdot I_{mpp}}{U_{OC} \cdot I_{SC}} \tag{2.23}$$

where:

- I_{mpp} = operating current at maximum power [A];
- U_{mpp} = operating voltage at maximum power [V];
- I_{SC} = operating current in short circuit conditions [A];
- U_{OC} = no-load operating voltage [V].

The coefficient K_f globally represents the influence of the diode and of the resistances R_s and R_{sh} on the characteristic. In crystalline silicon PV cells, K_f assumes values between 0.7 and 0.8.

Ultimately, a good performance cell has a high fill factor and a "square" current-voltage characteristic.

In reality, the complete I(U) characteristic of the solar cell extends into quadrants II and IV (see figure 2.24); in them the cell functions as a user with reverse voltage (U<0, I>0) and reverse current (U>0, I <0) respectively. These operating modes are acceptable only if the working points fall inside the respective hyperbole of maximum power dissipable by the cell (P_{dm}).

If the reverse voltage exceeds the breakdown voltage U_b (a few tens of volts for silicon cells), the cell finds itself in the situation of having to dispose of a thermal power higher than the maximum permissible, it gets too hot and is irreparably damaged.

2.4.6 Influence of irradiance and temperature on the functioning of the solar cell

The I(U) characteristic of the solar cell, at constant temperature T, varies as a function of the irradiance G: as it decreases, the short-circuit current I_{sc} decreases proportionally, while the open-circuit voltage U_{oc} decreases with a logarithmic law. Figure 2.25 shows the dependence of I(U) on irradiance and highlights the locus of the maximum power points P_{MAX}.

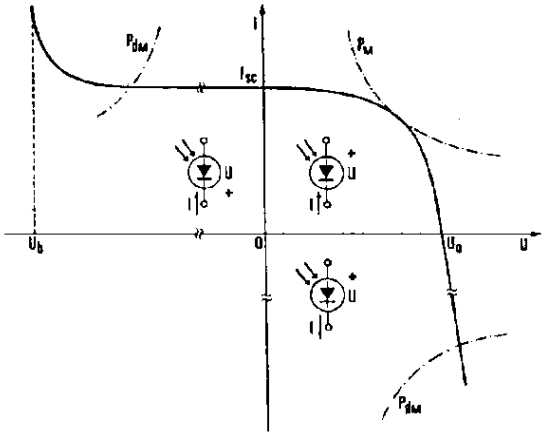

Figure 2.24: Modes of operation of a solar cell.

Therefore the U_{oc} is sensibly constant for considerable variations of G; only for low values of G, less than 50 $\frac{W}{m^2}$, it abruptly decreases. In silicon solar cells the variations of the I(U) characteristic, as the irradiance G varies, occur very quickly with time constants which, for silicon cells, are of the order of 10-20 μs.

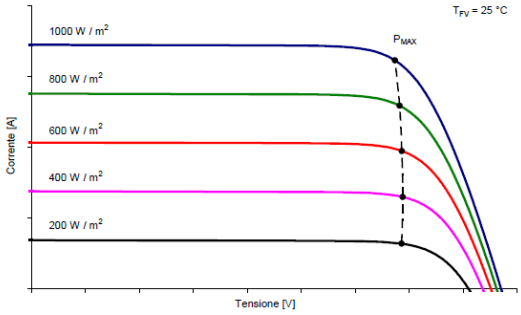

Figure 2.25: I (U) characteristic of a solar cell as a function of irradiance. T = const.

The I(U) characteristic also depends on the temperature (see figure 2.26). At constant irradiance, an **increase in temperature** causes:

- A **slight increase in the PV current** I_{ph} and therefore also in the **short-circuit current** I_{sc} (or in the current density J_{SC}), essentially due to the decrease in the energy gap of the material. This variation corresponds to approximately $\frac{dJ_{SC}}{dT} \approx 0.01 \frac{mA}{cm^2 K}$ for crystalline silicon, while it has higher values for amorphous silicon.
- An **increase in the current Ij in the diode**, which corresponds to a **decrease in the open circuit voltage** U_{oc}. The trend of the decrease is about $\frac{dU_{OC}}{dT} = -2.2 \frac{mV}{K \cdot cell}$.

The extent of these variations are such as to cause an overall decrease in the maximum

power that can be generated ($dP_{max}/dT \approx -0.5\%$ /°C for crystalline silicon, lower values for amorphous silicon)[2].

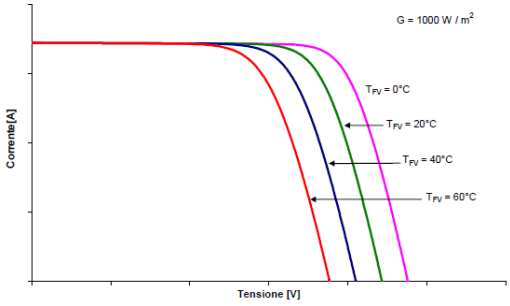

Figure 2.26: I (U) characteristic of a solar cell as a function of temperature. G = const.

2.4.7 Series and parallel connections of solar cells

A single silicon PV cell, under optimal irradiance and load conditions, generates a voltage of 0.4 - 0.6 V, independent of the illuminated surface. The current, on the other hand, depends on the surface. Current density values equal to J = 0.2 - 0.3 $\frac{A}{mm^2}$ are obtained (for cells with a diameter of 100 mm, I = 2 - 2.5 A).

The loads currently used require much higher voltages and currents than those supplied by the individual cells.

Therefore, to reach the required power levels, it is essential to connect several solar cells in series and / or in parallel, thus constituting the **PV module**. It is important to state that the characteristics of the PV cells (and therefore of the PV module), in reality, are subject to some variations that can be essentially summarized in two reasons: the natural variation of the parameters due to manufacturing problems and the various conditions of operation that occur (e.g. some cells of the module are in shadow).

These variations lead to a decrease in the performance of the PV module and are considered under the heading "*mismatching*".

The "mismatching" can lead to different problems depending on the type of connection of the PV cells.

Series connection

If N_s equal cells are connected in series with each other (in jargon "string") and one of them has a different characteristic from that of the others, for example because it is partially in

[2] in applications, it is often believed that the short circuit current I_{SC} depends only on the irradiance and that the open circuit voltage U_{OC} depends only on the temperature.

shadow, the resulting characteristic is formed by the sum, for a given current, the voltage of all other cells $(N_S - 1)$ not darkened and the voltage of the shaded cell.

In figure 2.27 it is possible to observe different curves that represent the voltage and current characteristics of the cells connected in series:

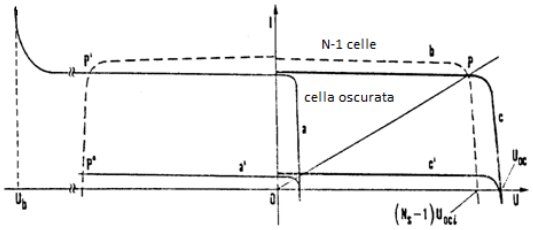

Figure 2.27: I(U) characteristic of cells connected in series, in case of mismatching.

Curve (a) I(U) curve different from the others due to a constructive defect.

Curve (a') I(U) curve different from the others because it is shaded.

Curve (c) resulting characteristic (relative to curve a) formed by the sum, for a given current, of the voltage $(N_s - 1)$U of the $N_s - 1$ cells equal with the cell voltage different due to a construction defect.

Curve (c') resulting characteristic (relative to curve a') formed by the sum, for a given current, of the voltage $(N_s - 1)$ U of the $N_s - 1$ cells equal to the voltage of the shaded cell.

Piecewise curve (b) I(U) curve resulting from the sum of the characteristics of the $(N_p - 1)$ normally functioning cells

The resulting curve can have a considerably decreased power (curve c'in the case of heavy shading) and in any case the **maximum power is always lower than the sum of the maximum powers of the cells connected to each other**.

The resulting curve itself has an open circuit voltage U_{OC} equal to the sum of the $U_{OC,i}$ of the individual cells and a short-circuit current I_{SC} theoretically equal to the short-circuit current of the cell that delivers the lowest current:

$$U_{OC} = \sum_i U_{OC,i} \tag{2.24}$$

$$I_{SC} \cong (I_{SC,i})_{min} \tag{2.25}$$

Now, if the cell is totally shaded, it stops generating current. When a cell is electrically connected in series with other PV cells and is subjected to 100% shading, its generated

current is 0 A. The other $(N_S - 1)$ cells, not being shaded, produce current and voltage which reverse bias the shaded PV cell. The shaded cell opposes the flow of current with its resistance which generates a voltage with the opposite direction to that generated by the other cells. The shaded cell becomes a load, with its electrical resistance, and therefore will dissipate heat, generating the phenomenon of the **hot-spot** (point P') [16] .

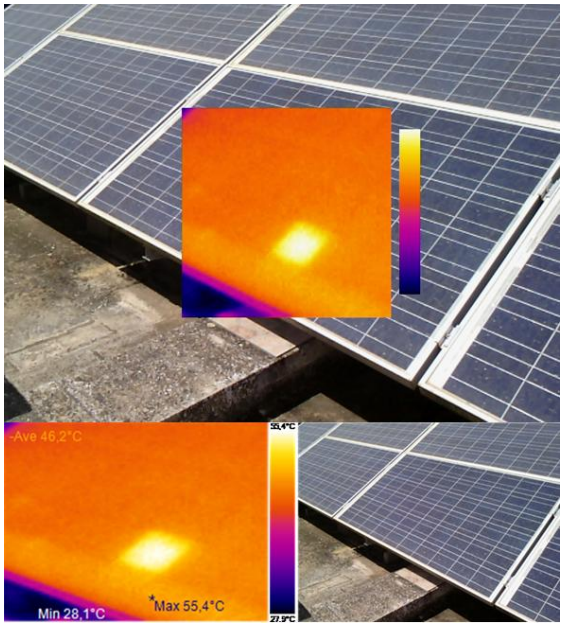

Figure 2.28: Typical example of a hotspot due to a faulty cell in the PV module.

After a time that depends on the entity of the overload and the cooling mode, irreparable failures can occur in the cell.

In fact, if the voltage $(N_S - 1)$U exceeds the maximum breakdown voltage U_b, the cell is instantly destroyed. Taking into account that for silicon cells the breakdown voltage is U_b = 25-50 V and that each cell supplies a voltage $U \approx 0.5V$, from thirty to sixty cells in series are required for the inversely polarized cell to break. A **diode D_P connected in parallel to the shadow cell** prevents this cell from functioning as a user with reverse voltage, as indicated in figure 2.29 , where the individual cells have been represented as current generators.

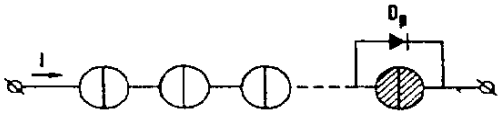

Figure 2.29: Protection diode connected in parallel to the cell.

The diode D_P has the task of ensuring that the short-circuit current of the string is no longer limited to the value of the current of the cell with the worst characteristic (a'), but is equal to that of the remaining cells in series with the best characteristic. Therefore, the power delivered by the string is reduced only by the contribution of the cell (a') and the abrupt power reduction that took place in the absence of the diode D_P, represented by curve (c') in figure 2.26 , does not occur. However, such a protection technique for each single cell is impractical, therefore the diode D_P connects in parallel to groups of cells in series forming a module, typically every 18-20 cells. Therefore, in the case of cells in series equipped with protection diodes in parallel, it is observed that:

- If a cell is interrupted, the entire series does not deliver current and therefore the power supplied is canceled;
- If a cell is short-circuited, the entire series delivers a power reduced only by the contribution of the short-circuited cell.

Parallel connection

Considerations similar to the previous ones show that, if among N_P cells connected in parallel, one has a different characteristic from that of the others (e.g. for shading), the resulting characteristic is given by the sum, for a given voltage, of the currents $(N_P - 1)$ I of the $N_P - 1$ unobscured cells and of the current of the shadow cell.

The resulting characteristic has a short circuit current I_{SC} equal to the sum of the short circuit currents I_{SC}, i of the individual cells and an open circuit voltage U_{OC} very close to that of the darkened cell:

$$I_{SC} = \sum_i I_{SC,i} \tag{2.26}$$

$$U_{OC} \cong (U_{OC,i})_{min} \tag{2.27}$$

It is observed that if a cell is darkened, the parallel of the cells behaves towards the load like the parallel of $N_P - 1$ illuminated cells. The worst condition for the darkened cell occurs with zero external load because in this condition the darkened cell is forced to absorb the current of the illuminated $N_P - 1$ cells.

Normally the overtemperature consequent to this high current determines the out of service of the cell and the parallel resumes to work with $N_P - 1$ instead of with N_P cells.

With regard to the load, the presence of a shadow cell in the parallel connection has a much less harmful influence than in the series connection.

A diode D_S connected in series to the single cells in parallel could prevent the shadow cell from functioning as a user with reverse current.

However, this protection is unacceptable for the parallel of single cells, since the voltage drop across the diodes is of the same order as the voltage generated, but it is applied to

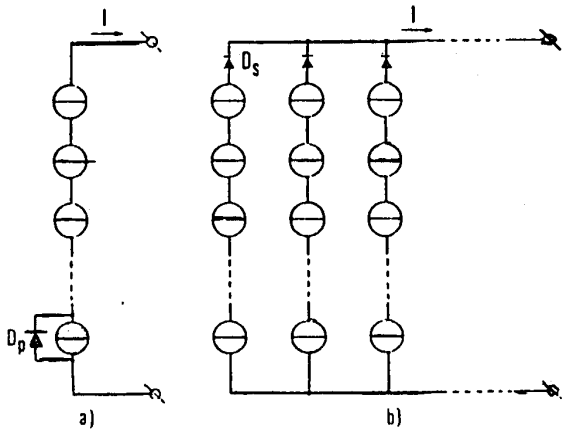

Figure 2.30: Protection diode connected in series.

strings of several cells in series. The preceding considerations show that in the series or parallel connection of cells to each other it is advantageous to use cells with characteristics as similar as possible.

This requires, in the construction phase, an accurate selection of the cells to be connected together. A first selection criterion is to verify that the values of the three parameters I_{SC}, U_{OC} and $_{Pmpp}$ are identical.

These checks cannot, however, prevent the maximum power of several modules, connected to each other, from being lower than the sum of their maximum powers: a loss of 2-3% is often assumed with respect to the nominal value.

2.5 The PV module

The production process of **crystalline silicon** modules is standardized, with few variations between the different manufacturers [16] .

The module manufacturing process is divided into various phases:

1. Electrical connection;
2. Encapsulation;
3. Mounting the frame;
4. Mounting the junction box.
5. Monitoring test

First of all it is necessary to solder suitable connection terminals on the front and rear contacts of the cell. These terminals are mostly in the form of copper "ribbon".

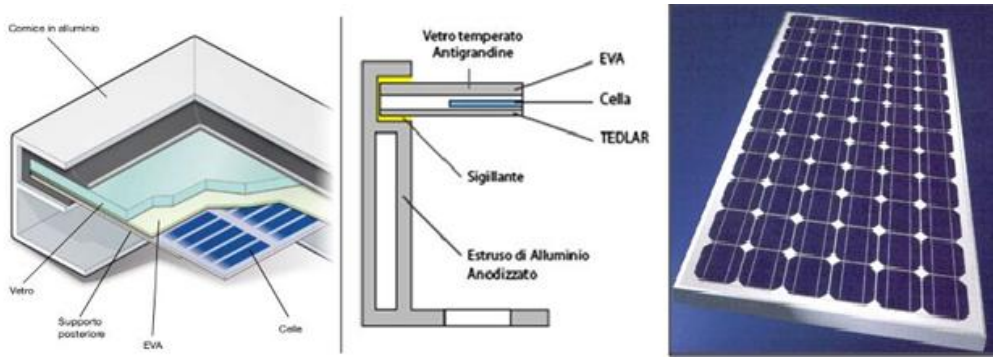

Figure 2.31: Section of a crystalline silicon PV module and its components.

The **electrical connection** consists in connecting the individual cells in series-parallel to obtain the desired voltage and current values, using special welding paths.

A sandwich is then constituted of which the cell surface constitutes the central part: the **encapsulation** consists, first of all, in fixing the cells to a glass plate by means of a transparent adhesive sheet, generally of EVA, and subsequently, affixing, in the rear part of the sandwich, another sheet of EVA and a sheet of synthetic covering, for example in Tedlar; the sandwich thus obtained is treated in a special oven, called lamination, in which the components are sealed by heating at about 150 °C. EVA (originally translucent) becomes transparent and the air and vapor contained between the interstices are eliminated from within the stratification, in order to avoid possible corrosion processes; a final heat treatment concludes the lamination operation, so that the entire slab takes on a monolithic character.

It is important that the encapsulation, in addition to protecting the cells, is transparent to solar radiation, stable to ultraviolet rays and temperature, has self-cleaning capabilities and allows the temperature of the cells to be kept low.

In principle, the life of a solar cell is infinite; it is therefore the duration of the encapsulation that determines the life span of the module, which can now be estimated at about 25 years.

Finally, there are two other types of encapsulation, namely Teflon and resin. The first type of processing is very similar to that previously described, but differs in the absence of the additional coating on the front because Teflon is resistant to UV rays, has good transparency characteristics, does not become opaque and does not reflect radiation; furthermore, this material, with a maximum thickness of 0.5 mm, is an excellent conductor of heat, which facilitates the cooling of the cells.

Encapsulation is carried out by fusion with resin casting: the cells are fixed between two sheets of glass, the resulting cavity is filled with a molten resin which, cooling down, hardens inside; the advantage of this process, which produces modules up to 2.50 $\times$ 3.80 m in size, is the precision with which the cells can be positioned.

Finally, the **assembly of the frame and the junction box follows**: the first, usually in extruded anodized aluminum, has the function of giving the module greater strength and allowing it to be anchored to the support structures; the second, in plastic material and placed on the rear side, has the purpose of protecting the terminal strips that protrude from the sandwich and, generally containing by-pass diodes, in case of malfunction of the module, to isolate it from the rest of the system.

At the end of the assembly the modules are visually **inspected** to identify any damaged cells. With an "artificial sun" the fundamental parameters (ISC, UOC, PMAX) are obtained, and on the basis of these measurements it is placed in a certain production batch. This phase is important because it allows the manufacturer to provide the customer with modules with similar characteristics, in order to minimize losses due to mismaching.

The modules must also pass a series of mechanical tests to verify their resistance to humidity, hail, frost and wind. In 2015, according to the ***Photon*** index on the prices of PV panels, which mostly refers to the German market ("spot market"), the average price of polycrystalline panels was around **0.66** $\frac{e}{W}$ for those in monocrystalline silicon ($\eta \approx 14 - 17\%$) and **0.51** $\frac{e}{W}$ for those in polycrystalline silicon ($\eta \approx 12 - 14\%$).

Finally, the production process of **amorphous silicon** modules is different.

In fact, in the case of amorphous silicon, innovative techniques and manufacturing methods are the subject of continuous interest.

The result is often original, versatile and effective components, especially if considered in relation to a prospect of future market enlargement and diversification of applications. Thus, we are witnessing the processing of flexible PV sheets, in which the cells are combined with synthetic and transparent materials, or, with small components, with a single cell exposed to the open air.

For amorphous silicon and thin films in general (even if the other materials remain, more than anything else, at the experimental stage), there are, therefore, no standard production processes, but variable techniques depending on the type of component desired.

The most popular method consists in the creation of modules similar to those of crystalline silicon, in which the amorphous silicon is deposited directly on the glass plate which will act as a transparent cover, avoiding the use of the sealant.

An advantage that should not be underestimated in this case is that the cells and interconnections can be made in a single process. After having deposited on the glass the tin oxide that will constitute the transparent front contact, this layer is divided into a series of longitudinal strips, 1-2 cm wide, which cross the entire module, by mechanical or laser engraving.

Then the amorphous silicon is deposited over the entire surface (generally in a multiple junction layering), which creeps into the grooves and covers the previous layer and which in turn is engraved according to grooves slightly out of phase with respect to those traced in the tin oxide. .

Finally, the rear metal contact is deposited, which fills the recesses in the silicon and

covers it, and is subsequently also engraved, according to slightly out of phase grooves with respect to those practiced in silicon.

The result is a PV module, of variable dimensions, composed of longitudinal cells, connected together in series.

The perimeter frame and the junction box can be added or not, depending on the type of use envisaged.

Alternatively, the module can be made on flexible transparent supports or, again, by connecting amorphous surface cells of some hundreds of cm^2 each, made separately.

In 2015, the average price of an amorphous silicon module stood at around **0.45** $\frac{e}{W}$.

2.5.1 Quality certification

The **IEC EN61215** standard describes all the tests to which a crystalline silicon PV panel (or **IEC EN 61646** for thin films) must be subjected to have a degree of quality and reliability over time that meets the expectations and needs of the European market [17].

Mechanical tests

The PV module is subjected to various mechanical tests.

Hail test : the panel is targeted in typical standardized points with ice spheres between 4.5 and 7.5 centimeters in diameter. These balls are fired at a speed from a minimum of 110 to a maximum of 142 $\frac{km}{h}$. This test simulates very severe conditions that are difficult to find in real conditions.

Mechanical load test : this test simulates the kinetic thrust of the wind or the static thrust of snow accumulations.

Termination robustness test : electrical terminations are stressed to check whether the terminals are capable of withstanding wiring operations.

Twist test : the module is fixed on three corners of the aluminum profile, while the fourth is raised by a certain standardized value.

Electrical tests

The electrical tests carried out on the modules are:

Performances at nominal working temperature (NOCT) : in this test the characteristic values of the electrical performance of the PV panel at the nominal working temperature are measured. The latter is defined as the average temperature at which the PV cells work inside the module when they are exposed to a light energy of 800 $\frac{W}{m^2}$ with an ambient temperature of 20 °C and a wind speed of 1 $\frac{m}{s}$.

The knowledge of NOCT (42-50 °C) allows to determine, through equation 2.28, the T_C cell temperature in the operating conditions of the module.

For a given irradiance G $[\frac{Wh}{m^2}]$ and ambient temperature Ta it is assumed that the difference between the cell temperature and the ambient temperature depends linearly on the irradiance G:

$$T_C = T_a + \frac{NOCT + 20}{0.8} \cdot G \tag{2.28}$$

STC performance : this test consists in raising the voltage-current characteristics of the module in the standard test conditions (STC) with illumination of 1000 $\frac{W}{m^2}$, ambient temperature of 25 °C and AM index equal to 1.5.

Electrical insulation test : measures the degree of electrical insulation between the module terminals and the aluminum frame by applying a test voltage.

Outdoor exposure test : the module is exposed to a total irradiation quantity of 60 $\frac{kWh}{m^2}$ (12 days with an irradiation of 1000 $\frac{W}{m^2}$ and 5 hours of exposure per day). After the test, the module must have no visual defects and must have maintained the electrical insulation equal to that prior to the test.

Thermal tests

Thermal cycle test : the PV module is subjected to a series of thermal cycles between -40 °C and +80 °C with a duration of each cycle of less than 6 hours. At the end of this series of tests, the module must have unchanged efficiency parameters and the power must remain above 95% of the initial one.

Cell overheating resistance test : some PV cells are obscured causing hot-spot phenomena that will determine the ability of the module to resist localized overheating effects that can lead to detachment of the welds or deterioration of the encapsulant.

The rules that regularize the tests on the various modules are:

CEI EN 61215 (CEI 82-8) : Crystalline silicon PV modules for terrestrial applications. Design qualification and type approval;

CEI EN 61646 (82-12) : Thin film PV modules for land use - Project qualification and type approval;

IEC 61730-2 : Safety qualification of PV modules - Requirements for testing.

2.5.2 The efficiency of the PV modules

Consider a PV module operating under standard STC conditions: irradiance G (1000 $\frac{W}{m^2}$), temperature T (25 °C) and air mass AM = 1.5. The solar power PS that reaches the module is given by the equation:

$$P_S = G \cdot A[W] \tag{2.29}$$

where with A we mean the total area (total of the edges) of the irradiated PV panel [m^2]. If P_M is the maximum deliverable power (**peak power** [W_p]), the overall efficiency of the PV module is η_M:

$$\eta_M = \frac{P_M}{P_S} \tag{2.30}$$

The overall efficiency of the PV module can be expressed as a product of partial efficiencies:

$$\eta_M = \eta_P \cdot \eta_{Ec} \cdot \eta_{IM} \tag{2.31}$$

where:

- η_P = filling efficiency
- η_{EC} = encapsulation efficiency
- η_{Im} = non-uniform irradiance efficiency

The filling efficiency η_P takes into account that not the entire area of the module affected by the luminous flux is useful for conversion purposes, but only that part of it which is made up of cells.

η_P is therefore defined by the ratio between the area occupied by the cells and the total area of the module ($\sim 85\%$). The encapsulation efficiency η_{EC} can be expressed as the product of three terms:

$$\eta_{Ec} = \eta_C \cdot \eta_T \cdot \eta_{Mis} \tag{2.32}$$

where:

- η_C is the PV conversion efficiency of the bare cell, i.e. directly hit by solar radiation without the interposition of the encapsulating resin and the cover glass;
- η_T is the optical transmission efficiency of glass and resin which takes into account the absorption operated by these materials ($\sim 95\%$);
- η_{Mis} is an efficiency which, with the same irradiance, depends both on the possible non-uniformity (mismatch) between the characteristics of the cells, and on the losses due to the Joule effect in the resistances of the connections between the cells ($\sim 95\%$).

The uneven irradiance efficiency η_{Im} takes into account that not all the cells of the module can be subjected to the same irradiance value ($\sim 98\%$).

In light of these values, the overall efficiency η_M of the module, when referred to standardized test conditions, assumes, according to the type of cell, values that are a few points lower than those previously indicated for bare cells ($\eta \approx 10 - 20\%$)[3].

2.5.3 Correction of the PV module parameters as a function of temperature and irradiation

The main operating parameters of the solar cell, and therefore of the PV module (voltage, current and power), depend on the operating temperature and solar radiation. There are therefore analytical formulations capable of describing these dependencies.

Analytical expression of the current I_{SC}

The link between the short-circuit current Isc and the radiation G and the cell temperature T_c is expressed with the following formula:

$$I_{SC}\,(G,T) = I_{SC}\,(STC) \cdot \frac{G}{1000} \cdot [1 + \alpha_{I_{SC}} \cdot (T_C + T_{STC})] \tag{2.33}$$

where:

$I_{sc}(STC)$ = short-circuit current measured under STC [A] conditions (this value must be provided by the manufacturer);

G = irradiance in the conditions in which the short-circuit current [W/m^2] is to be measured;

$\alpha_{I_{SC}}$ = thermal coefficient of the short-circuit current [% /°C] (this value must be provided by the manufacturer);

T_c = cell operating temperature [°C];

T_{STC} = temperature under standard conditions, equal to 25°C.

the thermal coefficient of the short-circuit current $\alpha_{I_{SC}}$ can be provided by the manufacturer expressed in $\frac{A}{°C}$, instead of in $\frac{\%}{°C}$. To switch from one mode of expression to another, simply use the following formula:

$$\alpha_{I_{SC}}\left[\frac{A}{°C}\right] = \frac{I_{sc}(STC)}{100} \cdot \alpha_{I_{SC}}\left[\frac{\%}{°C}\right] \tag{2.34}$$

[3]Solar panels are very resistant. Compared to other energy sources, they wear out very slowly. **Their effectiveness decreases by about 0.7-0.8% per year.** Producers, in fact, guarantee at 20 or 25 years that the yield does not fall below 80% of the initial value. Their life, however, also extends beyond 25 years.

Analytical expression of U_{OC} voltage

The link between the no-load voltage U_{OC} and the cell temperature T_c is expressed with the following formula:

$$U_{OC}(T) = U_{OC}(STC) \cdot [1 + \beta_{U_{OC}} \cdot (T_C - T_{STC})] \tag{2.35}$$

where:

$U_{OC}(STC)$ = no-load voltage measured under STC [V] conditions (this value must be provided by the manufacturer);

$\beta_{U_{OC}}$ = thermal coefficient of the no-load voltage [%/°C], supplied by the manufacturer;

T_c = operating temperature of the cell;

T_{STC} = temperature under standard conditions, equal to 25°C.

The thermal coefficient of the no-load voltage $\beta_{U_{OC}}$ can be expressed in V/°C, instead of in%/°C. To switch from one mode to another, simply use the formula:

$$\beta_{U_{OC}} \left[\frac{V}{°C}\right] = \frac{U_{OC}(STC)}{100} \cdot \beta_{U_{OC}} \left[\frac{\%}{°C}\right] \tag{2.36}$$

Analytical expression of P_M power

The link between the power P_M, the radiation G and the temperature Tc of the cell is expressed with the formula:

$$P_M(G,T) = P_M(STC) \cdot \frac{G}{1000} \cdot [1 + \gamma_{P_M} \cdot (T_C - T_{STC})] \tag{2.37}$$

where:

$P_M(STC)$ = maximum power measured under STC conditions [W_P], supplied by the manufacturer;

G = irradiance in the conditions in which the short-circuit current [W/m^2] is to be measured;

γ_{P_M} = thermal coefficient of power [%/°C], supplied by the manufacturer;

T_c = cell operating temperature [°C];

T_{STC} = temperature under standard conditions, equal to 25°C

The thermal coefficient of the power γ_{P_M} can be supplied by the manufacturer expressed in W/°C, instead of in%/°C. To switch from one mode of expression to another, simply use the following formula:

$$\gamma_{P_M} \left[\frac{W}{°C}\right] = \frac{P_M(STC)}{100} \cdot \gamma_{P_M} \left[\frac{\%}{°C}\right] \tag{2.38}$$

Analytical expression of η efficiency

The efficiency of the cell, understood as the ratio between the electrical power produced and the power input to the cell, can be expressed as follows:

$$\eta = \frac{P_M(G,T)}{G \cdot A} \tag{2.39}$$

where:

$P_M(G,T)$ = Power actually delivered by the PV module [W] under certain conditions of irradiance G and temperature T.

G = irradiance reaching the PV module [W/m^2].

A = surface of the PV module.

2.6 The PV system

To obtain a predetermined power it is necessary to connect several PV modules together. These groupings give rise to more complex structures, identified in the PV terminology by specific terms [10] [13] [14] .

Several **cells** connected together form a **module**. Several modules mechanically and electrically connected to each other form a **panel**. Several panels electrically connected in series make up a **string** and several strings, electrically connected in parallel to provide the required power, make up the **generator** or **PV field** (figure 2.32).

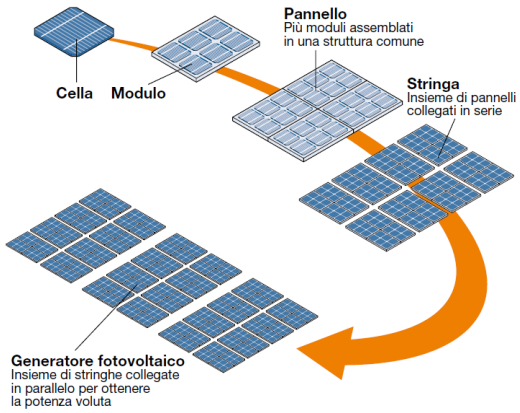

Figure 2.32: Photovoltaic terminology.

As previously mentioned for the PV cells, the phenomenon of *mismatch* can also be created between the strings of the PV generator, as a result of the inequality of the modules, different irradiation of the strings, shadows and failures of a string.

Therefore, to avoid reverse current circulation between the strings, **by-pass diodes** D_P are inserted. In this way, it is guaranteed that the power delivered by the string is reduced only by the contribution of the module, avoiding the *"out-of-service"* of the entire string.

Furthermore, for the protection against asymmetry in the parallel connections of the modules, a **protection** (or blocking) **diode** D_S is placed in series with the module, or with the string of modules in series (figure 2.33).

Finally, in the design of a PV generator it is very important to make an optimal connection of the various modules. They can be connected in **series** or in **parallel**.

By connecting multiple modules in series, the output voltages of the individual elements are added and the same current of the single element is obtained at the output of the series.

By connecting multiple modules in parallel, the output currents of the individual elements are added, while the output voltage remains unchanged.

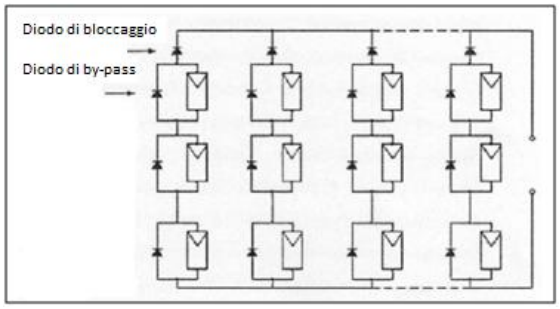

Figure 2.33: Blocking and by-pass diodes in a photovoltaic array.

Since the ohmic losses are a function of the current flowing through the cables and not of the voltage between the poles, from an energy point of view it would be convenient to connect all the modules in series with each other; however, this is not possible from a technical point of view, as it is necessary to comply with the input voltage specifications of the conversion system (*inverter*).

For a correct configuration of the system, then proceed to define the maximum number of modules that can be connected in series according to the characteristics of the conversion group, and then connect in parallel the number of strings necessary to reach the peak power required, thus defining the PV generator.

2.6.1 Photovoltaic systems

It is possible to classify PV systems based on their electrical configuration: isolated (*"stand alone"*) and connected to the network (*"grid-connected"*).

Stand alone systems

They are systems not connected to the electricity grid and consist of PV panels and, generally, of a storage system that guarantees the supply of electricity even in times of low light or in hours of darkness.

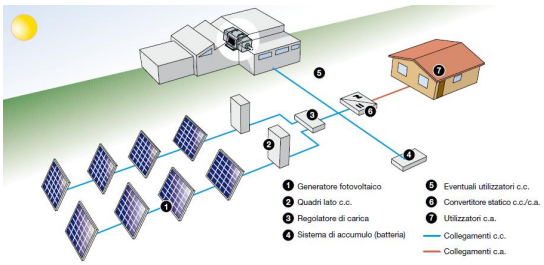

Figure 2.34: Isolated plant scheme.

Since the current supplied by the PV generator is of a continuous type, if the user system requires alternating current, the inverter must be interposed.

Such plants are technically and economically advantageous if the mains supply is absent or difficult to reach, often replacing the generators.

Furthermore, in a stand alone configuration, the PV field is over-sized in order to allow, during the hours of sunshine, both the power supply of the load and the recharging of the storage batteries, with a certain safety margin to take into account of little sunshine

Grid-connected systems

The systems permanently connected to the electricity grid absorb energy from it in the hours in which the PV generator is unable to produce the energy necessary to meet the needs of the user system.

Conversely, if the PV system produces electricity in excess of the needs of the user system, the surplus is fed into the grid: systems connected to the grid therefore do not require storage batteries (unless you want to maximize self-consumption of electricity).

These plants offer the advantage of distributed rather than centralized generation, in fact the energy produced near use has a greater value than that supplied by large traditional power stations, because transmission losses are limited and the economic burdens of large electric transport and dispatching systems are reduced.

Furthermore, the production of energy during sunny hours allows to reduce the demand to the grid during the day, just when the greatest demand occurs.

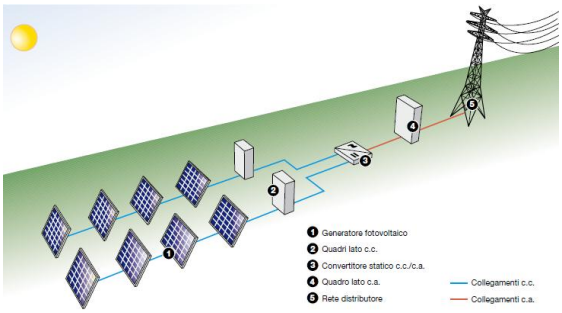

Figure 2.35: System diagram connected to the network.

2.6.2 Localization and arrangement of modules

The performance of a PV generator depends on the local sunlight conditions. Therefore, for the design of a PV system, it is necessary to know some parameters that define the paths that the Sun describes in the different periods of the year in order to determine the power of solar energy incident on a surface inclined at a certain angle, with a certain direction and at a given site.

Latitude of the site : is the angle formed by the line joining the site with the center of the earth and the equatorial plane.

Solar azimuth α_S : is the angle formed by the projection on the horizontal plane of the sun-earth junction at the reference site with the southern semi-axis.

Solar height γ_S : is the angle formed by the sun-earth junction in the reference site with the horizontal plane.

Surface azimuth of the α_{PV} **plane** : it is the angle formed by the projection on the horizontal plane of the normal to the surface in question with the south axis. The optimal value is 0 °, that is surface facing South. In case you have to choose between an orientation towards East or West, the second case is recommended, as generally the haze phenomena are less frequent in the afternoon hours.

Inclination of the surface in question β : is the angle formed by the surface in question with the horizontal plane of the place in which it is located.

Considering the variation of the angle of incidence of the sun's rays, it is possible to maximize the value of the energy captured in the different periods of the year only if the receiving surface is inclined with a certain angle β, the value of which depends on the latitude.

The angle of inclination β that allows maximum yield in the winter months is greater than the optimal angle of inclination for the summer months, due to the lower values of the height of the sun in the winter. As can be seen from the figure, a zero tilt angle β

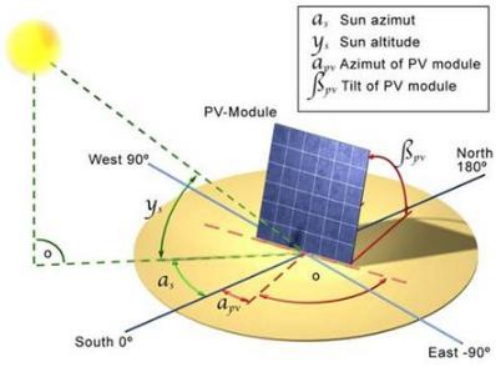

Figure 2.36: Graphic display of some solar angles.

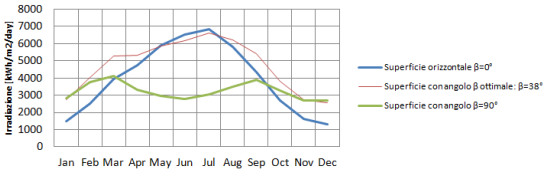

Figure 2.37: Variation of the average monthly irradiance with the variation of the tilt angle β - Turin - Source PVGIS.

favors an optimal yield in the summer months to the detriment of the winter ones. On the contrary, an angle β equal to 90°favors the winter months.

Therefore, in order to maximize the annual yield, the optimal tilt angle β will be between the two extremes: it will allow to obtain good performances during the winter months by only partially reducing those relating to the summer months, when usually even excesses of electricity production are obtained.

Finally, the minimum distance to be interposed between parallel rows of PV modules must be such as to avoid the phenomenon of shading. This calculation is made considering the data relating to the winter solstice, that is when the sun is characterized by a minimum solar height. The formula used is the following:

$$d_{min} = m \cdot \frac{\sin \beta}{\tan \alpha} \tag{2.40}$$

where:

β = tilt angle of the PV module

m = module length

P = footprint of the row of PV modules

α = solar height angle

h = vertical height of the PV module

d_{min} = minimum distance that must be guaranteed between the rows of PV modules to avoid the phenomenon of shading

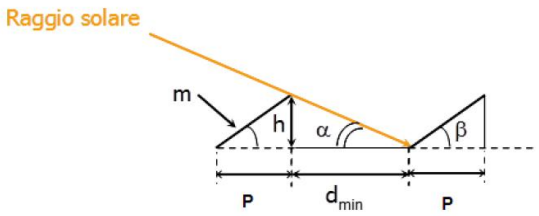

Figure 2.38: Minimum distance between two rows of PV modules.

For example, in the city of **Turin** ($\phi \approx 45°$), at the winter solstice ($\alpha \approx 21.55°$), considering a tilt angle $\beta \approx 38°$ and modules having a length of 1.660 m, the minimum distance between rows must be at least:

$$d_{min} = 1.660 \cdot \frac{\sin(38°)}{\tan(21.55°} \approx 2.59m \tag{2.41}$$

While the footprint of the same row of modules is:

$$P = m \cdot \cos\beta = 1.660 \cdot \cos(38°) \approx 1.3m \tag{2.42}$$

Therefore, each row of PV modules will occupy **3.89 m** ($P + d_{min}$).

Chapter 3

Power electronics conversion

3.1 DC-AC power converter (inverter)

The power control system consists of an electronic device called an inverter that transforms direct current into alternating current by controlling the quality of the output power for feeding into the grid also through an L-C filter inside the inverter itself [16] [18] .

It must be characterized above all by a particularly high conversion efficiency ($\eta > 90\%$) even at low loads and, therefore, have low no-load losses.

$$\eta_{inv} = \frac{P_{out}}{P_{in}} = \frac{V_{AC} \cdot I_{AC} \cdot \cos\phi}{V_{DC} \cdot I_{DC}} \tag{3.1}$$

where:

ϕ is the power factor and ϕ is the phase shift angle between voltage and current;

I_{DC} **and** I_{AC} is the current required by the inverter on the DC and AC side respectively;

V_DC **and** V_{AC} is the input voltage from the DC and AC side respectively.

Figure 3.1 shows the basic diagram of an inverter.

Where the main components are:

C_{rip} **capacitor** : used to compensate the fluctuation on the instantaneous power (single-phase system)

Inverter : controlled with PWM technique

L-C filter : aimed at obtaining a voltage waveform as sinusoidal as possible

Transformer : used to supply the voltage level required by the loads

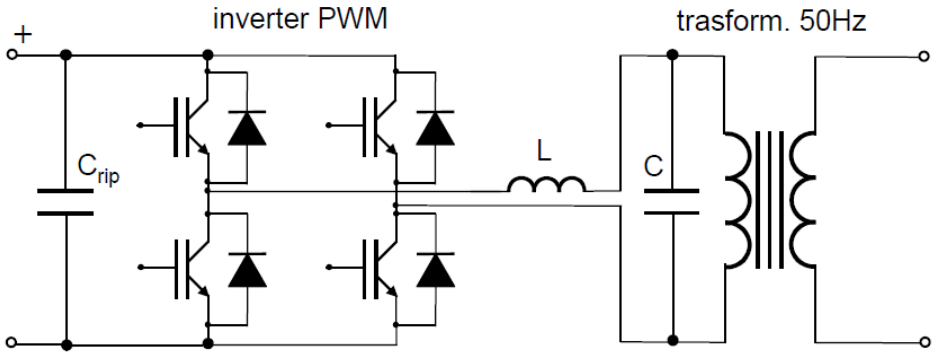

Figure 3.1: Principle diagram of a single-phase PWM inverter with low frequency transformer (50 Hz).

The transistors, used as static switches, are driven by an open-close signal which in the simplest, and therefore most economical form, would provide a square wave at the output.

To get as close as possible to a sine wave, the most sophisticated (PWM) technique is used, which allows to obtain an adjustment both on the frequency and on the effective value of the output waveform (figure 3.2).

3.2 Maximum Power Point Tracker

The power supplied by a PV generator depends on where it is operating. To optimize the energy produced by the system, the generator must be adapted to the load, so that the operating point always corresponds to that of maximum power [16].

For this purpose, a controlled chopper called **MPPT** is used in the inverter which identifies, moment by moment, the pair of voltage-current values of the generator for which the power supplied is maximum. Starting from the I-V curve of the PV generator:

The point of maximum power transfer corresponds to the point of tangency between the characteristic I-V for a given value of solar radiation and the hyperbola of equation $V \cdot I = const.$

The MPPT devices commercially used identify the point of maximum power on the curve characteristic of the generator causing small load variations at regular intervals that determine deviations in the voltage and current values, evaluating whether the new I-V product is greater or less than the previous one. If there is an increase, the load conditions continue to vary in the direction considered. Otherwise, the conditions are changed in the opposite direction.

If, for example, the load characteristic has the trend OA indicated in figure 3.3 , with irradiance G and temperature T, the MPPT to absorb the maximum power of the generator works at the input at voltage U_M and current I_M, while at the output, for supply this P_M,

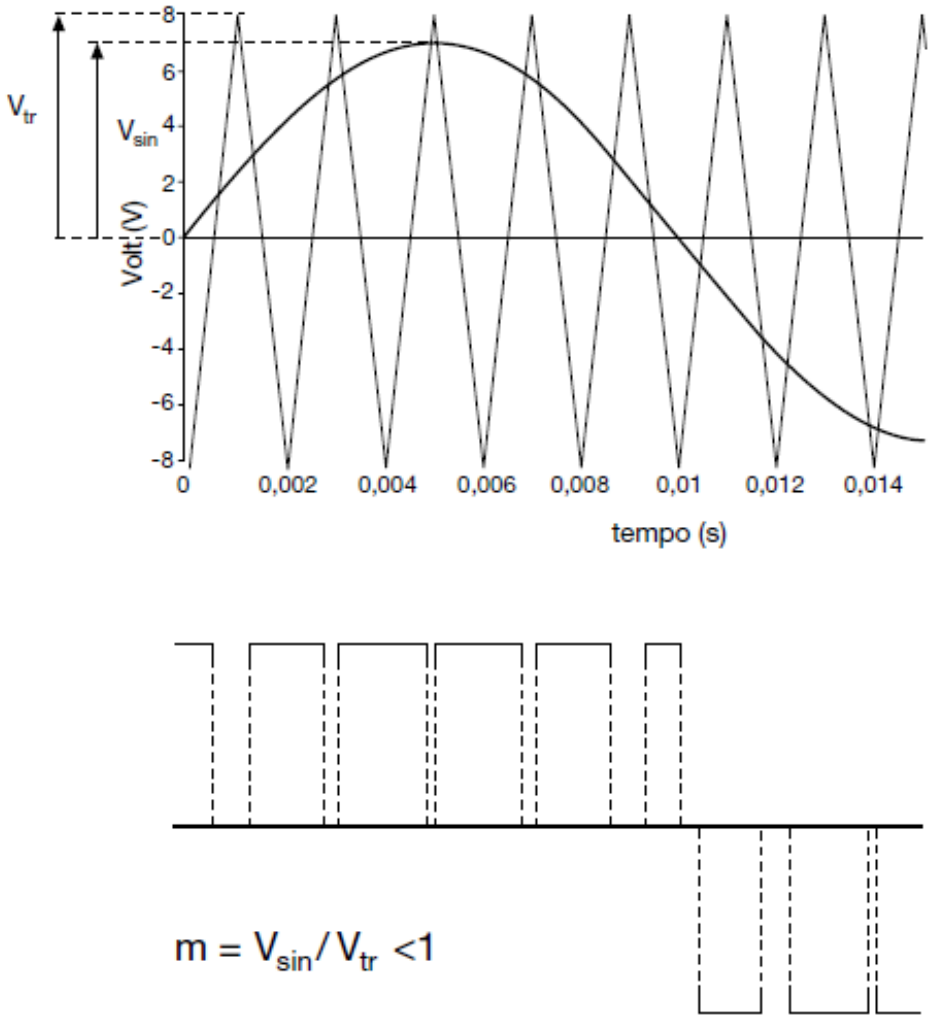

Figure 3.2: Principle of operation of the PWM technique.

must work at voltage $U'_M$and current I'_M, where $U'_M$and I'_M are the coordinates of M', the intersection point between the characteristic OA and the hyperbola at constant power, tangent in M to the characteristic of the generator (Unit yield MPPT). With reference to the voltage, this MPPT is called "step-down"; therefore an OB-type load characteristic requires a step-up MPPT; an OC-type characteristic requires a downward MPPT, for irradiance lower than G'and uphill for irradiance greater than G'.

The requirements of an MPPT are: pursuit of maximum power with efficiencies higher than 98%, within wide ranges of irradiance and temperature, and high reliability. In operation, the weak points, for the MPPT, are represented by the very fast variations (increasing or decreasing) of the irradiance or by the shading phenomena, concentrated

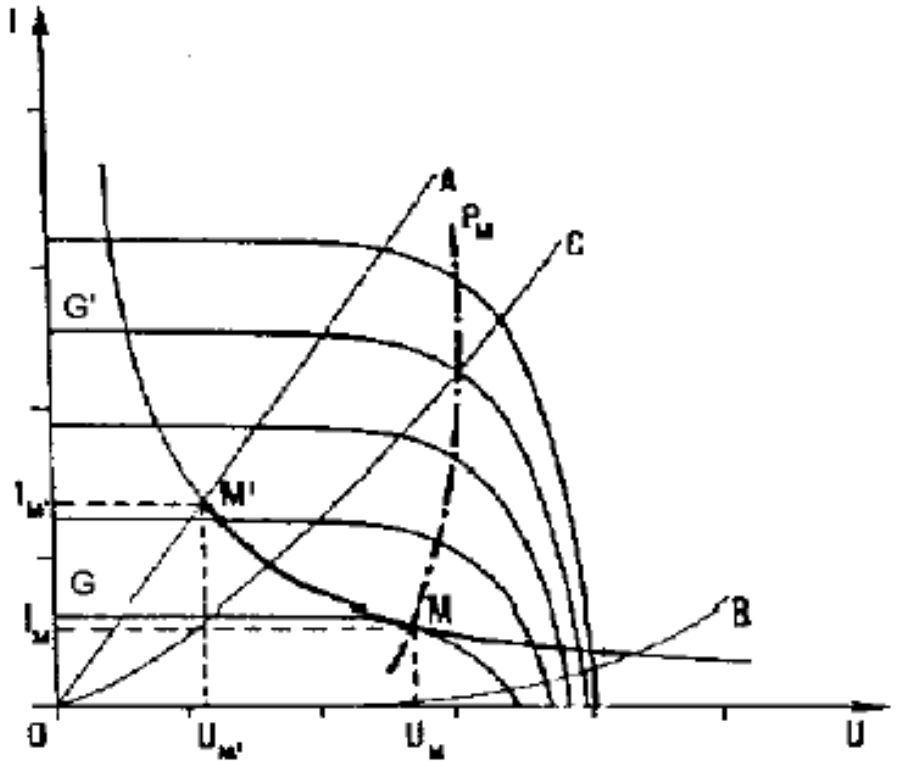

Figure 3.3: MPP maximum power point for a PV generator.

on part of the PV generator, which can determine a significant decrease in the maximum power voltage.

Due to the required performance characteristics, the inverters for stand-alone systems and for systems connected to the distribution network must have different characteristics:

- in **stand-alone** systems, the inverters must be able to supply a voltage on the AC side as constant as possible as the generation of the generator and the load request vary;

- in **grid-connected** systems, the inverters must reproduce, as faithfully as possible, the grid voltage, while trying to optimize and maximize the energy production of the PV panels.

The choice of the inverter and its size must be made on the basis of the nominal PV power that it must manage. The size of the inverter can be estimated by choosing the ratio between the active power fed into the grid and the nominal power of the PV generator between 0.8 and 0.9.

This ratio takes into account the decrease in power of the PV modules in real operating conditions (working temperature, voltage drops on the electrical connections) and the performance of the inverter itself. This ratio also depends on the installation conditions of the modules (latitude, inclination, ambient temperature) which can cause the generated power to vary. For this reason, the inverter is equipped with an automatic limitation of the power delivered to remedy situations in which the generated power is greater than that normally expected.

The inverter sizing features should include:

DC side

- rated and maximum power;
- rated voltage and maximum allowed voltage;
- MPPT voltage variation range in normal operation;

AC side

- nominal and maximum power that can be continuously supplied by the conversion unit, as well as the ambient temperature range at which such power can be supplied;
- rated current delivered;
- maximum current supplied that allows you to determine the contribution of the PV system to the short-circuit current;
- maximum voltage distortion and power factor;
- maximum conversion efficiency;
- efficiency at partial load and at 100% of the rated power;

It is also necessary to evaluate the nominal values of output voltage and frequency and the input voltage of the inverter.

3.3 DC-DC power converters

DC-DC converters are an essential part of the PV system in domestic and automotive applications. They usually perform two roles:

- Perform MPPT on the PV allray;
- Regulate the voltage prvided to the inverter.

For solar PV applications, these DC-DC converters are only required to support unidirectional power flow. Beyond this, there are some properties which are desirable for domestic solar PV applications:

- Low cost;
- Low input current ripple, to improve MPPT performance;
- Wide voltage conversion ratios (including both step-up and step-down), to provide flexibility in the number of series-connected panels, and to support a wide range of PV panel conditions (e.g. temperature has a significant impact on the MPPT voltage).

Other important characteristics of converters are: high efficiency, high stability. The DC-DC converters used for PV applications are the following:

- Buck/boost converter;
- buck-boost converter;
- isolated DC-DC converter;
- Ćuk converter;
- SEPIC converter.

In this application, only moderate voltage change ratios are needed as the series voltage of a solar PV string is similar to the DC voltage required by the grid-side inverter. A summarised comparison of the above DC-DC converters is provided in Table 3.1.

The component ratings for the converters are similar, so the primary factor influencing the cost of these converters is the component count, shown in Table 3.1. The primarily losses in non-isolated DC-DC converters are power electronic losses, inductor losses (eddy current and hysteresis), copper losses (inductor windings), and capacitor ESR losses.

The non-isolated converters in Table 3.1 all have an equal switch count so the power electronic device losses will be similar. For isolated converters, the additional switches and transformers cause higher losses and hence lower effciencies.

Converter	Voltage output	Input current	$\frac{V_{out}}{V_{in}}$	switches	diodes	inductors	capacitors
Buck/boost	Unipolar	Continuous	$\frac{1}{1-D}/D$	1	1	1	1
Buck-boost	Unipolar	Discontinuous	$\frac{D}{1-D}$	1	1	1	1
Isolated DC-DC	Carious	Various	Various	1-4	1-4	1-5	1
Ćuk	Unipolar	Continuous	$\frac{-D}{1-D}$	1	1	2	2
SEPIC	Unipolar	Continuous	$\frac{D}{1-D}$	1	1	2	2

Table 3.1: DC-DC converters used in PV applications.

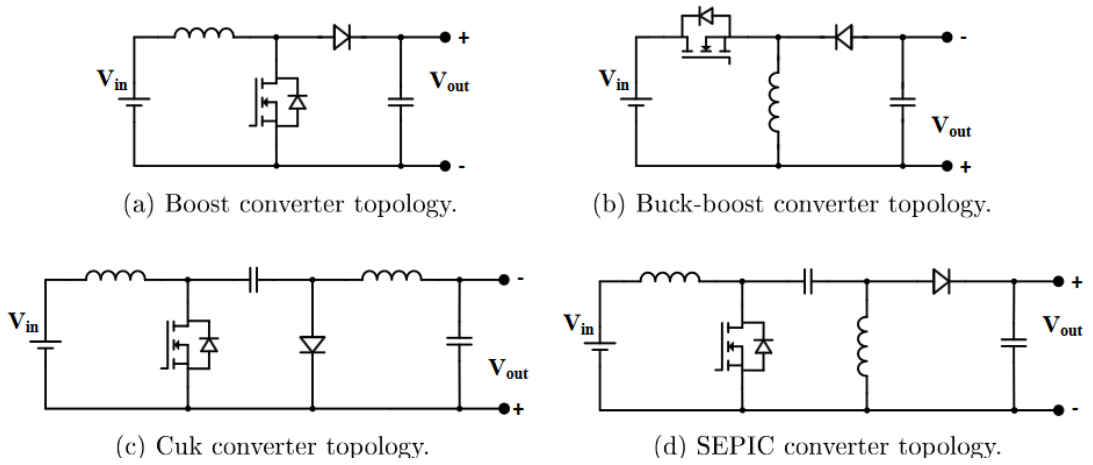

(a) Boost converter topology.

(b) Buck-boost converter topology.

(c) Cuk converter topology.

(d) SEPIC converter topology.

Figure 3.4: Layout of DC-DC converters commonly used in PV applications

3.3.1 Boost converter

As the name suggests, the standard boost converter (shown in Figure 2.12a) is capable of producing an output voltage which is higher than its input voltage. They have the lowest component count of the DC-DC converters, making them very cost effective. One drawback of this converter when compared with the others is the voltage conversion ratio, restricting the converter from providing a reduced output voltage and thus limiting its application flexibility.

3.3.2 Buck-Boost Converter

The single-switch buck-boost converter (shown in Figure 3.4) addresses the limitation of the boost converter by performing step-down voltage changes, into addition to step-up. One key difference is that the output voltage is inverted in polarity with respect to the input voltage. Buck-boost converters have the same low component count as the standard boost converter. The major drawback of this converter for solar PV applications is its discontinuous input current - necessitating a large decoupling capacitor to ensure smooth current flow from the PV array in order to operate close to the MPP.

3.3.3 Isolated DC-DC Converter

There are several isolated DC-DC converter topologies, including the forward, flyback, push-pull, isolated full bridge, and isolated half bridge. Most of these topologies are capable of providing both step-up and step-down voltage change ratios. The nature of the input current (continuous or discontinuous) and the size of the ripple are dependent on the topology. The number of active switching devices ranges from one to four, and the magnetics can range from a single inductor to four-winding transformers.

3.3.4 Ćuk Converter

The Ćuk converter is capable of both step-up and step-down voltage change ratios, though the output is inverted in polarity with respect to the input, as with the single-switch buck-boost converter. Unlike the buck-boost converter however, its input current is continuous, alleviating the need for a bulky decoupling capacitor between the PV array and the Ćuk converter's input. Another advantage of the Ćuk converter over the buck-boost converter is that the switch is ground-referenced, allowing a cheap, simple gate driver to be used. This converter does have a higher component count, with an extra inductor and capacitor required.

3.3.5 SEPIC Converter

The SEPIC converter shares many similarities with the Ćuk converter - both converters have the same component count, ground-referenced switch, voltage gain ratio, and continuous input current shape. The most notable operational difference between the two converters is the polarity of the output voltage: the SEPIC converter has a positive magnitude output voltage. Again, the size of the input current ripple may be problematic in solar PV applications, though the SEPIC converter's inductors may be coupled [19].

3.4 Estimation of energy productivity

In the design of a PV plant it is important to evaluate the electrical productivity as correctly as possible [15] [14] [13] . A formula that can be used is the following:

$$E_{AC} = H_g \cdot S_{PV} \cdot \eta_{STC} \cdot PR \left[\frac{kWh}{year}\right] \tag{3.2}$$

where:

- H_g = annual global irradiation on the inclined plane [kWh/m^2/year]
- S_{PV} = total area of the PV generator [$_m$2]
- η_{STC} = nominal efficiency of the modules []
- PR = "Performance Ratio", comparison parameter of PV plants []

Or:

$$E_{AC} = G_{STC} \cdot S_{PV} \cdot \eta_{STC} \cdot h_{eq} \cdot PR \left[\frac{kWh}{year}\right] \tag{3.3}$$

where:

- G_{STC} = irradiation in STC conditions (1000 W/m^2)

- h_{eq} = number of equivalent solar hours per year [h/year], which can be calculated as:

$$H_{eq} = \frac{G_g}{G_{STC}} \tag{3.4}$$

Various sources of leakage are included in the PR parameter. The main ones are:

- tolerance with respect to STC data and intrinsic mismatch of the current - voltage I-V characteristics of the modules;
- dirt and reflection of the front glass;
- solar spectrum different from the reference one (AM=1.5);
- wiring, blocking diodes, fuses and switches;
- overtemperature (or undertemperature) compared to 25 °C;
- non-uniform lighting on all modules (shading effect);
- MPPT and DC-AC conversion of the inverter.

The design value of the PR is therefore between 0.55 and 0.85.

Chapter 4

Energy storage

Electricity, as known, does not lend itself to being easily accumulated and, generally, must be produced at the same time it is requested by the user.

But with the development and consequent use of renewable energies as a source of electricity, it was necessary to develop technologies and strategies for using the accumulations, given the **random availability** of many of these sources **NPRS**. The presence, therefore, of storage systems expressly designed to cope with the non-programmable nature of the contribution of many renewable energies is and will be indispensable for the correct management of the entire electricity system (stabilizes the voltage and frequency of the grid), increasing its efficiency and reliability. If, then, we focus on **hybrid systems**

not connected to the electricity grid ("stand alone"), the accumulation of electricity is a fundamental requirement: it allows, in fact, to store the quantity of excess electricity for the immediate needs of consumption and then make it available when the generation plant is partially or totally inactive and, therefore, unable to satisfy the load (for example in the case of little or no solar radiation and / or wind). Therefore, it is avoided to oversize the generator system and the operating hours of the back-up generator set (and the related fuel consumption) are minimized. Therefore, the storage system can be seen as an effective

tool to be integrated with the hybrid generation plant based on NPRS to improve and optimize the management of the energy produced and that absorbed by the load.

The electrical storage systems can therefore be defined as systems that store electrical energy by converting it into another form of energy (electrochemical, mechanical, electrical, chemical and thermal).

The first and, in some ways, more general classification among electrical storage technologies is therefore based on the methods of energy conversion. **Electrochemical accumulators** (lead-acid batteries, lithium, etc.) convert electrical energy into chemical energy. The **mechanical accumulation** includes compressed air accumulation systems (CAES), high and low speed mechanical flywheels, water pumping. The **electrical storage** consists of capacitors, supercapacitors, SMES. **Chemical accumulation** is characterized

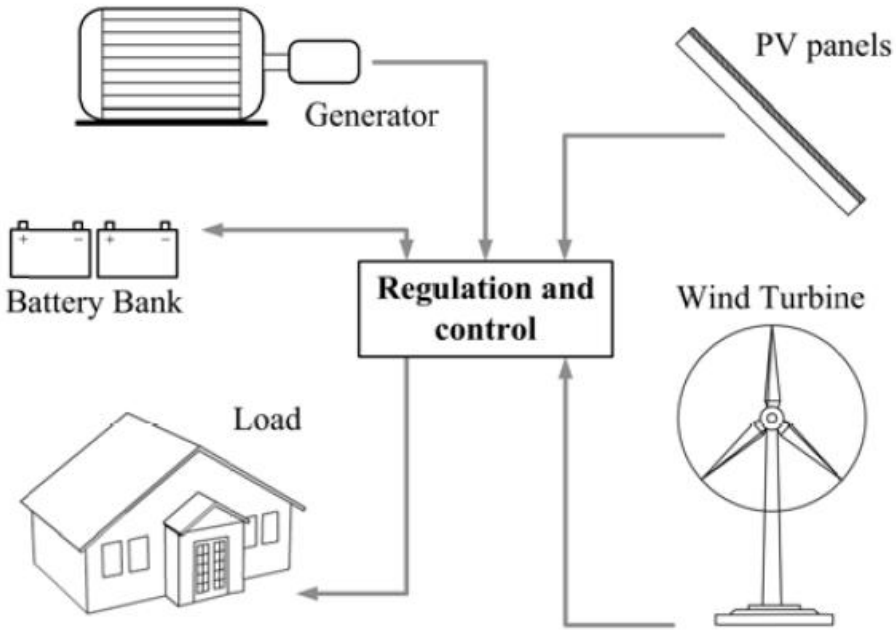

Figure 4.1: scheme of an NPRS hybrid plant.

by fuel cells through which hydrogen (fuel) is produced while **thermal accumulation** allows the storage of thermal energy. A second classification is based on the working methods and performances that characterize the technologies. There are therefore systems that work "**in energy**", capable of delivering powers with autonomy of a few hours, typical of peak-shaving applications or in coupling with renewable sources generators, and systems that work "**in power**", capable of deliver strong power for short times (from fractions of a second to a few tens of seconds) with very fast response times, suitable for *Power Quality* applications. Figure 4.2 shows, for the various categories identified, the main technological

alternatives existing and in the industrialization phase [20] [13] .

In hybrid NPRS off-grid systems, usually characterized by medium / small power (« 1 MW), electrochemical accumulators represent the most widely used technology as they generally have good performances both in terms of autonomy and response time and offer intermediate performances in terms of relationship between power offered and energy that can be stored as well as economically advantageous prices and extended useful life.

4.1 Electrochemical storage

Electrochemical accumulators, or *secondary cells*, are a sub-category of the so-called "stationary electromotive force generators", which also include primary cells (common

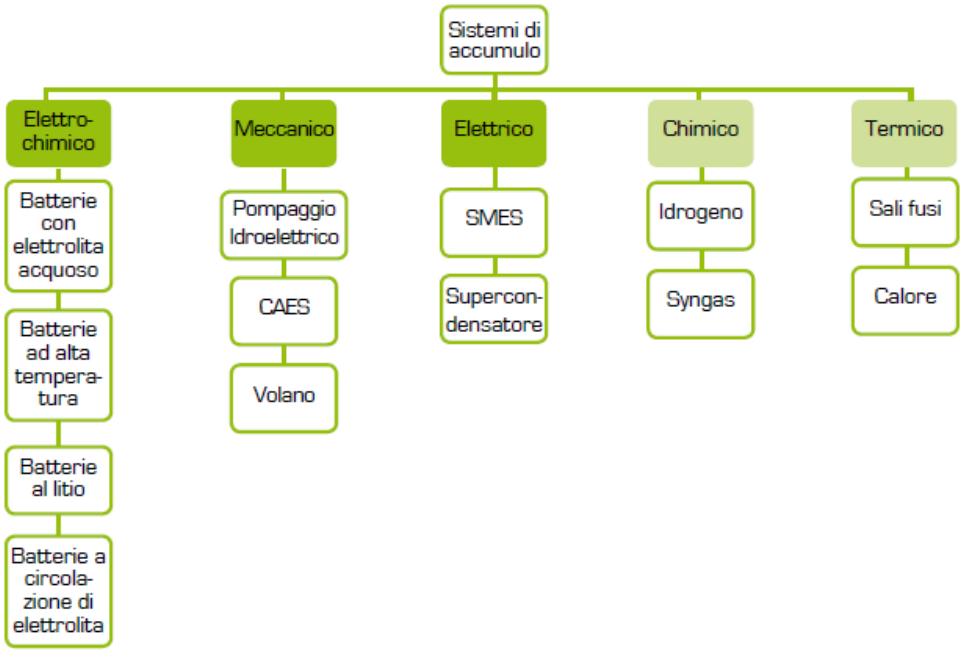

Figure 4.2: Classification of technologies for storage systems.

cells) and fuel cells [20] [21] .

Unlike primary batteries, secondary batteries are **rechargeable**, meaning the process of direct transformation of chemical energy into electrical energy is reversible. This allows the accumulation of electrical energy in the form of chemical energy, making it available at the right time.

The batteries consist of the combination, in series and / or parallel, of a certain number of electrochemical accumulators. Each of them generally consists of a structure composed of two half-cells separated by a porous septum, each of which contains a metal **electrode** (anode and cathode) immersed in an **electrolytic solution** (which typically contains ions of the same metal). The "ideal" operating principle through which an electrochemical accumulator allows the release and storage of electrical energy refers respectively to the **redox** and **electrolysis** reactions.

The first is realized in the fact that one electrode (**anode**) oxidizes, yielding electrons, while the other electrode (**cathode**) is reduced, acquiring the electrons lost from the first: through a conductor, this flow of electrons is intercepted, thus obtaining electric current . The second reaction, electrolysis, allows the system to be returned to its initial status: by applying an electric field from the outside, electrical energy is transformed into chemical energy.

The invention of the modern battery is the result of experiments conducted by the Italian physicist **Alessandro Volta**. He announced his discovery in a communication dated

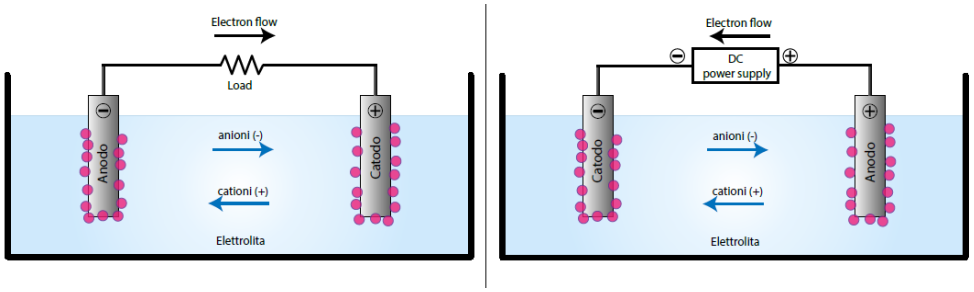

Figure 4.3: Diagram of an electrochemical accumulator during the discharge (left) and charge (right) process.

March 20, 1800 addressed to the president of the *Royal Society of Chemistry in London, Sir Joseph Banks* [20] . The different types of existing electrochemical accumulators, which

are at a different stage of technological development, are characterized by the material of which the electrodes and the electrolytic solution are made, as well as by the construction characteristics.

In particular, four main sub-categories can be identified, to each of which different variants belong:

- Accumulators with aqueous electrolyte
- High temperature batteries
- Lithium batteries
- Electrolyte circulation batteries

Finally, it is important to underline that the duration and functioning of electrochemical accumulators also depend on their correct use. It is important to prevent the batteries from being overloaded by the generator system, and by excessive withdrawal by the user. To this end, a **charge controller** is essential, an electronic device that serves to control and regulate the minimum and maximum charge level of the batteries, thus increasing their useful life (the storage system represents an important percentage of the investment). The actual operation of an electrochemical accumulator involves, in addition to the two

main reactions of oxidation-reduction and electrolysis, other secondary or "parasitic" reactions, which represent a negative phenomenon since they degrade the performance of the accumulator over time. For example, in electrochemical accumulators one of the best known parasitic reactions is the **gasification reaction** that takes place in the final phase of recharging for accumulators with aqueous electrolyte (lead / acid, nickel / cadmium, nickel / metal hydrides). The reaction is triggered when the gasification voltage is exceeded, which starts the electrolysis reaction of the water of the electrolyte producing hydrogen at the negative electrode and oxygen at the positive. The consequences of this parasitic

reaction are first of all the reduction of the recharging efficiency of the accumulator (which is not unitary, since a part of the recharging current is used in the parasite reaction), the consumption of the electrolyte water and the production of gases that can form potentially dangerous mixtures.

Even the self-discharge of an accumulator, or the discharge that occurs when the accumulator is at rest, is due to various parasitic reactions that slowly consume the charges present and lead to complete discharge over time. The extent of self-discharge varies depending on the type of accumulator; for example, in the lead-acid battery the self-discharge has a value equal to approximately 2-3% of the capacity per month. The

figure below shows a comparison between the main electrochemical pairs in relation to their most important characteristics.

Categoria	Coppia elettrochimica	Costruttori Sviluppatori	Stadio di sviluppo	Energia specifica		Efficienza conversione	Apparato di gestione	Rischi sicurezza	Costo materie prime
				Wh/kg	Wh/l				
Temperatura Ambiente Elettrolita acquoso	Piombo acido Pb	a livello mondiale	industriale consolidato	30	80	75%	normalmente non usato	accettati	medio basso
	Nichel-Cadmio Ni-Cd	a livello mondiale	industriale consolidato	50	60	60%	normalmente non usato	accettati	medio
	Nichel-Idr.Met Ni-MH	a livello mondiale	industriale consolidato	60	65	70%	controllo della carica	accettati	alto
	Nichel-Zinco Ni-Zn	a livello pre-indust.	limitato	70	70	60%	controllo della carica	accettati	medio
Litio	Li-Ioni	a livello mondiale	industriale su taglie piccole	150	200	90%	complesso	(instabilità termica)	molto alto
	Li-Ion Polimeri	a livello mondiale	industriale su taglie piccole	130	180	90%	complesso	limitati	molto alto
	Li-Metal	a livello preindustr.	sviluppo	180	150	90%	molto complesso	presenti	molto alto
	Li-Metal	Canada	avviata ma interrotta	120	120	88%	molto complesso	presenti	molto alto
Celle alta temperatura	Sodio-Zolfo Na-S	Giappone	industriale limitato	120	140	85%	complesso	presenti	medio
	Sodio-Clor.Met Na-$NiCl_2$	Svizzera	industriale limitato	120	120	85%	complesso	limitati	medio

Figure 4.4: Comparison between the different electrochemical pairs.

4.2 Reference parameters and characteristics

Electrochemical accumulators are characterized by a series of quantities that describe their behavior in quantitative terms and which are necessary to compare technologies of different types.

Capacity [Ah]: is the quantity of electric charge that can be extracted from the system during discharge until the minimum voltage value is reached. In most electrochemical accumulators the capacity is not a constant parameter, but depends on the regime, i.e. on the discharge current and on the working ambient temperature (at very low temperatures the electrolyte can freeze, undermining the performance of the battery, while on the contrary, by raising the temperature, the performance increases). It is

obtained from the product between the discharge current [A] and the time [h] elapsed until the final discharge voltage (cut-off) is reached. This is because the battery during the discharge phase typically lowers its voltage value up to the cut-off value.

$$C_t = \int_0^t I(t) \cdot dt[Ah] \tag{4.1}$$

As far as time is concerned, on the datasheets of the electrochemical accumulations, standard reference values are used which vary according to the type of battery and set by European regulations.

For example, considering a battery with a capacity of 100Ah:

- C / 10 or C_{10}: the battery delivers 10 A for 10 h.
- C / 5 or C_5: the battery delivers 20 A for 5 h.
- 2C: the battery delivers 200 A for 30 minutes.

Specific capacity : it is the accumulator capacity per unit of mass $[\frac{Ah}{kg}]$ or per unit of volume $[\frac{Ah}{dm^3}]$.

State Of Charge - SoC [%]: is the amount of charge present in the accumulator, compared to a reference value, very often coinciding with the nominal capacity, expressed as a percentage.

$$SoC = \frac{available charge[Ah]}{nominal charge[Ah]} \tag{4.2}$$

Depth of Discharge - DoD [%]: is the amount of charge delivered by the accumulator compared to a reference value, very often coinciding with the nominal capacity, expressed as a percentage.

$$DoD + SoC = 1 = 100\% \rightarrow DoD = 1 - SoC \tag{4.3}$$

Nominal energy [Wh]: is the energy that the system provides during discharge, starting from a fully charged condition up to complete discharge, and is given by the product of the capacity times the battery voltage. This parameter also depends on the working regime and the ambient temperature.

$$E = C \cdot U[Wh] \tag{4.4}$$

Power [W]: is the product of the current I [A] supplied by the corresponding voltage U [V]. The power that can be delivered by an electrochemical accumulator cannot be defined univocally, since it depends on the load applied, but it is useful for each accumulator to define a nominal power, i.e. the power corresponding to the discharge rate sufficiently representative of the operating rate at which the battery is destined, and the peak power at 30 seconds, defined as the power that the accumulator is able to sustain for 30 seconds with a DoD value of 80% (i.e. with an almost discharged battery).

Specific energy [$\frac{Wh}{kg}$ and energy density [$\frac{Wh}{l}$]]: are obtained by relating the energy that can be stored in the accumulator respectively to the weight and volume occupied by the same.

Specific power [$\frac{W}{kg}$ and power density [$\frac{W}{l}$]]: are obtained by relating the power of the accumulator to the weight and volume occupied by the same, respectively.

Energy efficiency [**-**]: it is defined as the ratio between the energy discharged and that spent to restore the storage system to its initial state of charge.

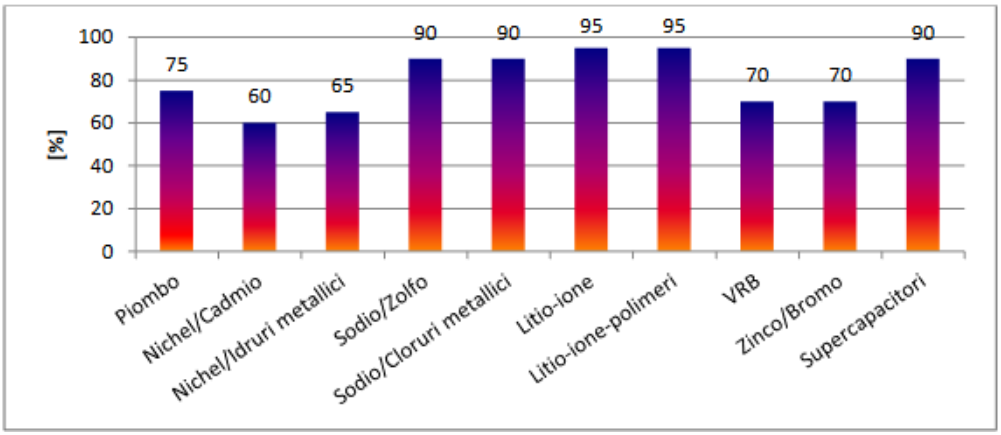

Figure 4.5: Energy efficiency of some storage technologies.

Amperor-metric efficiency [**-**]: is defined as the ratio between the quantity of charge, measured in Ah, delivered during the discharge and the quantity necessary to restore the initial state of charge. This parameter has a unitary value for some electrochemical accumulators (sodium / sulfur, sodium / nickel chloride, lithium / ions), while for many others, such as lead, due to parasitic reactions that occur during recharging, it has a value that is not constant and less than unity. A unitary amperor-metric efficiency significantly simplifies the management of the accumulator, because it allows you to measure the state of charge simply by integrating the charge / discharge current.

Life time [**years**]: means the overall operating time of the accumulator, which ends when the system performance degrades below the operating limits (for example, when the capacity is reduced by a predetermined percentage). The life span of an accumulator strongly depends on the working methods and is drastically reduced if it is subjected to incorrect management and if the accumulator works at a high temperature.

Life time [**cycles**]: represents the number of discharge cycles (up to a predetermined percentage of DoD) and full charge that a battery is able to complete before its performance drops below a minimum limit (typically before its capacity is reduced by 20%). The value changes according to the DoD value chosen, the typical working

regime and the working temperature; typically the number of cycles at 25 °C with 80% DoD is taken as a reference value.

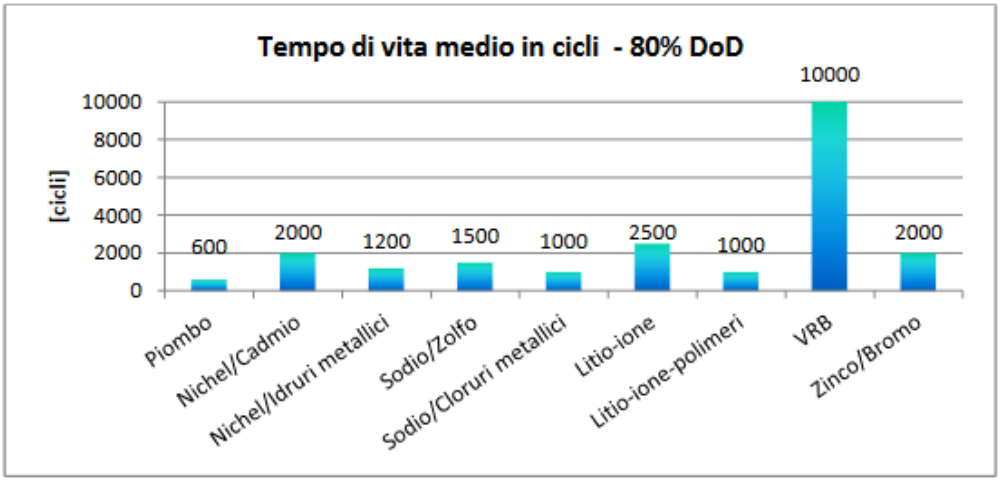

Figure 4.6: Life span expressed in cycles of various batteries.

Temperature [°C]: temperature range of the external environment within which the accumulator is able to work. The temperature at which it works has significant effects on the capacity and wear of the battery. In fact, the operation of the batteries is based on chemical reactions and these tend to slow down with lower temperatures (the electrolyte becomes more viscous and the speed of the ions decreases). Optimal usage temperatures vary between various battery types; generally 25 °C is the standard operating temperature for all types of battery, but there are no major differences in performance for temperatures between 20 °C and 40 °C.

Memory effect : the memory effect means that phenomenon in which certain batteries, such as Ni-Cd batteries, after having been repeatedly charged following a partial discharge, tend to replace the value of their capacity with that related to partial discharge, thus altering its performance. This characteristic is linked to an alteration of the internal materials. Fortunately, this alteration can in some cases be rewarded by a series of complete discharge and charge cycles.

Self-discharge : If left unused, batteries lose their stored charge over time, this phenomenon is called self-discharge (or even charge retention) [20] . This is also referred to as the rate of lost capacity per unit of time, usually months or years. The effect may also not be linear, neither with respect to the time elapsed nor with respect to the capacity stored at the time it is left inert. Self-discharge may be mainly due to several factors:

- Corrosion effects between electrode and electrolyte contact;
- Impurities in the electrolytes or in the electrolyte;
- Insulation defects between anode and cathode;

- High internal resistance;

Among the phenomena that tend to worsen the self-discharge phenomenon are in particular:

- Charging too fast;
- Low charge when left unused.

Clearly this phenomenon must be countered, this is done by keeping the accumulator constantly under charge with a low current, which is therefore sufficient to keep the charge level constant

4.3 Technologies for electrochemical storage

In this paragraph, the most important electrochemical battery technologies are described. More attention will be given to two technologies in particular, lead / acid and ion / lithium, as they are currently the most used in hybrid off-grid systems. For further information on the various electrochemical accumulator technologies, refer to the document [20] [13] [14] Reported in the bibliography.

4.3.1 Lead-acid batteries

Electrochemical batteries are the most conventional technology for the accumulation of electrical energy [20] [13] [14] . Although several electrochemical pairs are available on the market, lead acid batteries, due to their energy characteristics (energy density, power density) and their low costs, represent the most adopted solution for electrochemical storage both in industrial applications and in the distributed generation.

Their success is essentially due to the low cost and wide availability of lead, as well as a relatively simple and now established manufacturing technology. Finally, there are the advantages of good reliability and widespread and well-established service and recycling infrastructures. On the other hand, they have several negative aspects, such as a fairly low expected life, a not excessively high energy and power density, which results in the need for a large surface footprint, the need to install adequate ventilation systems since during the charging phase hydrogen production can occur at the terminals. Furthermore, one of the most critical aspects in the management of a lead-acid storage battery is linked to the fact that the amperometric efficiency is lower than the unit, and this considerably complicates the measurement of the state of charge. The unit cell of a lead accumulator consists of a

negative lead metal electrode and a positive lead dioxide electrode, while the electrolyte is an aqueous solution of sulfuric acid, about 37 % by weight, with high ionic conductivity .

During the discharge, the lead oxidizes at the negative pole, releasing electrons and forms insoluble crystalline lead sulphate ($PbSO_4$) by reaction with the sulphate anions (SO_4^-) of the electrolyte. At the positive pole, crystalline lead dioxide is reduced by

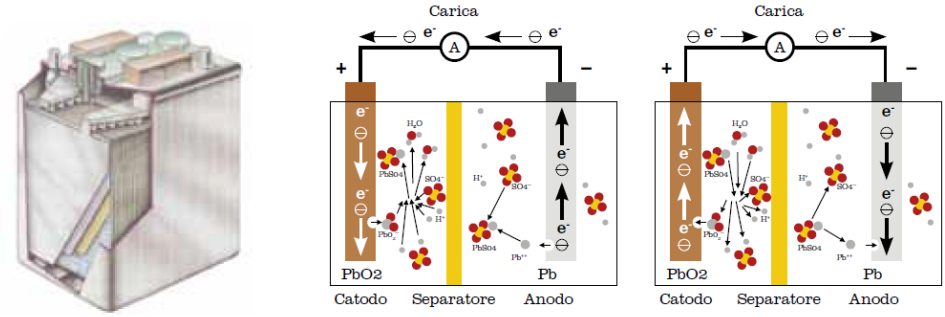

Figure 4.7: Lead / acid cell and charge and discharge reactions.

acquiring electrons and forming lead sulphate, also in this case by reaction with the electrolyte. Therefore, progressive transformations of both electrode materials occur, with profound changes in their crystalline structure, and the formation of lead sulphate and water, which reduces the density of the electrolyte. The reactions to the two electrodes are:

Positive side

$$PbO_2 + 4H^+ + SO_4^{--} + 2e^- \leftrightarrow PbSO_4 + 2H_2O \tag{4.5}$$

Negative side

$$Pb + SO_4^{--} \leftrightarrow PbSO_4 + 2e^- \tag{4.6}$$

which are summarized in the overall reaction:

$$PbO_2 + 2h_2SO_4 + Pb \leftrightarrow PbSO + 4 + 2H_2O + PbSO_4 \tag{4.7}$$

In this type of accumulator, the measurement of the electrolyte density can be used as an index of the state of charge.

During charging, the reactions described proceed in the opposite direction, the active materials Pb and PbO_2 are restored at the expense of the sulphate and the initial concentration of sulfuric acid is re-established. In addition to the main reactions, some parasitic reactions occur, among which the most important is the gasification reaction which takes place in the final phase of recharging. This reaction results in a reduction in recharging efficiency, the consumption of electrolyte water and the production of gases that can form potentially explosive mixtures.

The electromotive force of the lead / acid cell is nominally 2 V. Its actual value actually depends on the temperature and concentration of the reactants and reaction products.

Description of technology and performance

An elementary cell consists of a certain number of positive electrodes connected to each other, alternating with negative electrodes, also connected to each other, with the interposition of a suitable separator between each pair. In practical realizations, to optimize the size and weight, several elementary cells are often installed in a single container, electrically connected in series, which create monoblocks with a nominal voltage typically equal to 12 or 24 V. The design of the unit cell and the cell geometry influence the performance of the accumulator.

The electrodes can be "flat plate", in which the active material is a spongy paste spread on a metal grid generally made of lead with added calcium or antimony to obtain greater mechanical resistance, more rarely in pure lead; or "tube", in which the elementary component is a tube containing the active material, crossed by a thin lead wire for the supply of current.

There are therefore many types of accumulators, which can be grouped into two main categories:

- open accumulators, or VLA
- hermetic accumulators, or VRLA

VLA accumulators, still the most popular, are characterized by the presence of an opening that allows the release of hydrogen and oxygen produced during the parasitic reactions in charge. These accumulators are widely used in stationary and traction applications. In open-type accumulators, periodic topping up of the water contained in the electrolyte is required, which is consumed by evaporation and electrolysis. If subjected to proper management and regular maintenance, these batteries can have an expected life of up to 20 years. However, they require a large surface area with appropriate support racks, in environments equipped with ventilation systems to avoid the risk of the formation of thundering mixtures. In VRLA accumulators, the hydrogen produced on the negative plate is conveyed towards the positive where it recombines with oxygen, reconstituting water.

Hermetic accumulators are now widely used thanks to some advantages that characterize them, such as the fact that they require less maintenance, less space and to emit limited quantities of hydrogen, thus requiring less burdensome ventilation measures.

Over time, several limitations of this technology have been highlighted. The main ones are:

- the strong constructional inhomogeneity, which is a problem in installations consisting of numerous elementary accumulators connected in series and in several branches in parallel, complicating their management both in discharge and in charge.
- the gases produced recombine completely only up to a certain value of the recharge current, beyond which part of them is evacuated into the external environment

through the safety valves. This gas loss involves a gradual consumption of the electrolyte (dry out) and results in an abnormal degradation of the battery.

In VRLA, the recombination reaction is exothermic and is favored by the increasing temperature, therefore they can be the site of the phenomenon - as characteristic as it is dangerous - of thermal runaway which, if not interrupted, ends with the destruction of the accumulator. It is therefore important during installation to position the various accumulators so that their ventilation is favored.

For these aspects, the life span of hermetic accumulators is significantly lower than open ones. Although the lead-acid battery has reached a good technological and commercial maturity, research activities are still underway to improve performance. In particular, we try to increase the life time of the battery by studying new types of electrodes, on the estimation of the state of charge of the battery and on the development of management systems (BMI) and diagnostics to simplify and improve battery management.

Parametro	Valore Tipico	Commento
Tensione nominale [V]	2	
Capacità delle celle in commercio [Ah]	1 ÷ 10.000 Ah	
Potenza specifica [W/kg]	20 ÷ 40 70 ÷ 80	Per gli accumulatori VLA Per gli accumulatori VRLA
Energia specifica [Wh/kg]	15 ÷ 25 20 ÷ 40	Per gli accumulatori VLA Per gli accumulatori VRLA
Efficienza energetica [%]	70 ÷ 85	
Efficienza amperorametrica [%]	80	Non è unitaria a causa delle reazioni parassite in fase di carica e il suo valore non è costante ma dipende dalle modalità di carica
Autoscarica mensile [%]	1÷2	
Vita attesa DoD 80% [cicli]	800	

Figure 4.8: Typical performance parameters of lead / acid cells.

4.3.2 Lithium-ion battery

One of the most promising electrochemical storage technologies is represented by lithium batteries, which have had a very rapid development in recent years, partly driven by the possibility of use for powering electric vehicles and which is now testing the first applications also in the stationary. A lithium / ion battery is composed of thin layers constituting the cathode, the separator and the anode, immersed in an electrolyte that allows the transport of lithium ions [20] [21] .

In a lithium / ion battery the cathode is usually made up of a lithium oxide of a transition metal ($Li(TM)O_2$ with $TM = Co, Ni, Mn$), which guarantees a layered or

tunnel structure where the lithium ions can be inserted and extracted easily . The anode is generally made of graphite in the lithiated state, Li_xC_6 ($0 < x < 1$) in which each atom is bonded to three others in a plane composed of hexagonal rings fused together and which, thanks to the delocalization of the electronic cloud, conducts electricity . The electrolyte is typically composed of lithium salts, such as $LiPF_6$, dissolved in a mixture of organic solvents (dimethyl and ethylene carbonate) and the separating membrane is normally made of polyethylene or polypropylene. In polymeric electrolytes, the liquid electrolyte is melted into a host polymeric matrix to form a gel, ensuring the same performance as the liquid electrolyte but with a higher degree of intrinsic safety.

Current collectors are generally made of metals that do not have to react with the electrolyte and are usually copper for the anode and aluminum for the cathode.

In all lithium batteries, during the redox reactions associated with the charging and discharging processes, the lithium ions migrate reversibly from one electrode to the other.

When the cell is completely discharged, all the lithium present is contained in the cathode. During the charging process of the accumulator, the lithium ion is extracted from the metal oxide constituting the cathode and transferred to the anode, while the electrons migrate from the cathode to the anode through the external circuit and the metal of the cathode is then oxidized. At the anode, the charging process determines the trapping of the lithium ion, which is reduced to lithium in the graphite matrix acquiring the electrons from the external circuit. During the discharge, the lithium intercalated in the graphite matrix oxidizes releasing the electrons to the outside, while the lithium ions migrate through the electrolyte to the cathode, which is reduced.

During the first charge cycle, in addition to the transfer of lithium ions into the graphite, a passivating layer is also formed between the electrolyte and the negative electrode, called SEI, and composed of oxides, hydroxides, carbonates and fluorides. This layer is important for battery performance as it affects the number of cycles, capacity and safety. The following figure shows the structure of a cylindrical lithium cell and the charging mechanism and discharge for a cell with $LiCoO_2$ cathode, graphite anode and liquid electrolyte.

Regime di scarica tipico [C rate]	**C/10** **C/3**	Per applicazioni stazionarie Per applicazioni di trazione
Massima corrente in scarica e in carica [C rate]	**10C in scarica** **C/4 – 1C in carica**	In carica il superamento della tensione di gassificazione porta alla produzione di idrogeno e al consumo d'acqua, molto dannoso per le batterie ermetiche
Intervallo di temperatura di lavoro	**-20 ÷ 60 °C quando la batteria è carica** **0 ÷ 60 °C quando la batteria è completamente scarica**	Quando la batteria è scarica la temperatura minima di lavoro è di 0 °C perché l'elettrolita è composto quasi completamente di acqua
Ausiliari	**Necessario un sistema di ventilazione con portata d'aria adeguata per evitare l'accumulo di idrogeno nel locale**	

Figure 4.9: Cylindrical lithium / ion cell and charge and discharge reactions.

Description of technology and performance

The lithium / ion cells have a structure consisting of overlapping layers, which allows the simplification of the production process. The electrode materials are diffused on a thin metallic substrate which also constitutes the collector for the current. The cells with liquid electrolyte can be made with a cylindrical, prismatic, button structure, while the polymeric cells are flat.

Polymer electrolyte cells have a structure consisting of very thin and often foldable flexible sheets (polymer laminate), which allow for a simple and prospectively less expensive manufacturing process.

Lithium / ion batteries are a family of electrochemical accumulators that differ from each other as well as for the electrolyte technology, liquid or polymeric, also for that of cathode and anodic materials.

The different combinations of electrodes and electrolyte give rise to a multitude of possible variants, each of which is better suited for certain applications. Figure 4.10 shows some of the main cells that use this technology, highlighting the characteristics that distinguish it, from which a clear trade-off emerges between the maturity of the technology (and relative performance) and the level of security guaranteed by the solution itself.

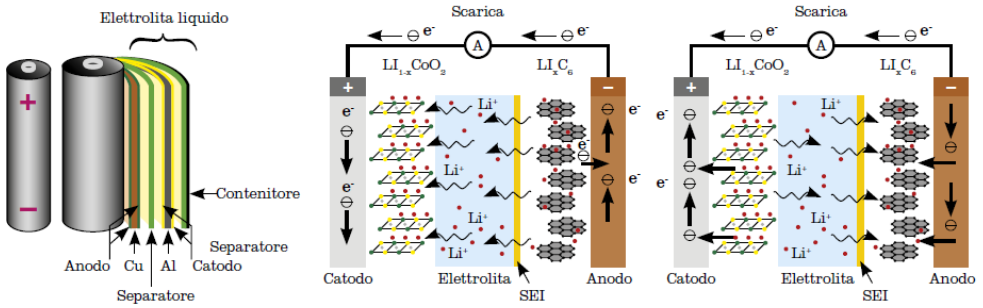

Figure 4.10: Characteristic parameters of the main cells using lithium-ion technology (Source: RSE).

The most used cathode material in the past, and the first to be used, was $LiCoO_2$, which has a good capacity to store lithium ions, adequate chemical stability and good electrochemical reversibility. However, this material is critical when overloading of the cell occurs, which can lead to the collapse of the structure of the material with consequent release of a large amount of heat. In addition, the mild toxicity and the high cost of cobalt has resulted in recent efforts to seek better alternatives.

For this purpose, cathodes made of mixed oxides with three transition elements based on nickel / cobalt are now produced to improve stability and reduce costs, which allow for higher performance than cobalt oxide at significantly lower prices. Although these materials are safer than cobalt oxide, it is still necessary to increase the safety level of the positive electrode.

Another type of cathode is made up of lithium / manganese compounds (LiMn2O4) which have a greater thermal stability than nickel / cobalt and therefore a higher safety but similar characteristics in terms of work cycles.

In recent years, the use - as a cathode material - of $LiFePO_4$, also called LFP, has taken up more and more space, by virtue of its low cost and the greater safety offered compared to other types of metal oxides, as a consequence of the low electrochemical potential.

Unfortunately, this technology has the drawback of having a reduced ionic conductivity, which leads to a lower flow of lithium ions and therefore a greater internal resistance. The increase in the ionic conductivity of the electrode is however carried out through various techniques, such as the doping of the oxide using elements such as rare earths, the realization of nano-structured oxides and, lastly, the coating of the entire electrode with atoms of carbon.

The anodic material most used in lithium batteries is carbon in the allotropic form of graphite, since it allows to obtain a capacity close to that of metallic lithium.

In recent years, batteries with $Li_4Ti_5O_{12}$, also called LTO, are spreading, which guarantee greater tolerance to overcharging phenomena. The absence of parasitic reactions with the electrolyte, by virtue of the high electrochemical potential, guarantees the lack of formation of the SEI, which in traditional cells with carbon anode constitutes a limit to the number of life cycles, at the maximum charging power and at the working temperature. For these reasons, $Li_4Ti_5O_{12}$ offers advantages from the point of view of charging time and life cycles compared to carbon compounds, but results in a lower working voltage and therefore a lower specific energy than traditional cells with graphite anode.

The main feature that distinguishes this technology refers to the **high specific power**, significantly higher than other electrochemical storage technologies, hence that this technology is particularly suitable for "power" applications. On the other hand, the specific energy is important and flexibility in terms of discharge rate make this technology “transversal”, i.e. also suitable for “energy” applications.

Finally, it should be noted that lithium / ion cells can give rise to dangerous situations if subjected to electrical and / or thermal overload conditions, hence the need to use a cell voltage balancing system and a BMS that monitors the cell and battery sizes and intervenes in the event of abnormal.

4.4 Charging controllers

In systems characterized by low peak powers required by the load, systems defined as charge regulators are applied to control the entire energy flow circulating between the PV field, storage system and load [22] .

The typical functions performed by the charge controller are aimed at managing the charging processes e discharge of the storage system, avoiding deep discharges and overloads

	NCA	NMC	LMO	LFP	LTO
Tensione nominale (V)	3,7	3,7	3,7	3,3	2,2
Tipo di catodo	$LiNiCoAlO_2$	$LiNiCoMnO_2$	$LiMn_2O_4$	$LiFePO_4$	$LiMn_2O_4$
Tipo di anodo	C	C	C	C	$Li_4Ti_5O_{12}$
Potenza (W/kg)	Alta	Buona	Media	Media	Media/Bassa
Energia (Wh/kg)	Alta	Alta	Buona	Media	Bassa
Vita cicli	Buona	Buona	Media	Media	Alta
Vita calendario	Buona	Buona	Bassa	Bassa per T>30 °C	Buona
Livello di sviluppo	Matura	Crescita/Matura	Matura	Crescita	Crescita
Sicurezza catodo	Bassa	Bassa	Media	Buona	Media
Sicurezza cella	Scadente	Bassa	Bassa	Media	Buona

Figure 4.11: Typical performance parameters for lithium / ion cells.

in order to guarantee greater availability and preserve the useful life of the accumulators.

These functions are automatically performed by the regulator on the basis of threshold voltages which they are HVD and LVD respectively. These disconnection processes, carried out automatically by the regulator, are based on a parameter calculated and kept updated by the regulator itself, namely the SoC.

A further parameter based on the SoC is the LVR. Using this parameter, the regulator is able to understand when the accumulators are charged enough to be reconnected to the load (since with the LVD protection the accumulators could be disconnected from the load).

Figure 4.12: Charge regulators.

Chapter 5

Case study

In this section the main topic of this thesis will be discussed, describing the LIFE-SAVE project in detail, and my personal contribution to itPV Some of the concepts mentioned in this chapter won't be examined in depth for sake of brevity, although further explanation will be in the bibliography and in the appendix.

5.1 The LIFE-SAVE project

LIFE-SAVE (LIFE16 ENV / IT / 000442) is a project funded by the European LIFE program for the development and industrialization of a system to convert cars into hybrid-solar vehicles, with very low costs compared to purchase of a new hybrid or electric vehicle. The purpose of the project LIFE-SAVE, started in September 2017, is to produce a version of this technology ready to be placed on the market (TRL = 9).

Figure 5.1: The project mounted on a FIAT Punto

The motivations

Currently, the means of transport are responsible for 63% of global oil consumption and 29% of CO2 emissions and achieving a more efficient, flexible and safer (and less invasive) transport for the environment is now a widely pursued goal.

The European Union is committed to reaching a ceiling of CO2 emissions of 95 $\frac{g}{km}$ by 2020 and with additional restrictions expected by 2025 (68-78 $\frac{g}{km}$).

The 2008 Air Quality Directive has also limited emissions of NOx and all major European countries want to achieve a higher degree of energy independence and implement a transport system no longer based only on an intense use of oil. The statistics also show an increase in the number of electric vehicles in the European Union, motivated by the choice of consumers and a fully transitioned automotive industry.

A sustainable and achievable solution

The best option would be the electric car, but several problems remain to be overcome. Above all, a mass conversion to electric cars is not achievable in the short term, for various reasons:

- a notable increase in electricity production would be required, and obtained from renewable sources (otherwise the CO2 reduction target would be lost);
- the charging power of the batteries is still too low, and therefore the charging times are much higher (even by a factor of 100!) compared to those to which we are accustomed to motor vehicles;
- the current electricity grid would be thrown into crisis by a general recourse to the recharging of electric vehicles, before major adjustments to the network structure and its "philosophy" (Smart-Grid).

Hybrid vehicles are certainly a good solution in the short and medium term to the demand for cars that consume and pollute less. But even in this case a large-scale transition to hybrid traction would clash with some problems: the cost of hybrid cars, more expensive than traditional cars, and especially the need to scrap a large part of the circulating fleet, often made up of good cars conditions.

Instead, the system allows you to convert cars into hybrid-solar vehicles at a low cost, thus allowing you to reduce fuel consumption and emissions, to access restricted traffic areas, to increase vehicle autonomy and performance, and to avoid the scrapping of cars often still in good condition, allowing reuse, which is one of the pillars of sustainability.

The benefits of car conversion in terms of LCA have been carefully evaluated and quantified by the partners of the LIFE-SAVE project .

Moreover, the solar hybridization of cars meets most of the SDG as defined in the 2030 Agenda for Sustainable Development by the UN .

The LIFE Program

Made in its first edition of 1992, LIFE is one of the "historical" programs of the European Union. In the current 2014-2020 programming phase, the LIFE program supports the implementation of the Seventh Environment Action Program (Decision No. 1386/2013 / EU of 20/11/2013) "Living well within the limits of the our planet ". It is divided into two main components: an "**Environment**" sub-program and a "**Climate Action**" sub-program, which are in turn organized into priority sectors and types of action.

The European Commission regulates and coordinates the activities of the LIFE program, implementing many activities and sectors within the EASME which determines the methods of implementation and its implementation (management of tenders, awarding proposals, project management, monitoring and evaluation).

The strategic management of the program (definition of budget, objectives and priorities) lies with two Directorates General of the European Commission, the DG Ambiente for the "Ambiente" sub-program and DG Clima for the "Azione per il clima" sub-program. The European Investment Fund monitors the financial instruments and methods through which companies can benefit from LIFE's support.

The evaluation system of LIFE projects has been planned by the European Community, and pays particular attention to the contribution of the project itself to promote environmental, economic and social improvements in the medium and long term. The degree of innovation, adherence to environmental protection policies and the cost / benefit ratio are the key criteria for positively evaluating a project to be funded.

5.1.1 How does it work

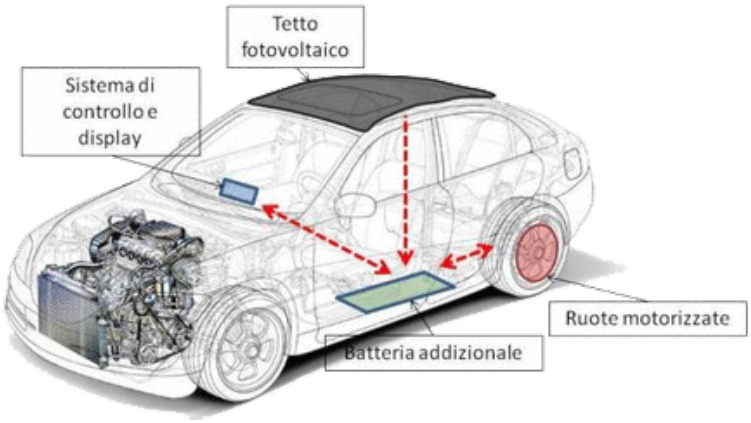

Figure 5.2: Description of the system

How it is composed

- In the rear wheels two electric motors are integrated that transform the car into a 4×4 hybrid drive (conventional traction on the front wheels and electric on the rear wheels)

- The electric motors are powered by an additional lithium battery mounted in the boot (instead of the "wheel"). The battery can be recharged by solar panels, by the vehicle itself (during braking or descents, or by absorbing the additional torque generated by the engine in order to optimize the overall performance), or by the network (Plug-In option)

- High-performance flexible solar panels (produced by Solbian, partner of the LIFE-SAVE project), are mounted on the roof and on the bonnet of the car, with the function of recharging the vehicle's battery, both during driving and during the phases parking, free and without CO2 emissions

- A control system, connected to a display, drives the electric motors based on the requests of the driver and the state of charge of the battery, connecting to the vehicle through the OBD port, normally used for diagnostics, and without interfering with the control unit of original vehicle check

The advantages

- The internal combustion heat engine works less, because part of the power required for traction is provided by electric motors, and this translates into lower fuel consumption and lower emissions of polluting gases. The benefit can reach 20-25% for a typical use in urban areas (one hour of driving a day) and on sunny days, but it is still appreciable even in the absence of sun, for the benefits related to hybridization (recovery of the braking energy and downhill, optimization of the efficiency of the thermal engine)

- The car, now comparable to a hybrid in terms of fuel consumption and emissions, can have access to restricted traffic areas (ZTL) , where it can move in a predominantly electric mode

- Unlike what happens with an electric car, the car has no recharging and autonomy problems, which on the contrary is also increased compared to the traditional vehicle of departure due to the presence of the additional battery

- Compared to the starting car, the car will perform better thanks to all-wheel drive. In particular, the presence of two electric motors in the rear wheels gives better capacity during acceleration, which translates into a reduction of more than 20% of the time to go from 0 to 100 km/h

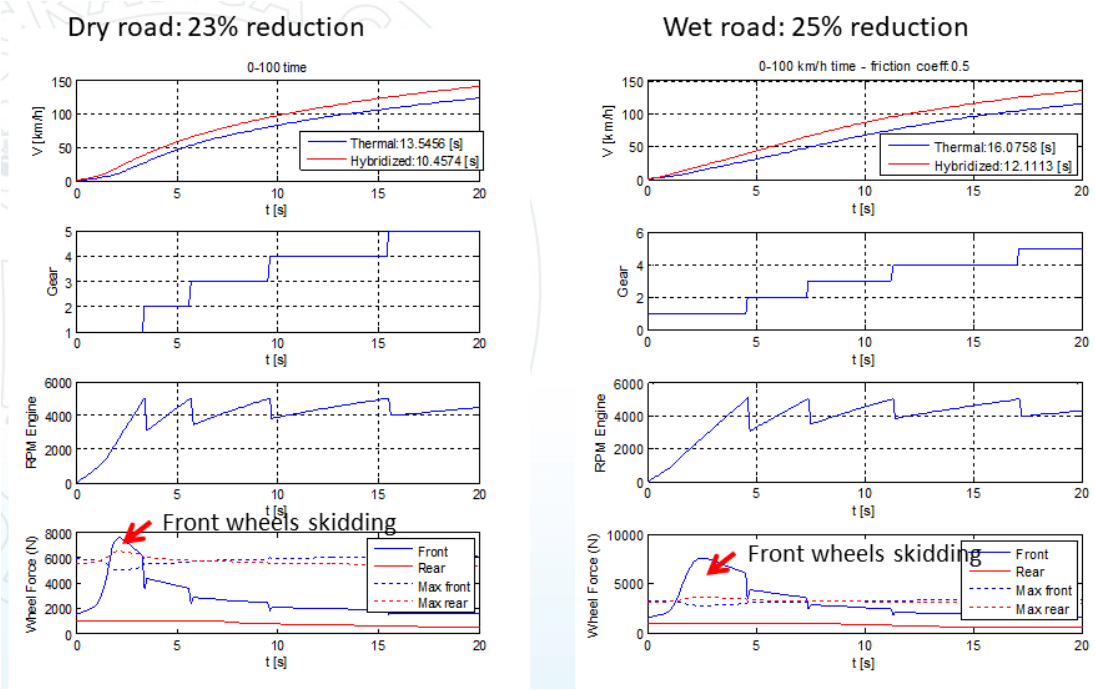

Figure 5.3: Test 0-100km/h – match between hybrid vehicle and normal one

5.1.2 LIFE-SAVE vs other solutions

The system developed by LIFE-SAVE project is a unique product, covered by patents: there are no alternative products or patents that provide hybridization of vehicles together with solar recharge.

Apart the convenience for the customer, this solution would allow the REUSE of cars often still in good conditions, avoiding a massive scrapping of the present fleet. The benefits in terms of energy consumption and CO2 emissions are analysed later .

A synthetic analysis of the advantages and disadvantages of the system compared to both the conventional vehicle and the possible alternatives follows.

Conventional vehicle (petrol or Diesel)

Pros : Reduction in consumption and emissions (up to 20% in typical urban use). Better performance (acceleration, driveability) thanks to the 4×4. The car can be classified as an ecological vehicle (it is similar to a hybrid) and can access the Limited Traffic Zones.life-save

Cons : Additional cost. Slight increase in vehicle weight (around 60 kg). Space occupied by the additional battery (instead of the spare wheel).

Conventional natural gas or LPG vehicle

Pros : With LIFE-SAVE solution the reduction in operating costs is due to a lower fuel consumption (which is one of the main targets of LIFE-SAVE project), while in a vehicle fueled by methane or LPG is linked only to a lower cost of fuel, which in Italy is currently burdened by a lower taxation than gasoline and diesel. It is clear that this advantage could change as a result of political decisions (even diesel fuel years ago cost much less than gasoline, but then the gap has been reduced after the diffusion of Diesel engines). The system also offers an increase in performance thanks to the 4×4 architecture. However, it can also be applied to CNG or LPG vehicles.

Cons : Installing LIFE-SAVE system is more expensive than installing a CNG or LPG system.

Hybrid vehicle

Pros : despite having the typical advantages of a hybrid vehicle (reduction of consumption and emissions, high range, high performance, braking energy recovery, etc.), it costs much less than a hybrid vehicle. In addition, it allows a partial solar recharge, an option not present today except on some “Concept” (however, far behind the development stage of LIFE-SAVE) and on the top model of Toyota Prius Prime Plug-In, currently only in the Japanese market (at a much higher cost compared to

LIFE-SAVE solution...). Moreover, a general switch to hybrid vehicles would mean a massive scrapping of the circulating fleet, while their conversion would allow the reuse of cars in many cases still in good condition. This solution is therefore much more sustainable, as the reuse is one of the pillars of sustainability together with the reduction and recycling (the three Rs).

Cons : A vehicle designed "ab ovo" as hybrid can, in theory, optimize consumption and performance better. However, this gap is offset by the presence of solar recharge.

Electric Vehicle

Pros : LIFE-SAVE system costs much less than an electric vehicle. It does not have the problems of limited range and difficulty and length of recharging which still afflict electric vehicles (problems related to charging and the impact on the electrical network today constitute a serious limit to the mass uptake of electric vehicles). It should be noted that an electric vehicle does not allow to avoid CO2 emissions, unless the electricity for charging does not come from a renewable source, while the reduction of CO2 ensured by LIFE-SAVE system is based on a lower consumption of energy related to hybridization and the availability of electricity from a PV source. With LIFE-SAVE solution, as for conventional vehicles, it is possible to heat the passenger compartment due to the waste heat of the internal combustion engine, while the winter heating (such as the air-conditioning during summer) seriously reduce the range in an electric vehicle.

Cons : The electric allows you to move in zero emission mode, within its range. LIFE-SAVE system allows "Full Electric" mode with reduced power, and with lower range than a native electric vehicle, as it is normally equipped with a smaller battery. It can however, with an additional cost, accommodate a larger battery, extending the range in "Full Electric" mode.

Hydrogen

Pros : Unlike LIFE-SAVE solution, the hydrogen-powered vehicles (with Fuel-Cell) represent today only alternative to long term, having to solve problems of cost of Fuel-Cell, safety, availability and distribution of hydrogen. As with the electric vehicle, the CO2 reduction associated with the use of hydrogen is only realized if the hydrogen itself (which is not found as it is in nature) is produced from a renewable source.

Cons : As for electric vehicles, a hydrogen vehicle allows you to move in Zero Emission mode, within its range. LIFE-SAVE system allows this mode only with reduced power and with lower range, as it is usually equipped with a smaller battery. It could however, with an additional cost, accommodate a larger battery, extending the range in "Full Electric" mode.

Bio-fuels

Pros : it allows to reduce operating costs, consumption and emissions compared to a conventional vehicle fueled with bio-fuels, also increasing its performance. Bio-fuels, available today and also in the near future in relatively small quantities, allow to reduce global CO2 emissions, but do not offer substantial advantages in terms of urban emissions, performance or operating costs (unless there are incentives). It should be noted that the system developed by LIFE-SAVE project can also apply to vehicles that use bio-fuels, adding the advantages.

Cons : Additional cost for the plant.

5.1.3 The PV contribution

There are important differences between the use of solar energy and all other modes of powering the cars. PV is the only case in which the primary energy can be used on the car, coming directly from nature, in a sort of "short supply chain". In all other cases, an "energy vector" is used: the primary energy is "incorporated" into a "vector" (fossil fuel, bio-fuel, electricity, hydrogen ...), transported, distributed, sold and taxed.

It is a relevant difference: in fact, energy transmission always involves energy consumption and, in many cases, CO2 emissions, energy costs and emissions that would instead be avoided by using direct primary energy on the vehicle, through PV.

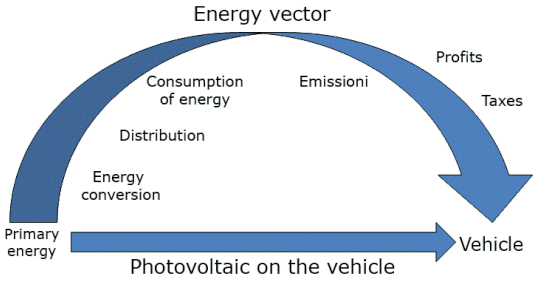

Figure 5.4: The power of cars with PV creates a "short supply chain"

What contribution can PV make on a car?

Let's now try to evaluate the savings that can be achieved by integrating the PV system into a vehicle. The skepticism that has accompanied the use of solar energy in the automotive field for a long time is due to the fact that the power of a solar panel that can be housed in a car with a normal size, of 300 W, is much lower than the power of a medium-sized car, of the order of 50-60 kW. But this observation is as elementary as it is misleading: it would be correct to think so if both systems always operate at maximum power. In the case of a car, this happens almost only when you run at Le Mans "24 hours"PV

In reality, most of the motorists (about 50%) use the car mainly in the city, for no more than an hour a day and almost always with only the driver on board. In these conditions, the "average" power required in an urban environment is of the order of 8 kW, considering the partial recovery of the power needed to brake. If the car is used one hour a day, the daily energy required for traction is therefore equal to 8 kWh.

Now let's go back to the solar panel: not even this, of course, always works at maximum power, at least because at night the sun goes away. However, if we consider a panel exposed in a sunny place, the energy obtainable is roughly equal to that obtainable in about ten hours per day operating at a power of 2/3 of the maximum power: in the case of a panel with a maximum power of 300 W , we can estimate the daily energy obtainable on an average day by multiplying the average power (200 W) for 10 hours, obtaining a daily energy of 2 kWh. The photovoltaic panel can therefore provide about 25% of the approximately 8 kWh per day required for traction, in a typical urban use, a value well over 0.5% that an apparently common sense but superficial analysis, based only on the maximum power , he would have attributed to him.

The Flexible photovoltaic used in the LIFE-SAVE project is developed by Solbian.

A more precise evaluation of the potential contribution achievable by PV panels located on a car (in almost horizontal position) is given by the following graphs. The values of mean and maximum daily net energy are computed for different cities at various latitudes by using the database PVWatts, developed by the NREL of US.

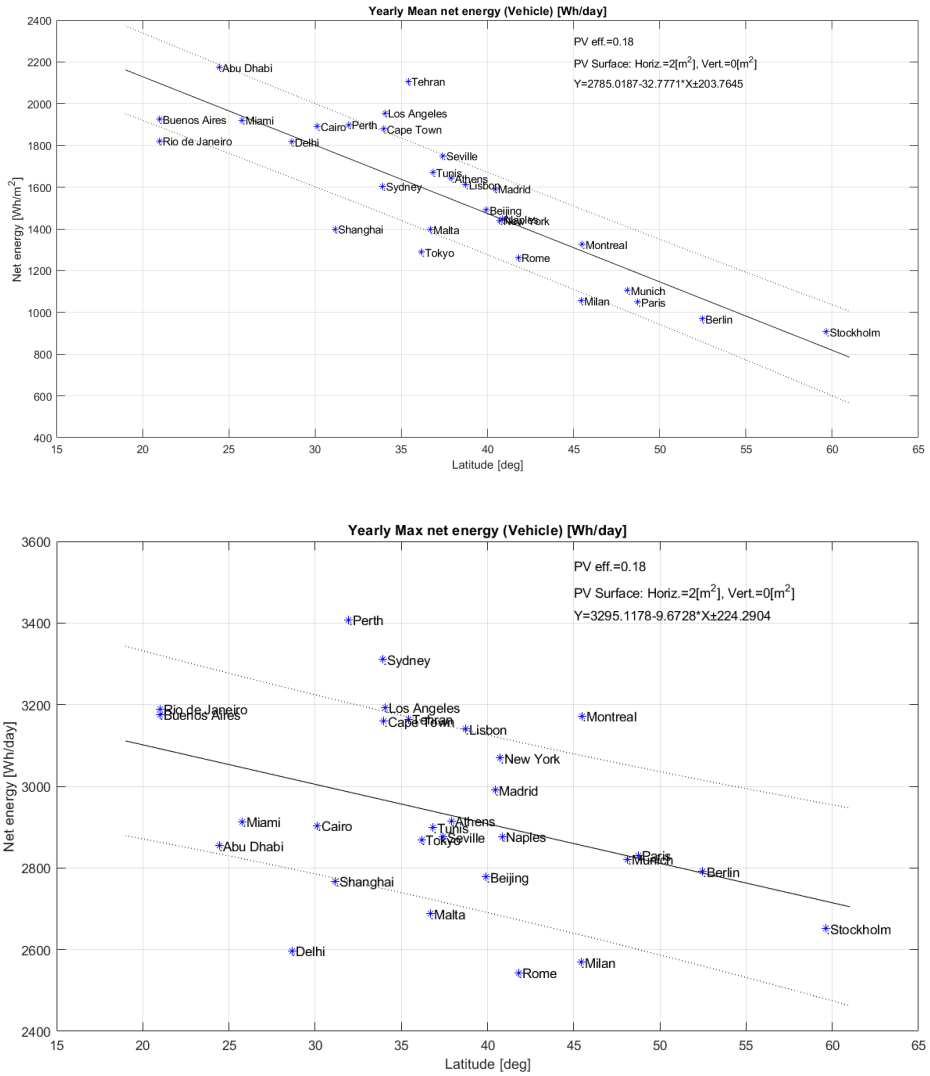

Figure 5.5: Estimated energy output with just the roof panels

It can be seen that, for a 2 sqm panel surface (compatible with our prototype and with most of cars) the maximum daily contribution can be over 3000 Wh/day in some locations, while mean contribution (considering also winter time) range from 1000 to 2000 Wh/day.

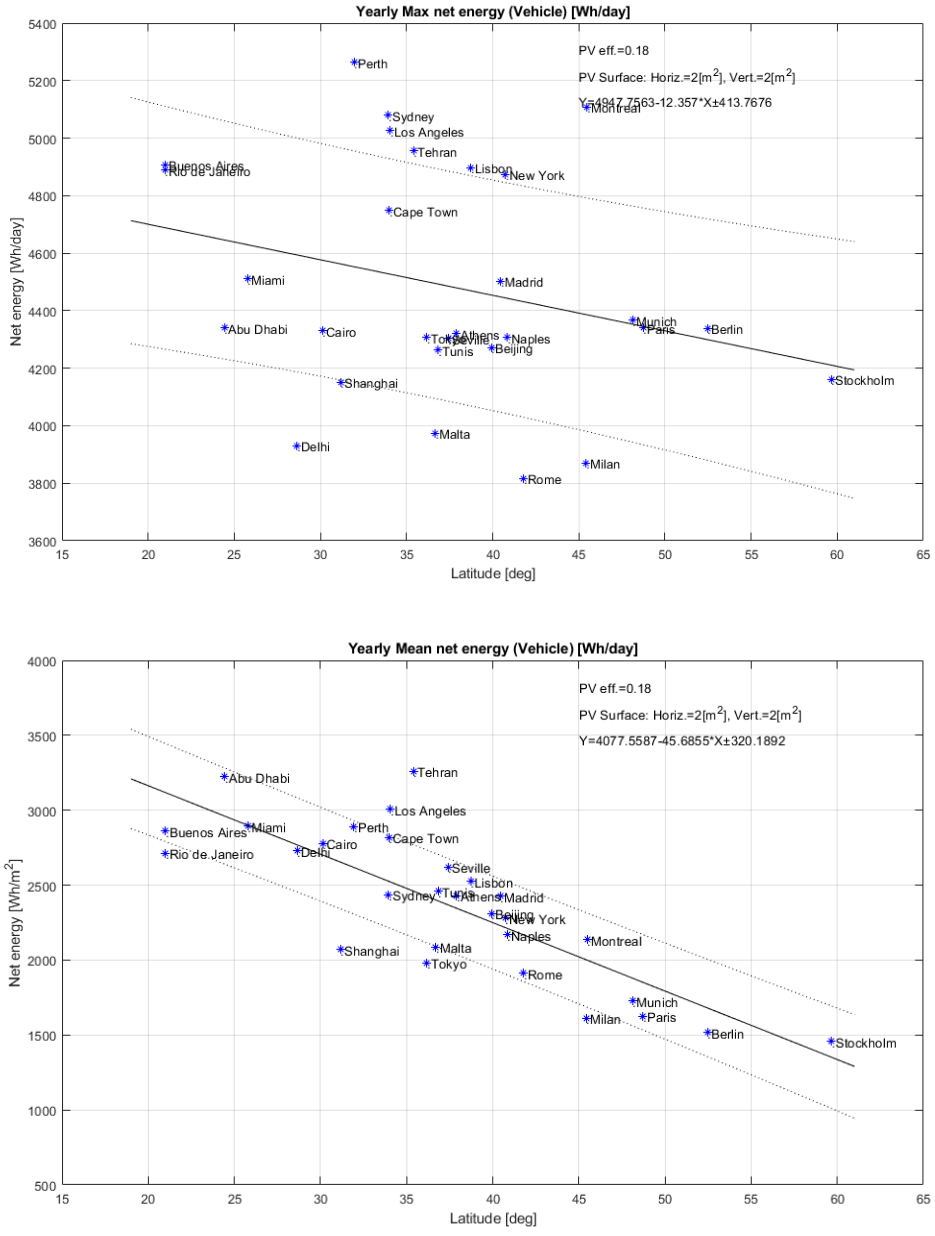

Figure 5.6: Estimated energy output with the roof and side panels

The use of PV panels on lateral sides also results in a significant increase of energy harvesting. Average yearly daily contributions range from 2000 and 3000 Wh for most world locations, with maximum values exceeding 5000 Wh/day in some locations. These results have been obtained considering $2m^2$ of panels in horizontal position and $2m^2$ on vertical position, on car lateral sides. It is worth mentioning that the solar contribution

presented above can be achieved if the PV panels are not shadowed. Shadowing (due to trees, tunnels, buildings and other obstacles) is more likely to occur during driving phases, while it can be avoided or minimized during parking with a proper choice of the parking slot. For most of cars used in typical urban commuting, that usually spend most of time when parked, the estimation presented above can be considered a reasonable approximation.

5.2 Testing bench

The main objective of this project is to evaluate the efficiency of the DC-DC converter installed on the car. For this purpose, a sensor was developed specifically that could satisfy the need to simultaneously measure the electrical input and output power, have high precision on different scales (30V-120V), as well as save data on a micro card. SD.

The lack of sensors on the market with these characteristics has led to invest a lot of time in development, evaluating different types of solutions. Using an Arduino-based system as a controller was an obvious choice due to its ease of use and low cost.

Arduino is an open-source platform used for building electronics projects. Arduino consists of both a physical programmable circuit board (often referred to as a microcontroller) and a piece of software, or IDE (Integrated Development Environment) that runs on your computer, used to write and upload computer code to the physical board.

The Arduino platform has become quite popular with people just starting out with electronics, and for good reason.

5.2.1 Microcontroller used as sensor

Arduino Uno

Unlike most previous programmable circuit boards, the Arduino does not need a separate piece of hardware (called a programmer) in order to load new code onto the board – you can simply use a USB cable. Additionally, the Arduino IDE uses a simplified version of C++, making it easier to learn to program. Finally, Arduino provides a standard form factor that breaks out the functions of the micro-controller into a more accessible package[23].

One of the most popular Arduino boards out there is the Arduino Uno. While it was not actually the first board to be released, it remains to be the most actively used and most widely documented on the market.

Board Breakdown

Here are the components that make up an Arduino board and what each of their functions are.

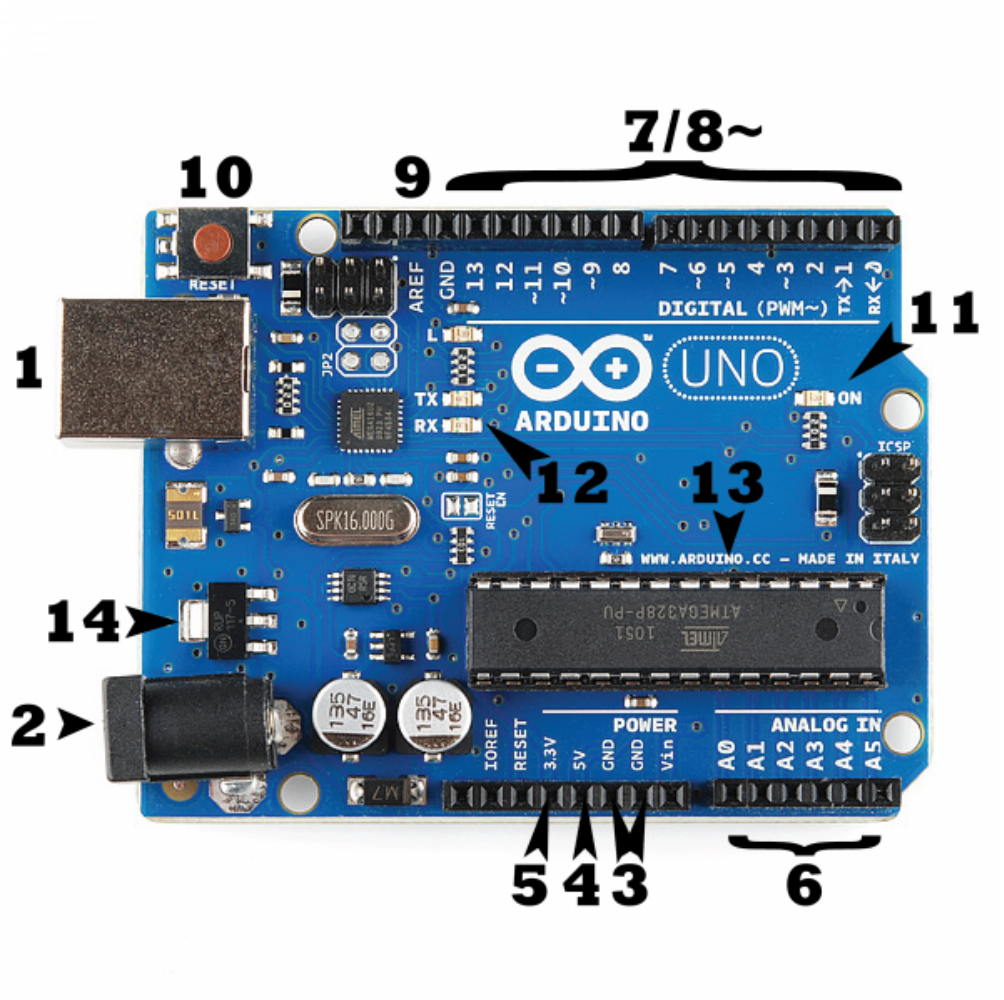

Figure 5.7: An Arduino Uno

1. Reset Button – This will restart any code that is loaded to the Arduino board
2. AREF – Stands for "Analog Reference" and is used to set an external reference voltage
3. Ground Pin – There are a few ground pins on the Arduino and they all work the same
4. Digital Input/Output – Pins 0-13 can be used for digital input or output
5. PWM – The pins marked with the (∼) symbol can simulate analog output
6. USB Connection – Used for powering up your Arduino and uploading sketches
7. TX/RX – Transmit and receive data indication LEDs

8. ATmega Microcontroller – This is the brains and is where the programs are stored
9. Power LED Indicator – This LED lights up anytime the board is plugged in a power source
10. Voltage Regulator – This controls the amount of voltage going into the Arduino board
11. DC Power Barrel Jack – This is used for powering your Arduino with a power supply
12. 3.3V Pin – This pin supplies 3.3 volts of power to your projects
13. 5V Pin – This pin supplies 5 volts of power to your projects
14. Ground Pins – There are a few ground pins on the Arduino and they all work the same
15. Analog Pins – These pins can read the signal from an analog sensor and convert it to digital

In order to work properly as a sensor Arduino needs a reliable voltage reference to compare its input with. the USB power supply is an easy way to communicate and power the board, but as the power consumption rises, the voltage provided by USB decreases[24].

So an external 9 V power supply has been used for the tests.

It's also crucial to evaluate the resolution of the microcontroller, the reference voltage is 5 V and the resolution of the Arduino Uno R3 is 10 bits as seen in the documentation[25].

With the resolution is easy to calculate the sensibility (such as what is the step for every bit in terms of voltage, also known as quantization error).

$$\Delta V = \frac{FSR}{2^{N_{bits}}} = \frac{5V}{2^{10}} = 4.883mV \tag{5.1}$$

Where:

FSR is Full Scale Resolution,

N_{bits} is the total number of bits of the controller

5.2.2 Measurement circuit under study

To measure the power it is necessary to know the current and the voltage:

$$P[W] = V[V] \cdot I[A] \tag{5.2}$$

The voltage is easily measured through a resistive divider connected to an analog input of the Arduino, while for the current there are different ways of measuring with pros and cons.

Voltage divider

In electronics, a voltage divider (also known as a potential divider) is a passive linear circuit that produces an output voltage (V_{out}) that is a fraction of its input voltage (V_{in}). Voltage division is the result of distributing the input voltage among the components of the divider. A simple example of a voltage divider is two resistors connected in series, with the input voltage applied across the resistor pair and the output voltage emerging from the connection between them.

Resistor voltage dividers are commonly used to create reference voltages, or to reduce the magnitude of a voltage so it can be measured, and may also be used as signal attenuators at low frequencies. For direct current and relatively low frequencies, a voltage divider may be sufficiently accurate if made only of resistors; where frequency response over a wide range is required (such as in an oscilloscope probe), a voltage divider may have capacitive elements added to compensate load capacitance. In electric power transmission, a capacitive voltage divider is used for measurement of high voltage[26].

A resistive divider is the case where both impedances, are purely resistive:

Hall effect sensor

The first approach used to create the circuit was to use a Hall effect current sensor.

If an electric current flows through a conductor in a magnetic field, the magnetic field exerts a transverse force on the moving charge carriers which tends to push them to one side of the conductor. This is most evident in a thin flat conductor as illustrated. A buildup of charge at the sides of the conductors will balance this magnetic influence, producing a measurable voltage between the two sides of the conductor. The presence of this measurable transverse voltage is called the Hall effect after E. H. Hall who discovered it in 1879.

Note that the direction of the current I in the diagram is that of conventional current, so that the motion of electrons is in the opposite direction. That further confuses all the "right-hand rule" manipulations you have to go through to get the direction of the forces.

The Hall voltage is given by

$$V_H = \frac{I \cdot B}{n \cdot e \cdot d} \tag{5.3}$$

where

n = density of mobile charges

e = electron charge.

d = thickness of the conductor

The Hall effect can be used to measure magnetic fields with a Hall probe[27].

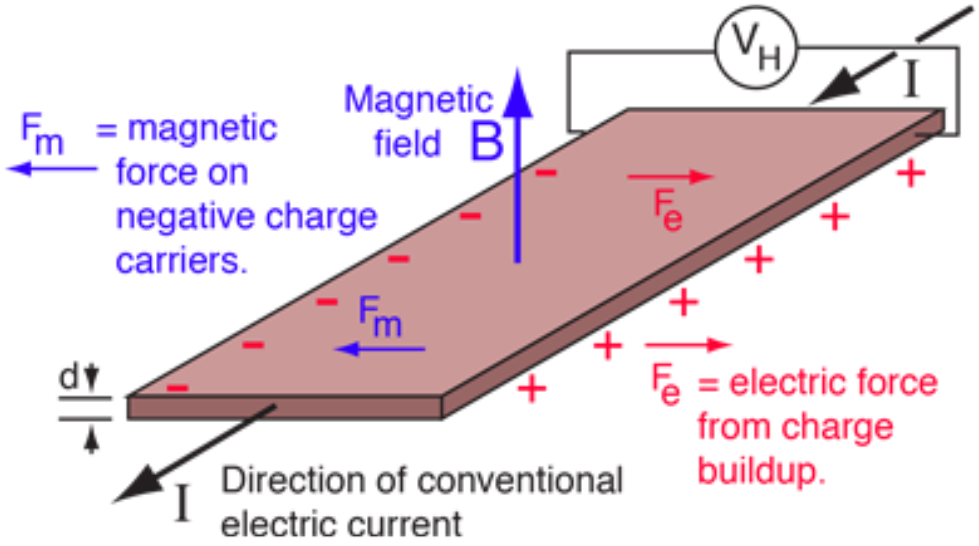

Figure 5.8: Hall effect phenomenon

ACS712

Hall Effect Sensors are transducer type components that can convert magnetic information into electrical signals for subsequent electronic circuit processing. Generally, current sensors use the Hall Effect to convert current inputs into voltage outputs. In the Hall effect, electrons from an electric current flow through a magnetic field plate. The field then causes the electrons to "push" to one side of the plate and produce a voltage difference between the two sides. The difference in voltage from the side of the plate is the output of the sensor.

ACS712 is a current sensor that can operate on both AC and DC. This sensor operates at 5 V and produces an analog voltage output proportional to the measured current. This tool consists of a series of precision Hall sensors with copper lines.

The output of this instrument has a positive slope when the current increases through the copper primary conduction path (from pins 1 and 2 to pins 3 and 4). The internal resistance of the conduction path is 1.2 $m\Omega$[28].

This would have been an optimal choice as it is a non-invasive measuring device (it does not absorb current from the power circuit), but unfortunately the measurements proved to be unreliable and not at all stable.

where:

- R1,R2,R3 and R4 are resistors used for the voltage divider in order to measure the voltage,
- F1 and F2 are 10 A fuses used for over-current protection,

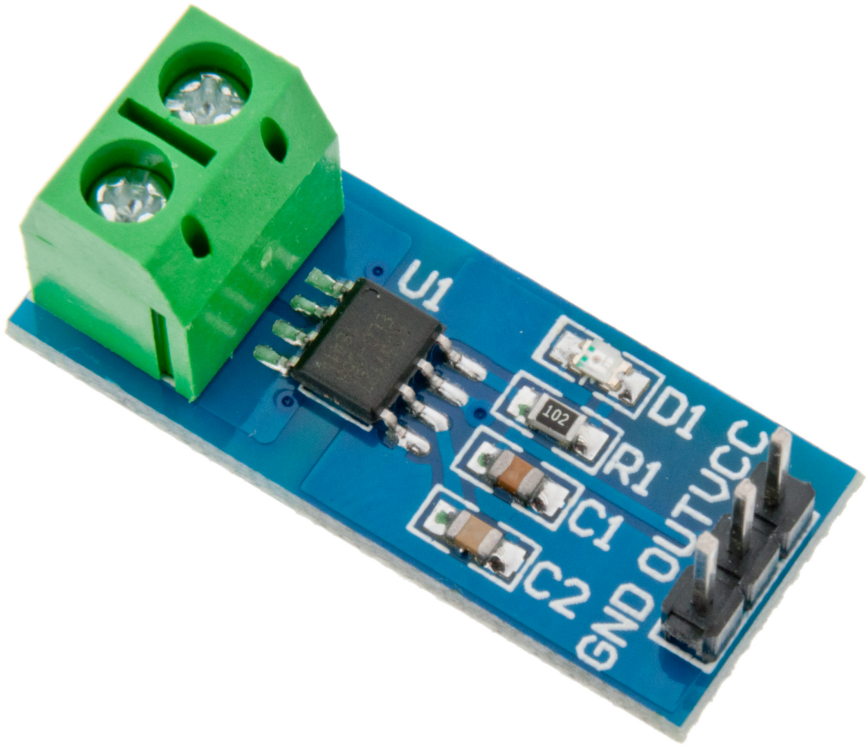

Figure 5.9: ACS712

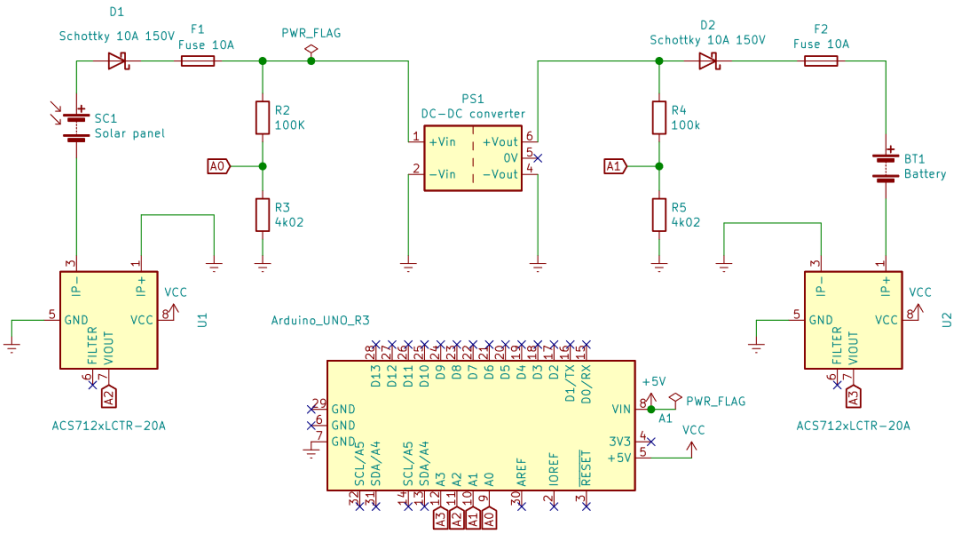

Figure 5.10: Electrical scheme of ACS712 circuit

- D1 and D2 are Schottky diodes used to protect the circuit from inverse currents.

Shunt resistor and amplifier

A different approach to circuit design was used to solve the problem. Instead of using a Hall effect sensor, it has been opted for a shunt resistor and an amplifier in order to have reliable and accurate readings. Shunt resistors are low resistance resistors connected in series to the load, the voltage drop allows to measure the current flowing through:

$$I[A] = \frac{V[V]}{R[\Omega]} \tag{5.4}$$

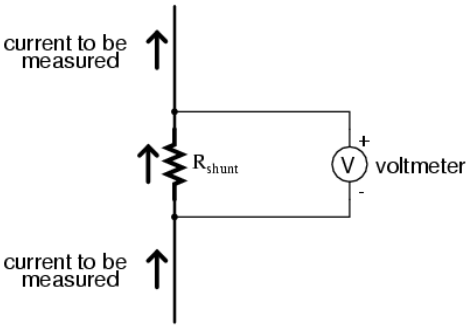

Figure 5.11: Measuring shunt voltage

Figure 5.12: Shunt resistance

To monitor the current with a shunt resistor it can be employed at the high voltage side or at the lo voltage side, meaning that the resistor will be placed before or after the load.

Both of these approaches have their pros and cons. High-side current sensing has the benefit of being able to detect current related faults, such as short-circuits or an open circuit that could affect the load. Also, with high-side current sensing, the load can be referenced directly to ground, as we'll explore later. The main disadvantage of high-side current sensing is that the common mode voltage is relatively high (based on the supply voltage), hence a high common mode amplifier is required.

As opposed to high-side current sensing, on the low-side the common mode is referenced to ground, hence a cheaper, more readily available low voltage amplifier can be used. As eluded to earlier, one disadvantage of low-side current sensing is that the shunt resistor is placed between the load and ground, which can cause ground loop issues since the load may not be at the exact same ground potential as the rest of the circuitry.

As mentioned earlier, for low-side current monitoring, essentially any single-supply, low

voltage amplifier can work, as the common mode voltage is ground referenced. Selecting the best amplifier for this situation depends on price versus required performance, as the amplifiers offset voltage, offset drift, common mode and power supply rejection and transient response may all be critical considerations.

For high-side current sensing, the amplifier must be able to support the higher common mode range, as well as handle any voltage transients that may occur on the power line. A system designer can again use a standard operational amplifier configured as a difference amplifier, as shown in figure 5.13.

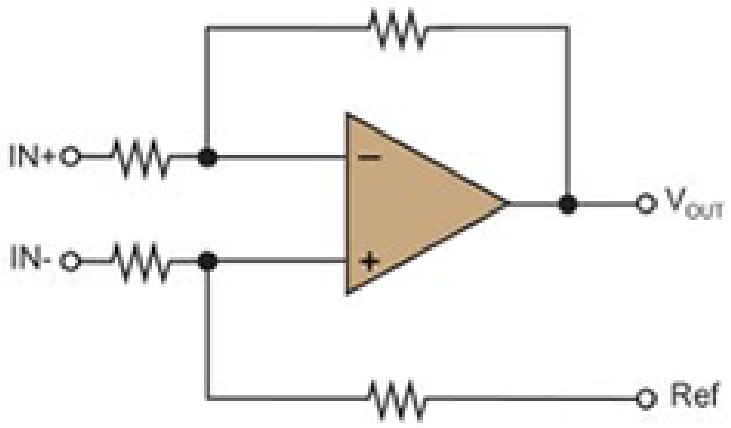

Figure 5.13: Difference amplifier

.However, there are some limitations to this approach. First, the input resistance is relatively low, determined by the external resistors, not to mention that the input currents are not matched, which will limit the common mode rejection. Speaking of which, the common mode rejection will also be limited by how well matched the resistors are, which leads to subpar performance.

The first type of connection was with the shunt resistor on the high voltage side. This configuration allows to eliminate problems related to the ground-loop, that is cases in which the negative sides of the two circuits are not exactly at the same voltage, having repercussions on the current measurements.

As seen before the Arduino Uno has a sensibility of 4.883 mV which in FSR of 0.8 V is not enough to cover the whole range of measurements effectively. In order to improve the

performances of the sensor, an amplifier must be used.

An amplifier, as the name suggests amplifies voltages. It achieves the opposite goal of a voltage divider, linearly increasing the voltage by a set amplification ratio. In electronics the most employed integrated circuits (IC) for this purpose are called Operational Amplifiers (Op Amp).

There are many different important characteristics and parameters related to Op Amps (see Figure 5.14).

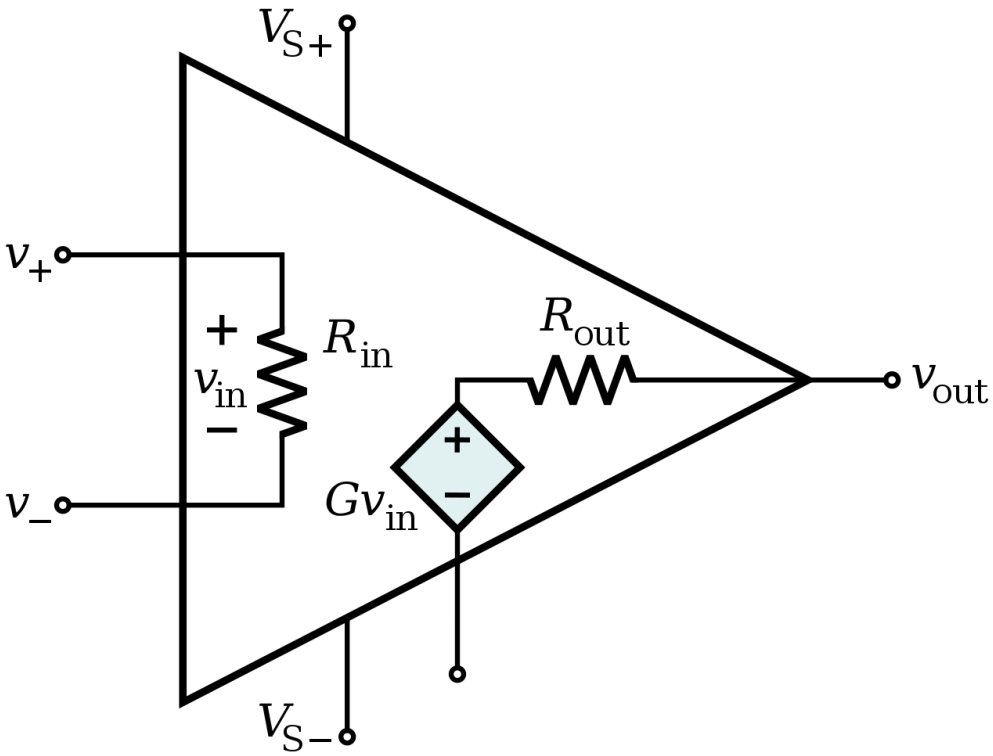

Figure 5.14: Operational amplifier

These characteristics are described in greater detail below.

Open-loop gain : The open-loop gain of an operational amplifier is the measure of the gain achieved when there is no feedback implemented in the circuit. This means the feedback path, or loop, is open. An open-loop gain often must be exceedingly large (10,000+) to be useful in itself, except with voltage comparators.

Voltage comparators compare the input terminal voltages. Even with small voltage differentials, voltage comparators can drive the output to either the positive or negative rails. High open-loop gains are beneficial in closed-loop configurations, as they enable stable circuit behaviors across temperature, process, and signal variations.

Input impedance : Another important characteristic of Op Amps is that they generally

have high input impedance ("R_{IN}" in figure 5.14). Input impedance is measured between the negative and positive input terminals, and its ideal value is infinity, which minimizes loading of the source. (In reality, there is a small current leakage.) Arranging the circuitry around an operational amplifier may significantly alter the effective input impedance for the source, so external components and feedback loops must be carefully configured. It is important to note that input impedance is not solely determined by the input DC resistance. Input capacitance can also influence circuit behavior, so that must be taken into consideration as well.

Output impedance : An operational amplifier ideally has zero output impedance ("R_{OUT}" in figure 5.14). However, the output impedance typically has a small value, which determines the amount of current it can drive, and how well it can operate as a voltage buffer.

Op Amps can be employed as differential amplifiers using their characteristics[29]:

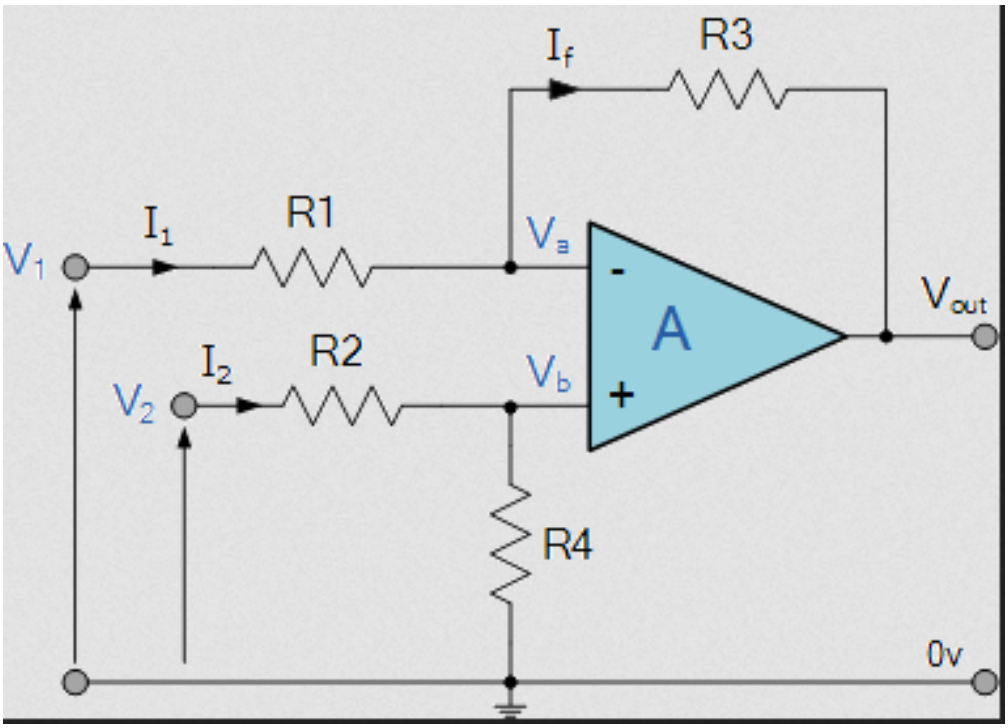

Figure 5.15: Differential amplifier circuit

With this layout the amplifier amplification can be controlled and used to sense tiny voltages. The equation for the output voltage is:

$$V_{out} = A_r \cdot (V_2 - V_1) = \frac{R_3}{R_1} \cdot (V_2 - V_1) \tag{5.5}$$

where $\frac{R_3}{R_1} = A_r$ is the amplification ratio.

After the amplifier, a Analog to digital converter ADC must be employed to save the data in the board. the ADC needs at least 4 channels because each side of the circuit uses 2 (2 for battery side and 2 panel side).

To select the interested channels the ADC needs a Multiplexer (Mux). A multiplexer, also known as a data selector, is a device that selects between several analog or digital input signals and forwards the selected input to a single output line. The selection is directed by a separate set of digital inputs known as select lines[30].

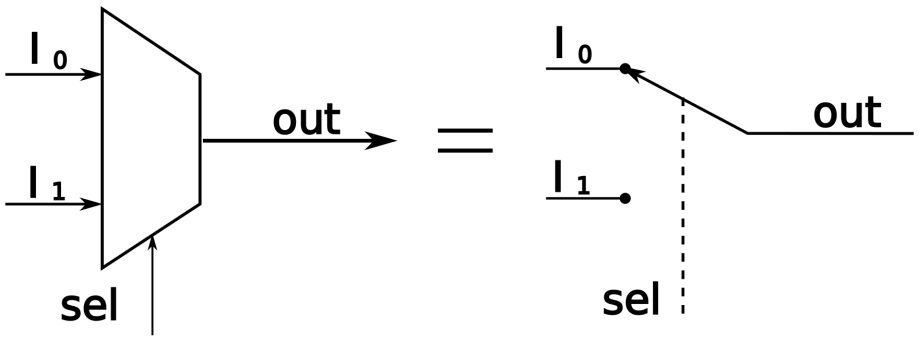

Figure 5.16: Working principle of multiplexer

Moreover a Programmable gain amplifier is useful to select the right range of voltage to be measured. A PGA is an electronic amplifier (typically based on an operational amplifier) whose gain can be controlled by external digital or analog signals.

The gain can be set from less than 1 V/V to over 100 V/V. Popular applications for these products are motor control, signal and sensor conditioning[31].

High side layout

However, this system is not optimal for the amplifier used as it can withstand a maximum voltage of 7V, while the power circuit easily exceeds 100V. This would require a much more expensive amplifier, or a divider to lower the voltage to acceptable values, greatly reducing the accuracy of the measurement.

The choice of the amplifier fell on an external ADS1115 module, consisting of a differential amplifier and a 16-bit ADC converter. This is capable of detecting 65536 different voltage values compared to the 1024 of the Arduino, also thanks to its programmable gain it is possible to significantly increase the precision. This system communicates with the main board via the i^2c digital connection, which does not generate contact problems and fluctuations within the circuit.

The shunt resistance chosen is 0.1 *Omega*, with an accuracy of 1 % and a maximum

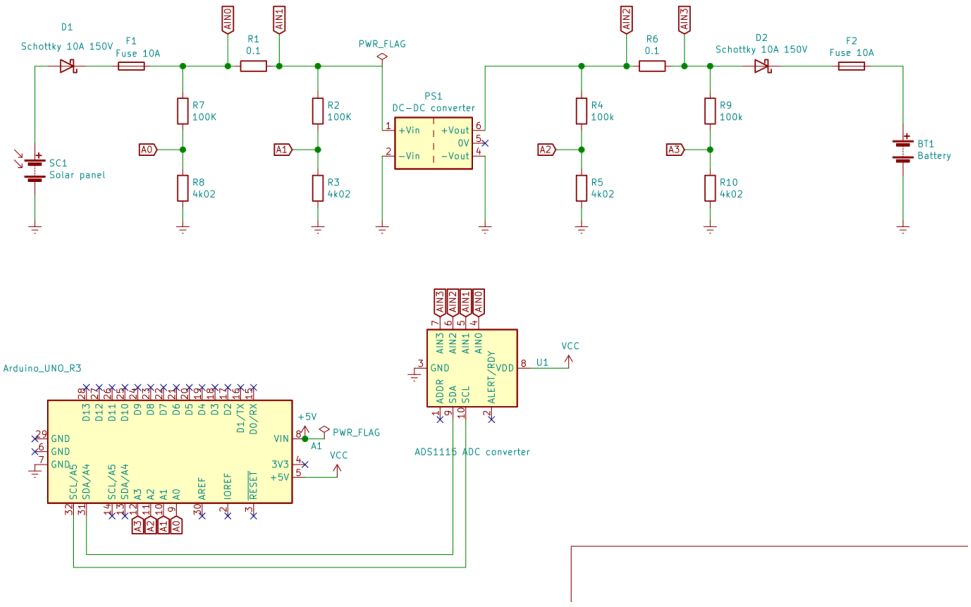

Figure 5.17: Electrical scheme of high side sensing circuit

dissipable power of 10 A, a value consistent with the loads applied to the converter.

The 0.1 Ω resistor leads to a voltage drop of 0.8 V when the current flowing through it is 8 A (limit case), comparing with the datasheet in table 3 it is noted that the optimal range for this measurement is equal to 1.024 V FSR (125μV LSB). Consequently, the gain is set with a value of 4x[32].

In the third and latest stage, the shunt resistor are moved from the high voltage side to the low voltage side, so the amplifier is connected directly to the resistor, eliminating a divider and not risking damage to components.

As previously mentioned, the current measurement on the low voltage side can lead to ground-loop phenomena.

Ground loop

A ground loop is an undesirable current path in an electrical circuit. Ground loops occur whenever the ground conductor of an electrical system is connected to the ground plane at multiple points.

Not only can ground loops induce noise in instrument signal cables, but in severe cases it can even overheat the instrument signal cable and thus present a fire hazard!

The phenomenon of ground loops is illustrated in the schematic diagram below:

There are several causes of ground loops in any instrumentation installation. Some of them are itemized below:

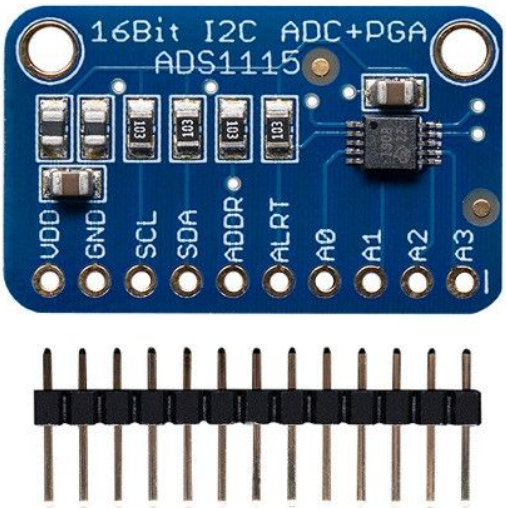

Figure 5.18: ADS1115

- Differences in potential between the points of the ground plane to which the ground terminals have been connected.
- Inductive coupling
- Capacitive coupling
- Use of internally grounded instruments inside an already grounded loop
- Cable shields grounded at both ends
- Grounded thermocouples with non-isolated transducers
- Four wire transmitters used as input to a receiver instrument grounded to a different ground connection

There are several methods of curbing ground loops that introduces undesirable noise voltage into instrument signal cables.

However, two of the most effective methods of reducing ground loops are:

- Single Point grounding
- Use of Differential Inputs

Single point grounding involves grounding the instrumentation installation at a single point. This approach significantly reduces the noise voltage generated due to ground loops from multiple grounding points.

Differential inputs are used to cancel out the noise voltage that may appear in the instrumentation circuit.

One very effective way to completely isolate an instrumentation system from ground loops is to use battery powered instruments. However because of the limited life of a battery, they are seldom used.

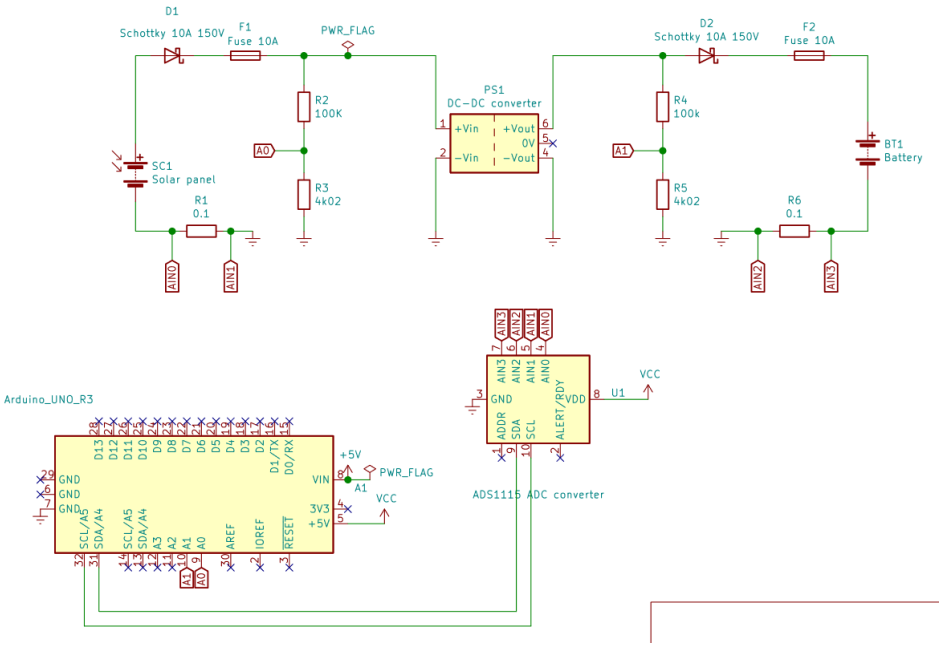

Figure 5.19: Electric scheme of low side sensing circuit

Final design

Another resistance has been added to the circuit in order to change the measurement range of the voltmeter integrated in the circuit without having to unsolder the components, by

connecting these to a diverter the selection system is very simple and compact.

The Arduino Uno R3 board has been replaced by an Arduino Nano to reduce the overall dimensions and for its possibility to be soldered on a prototype board directly. The latter is a perforated base that is used to create soldered circuits and test before producing printed circuit boards (PCB).

The PCB is a finished board, where the circuit is printed directly at the time of construction, this represents the final product in terms of shape and size.

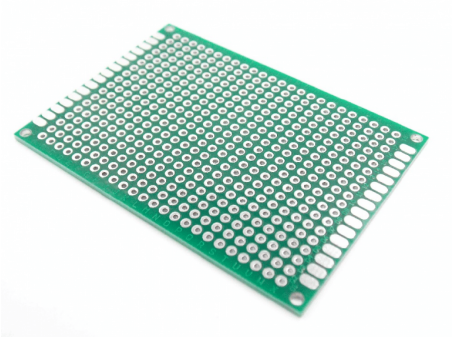

Figure 5.20: A prototype board

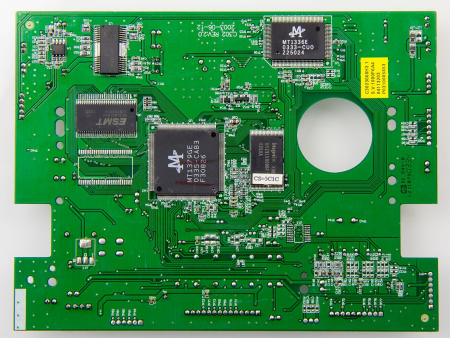

Figure 5.21: A printed circuit board

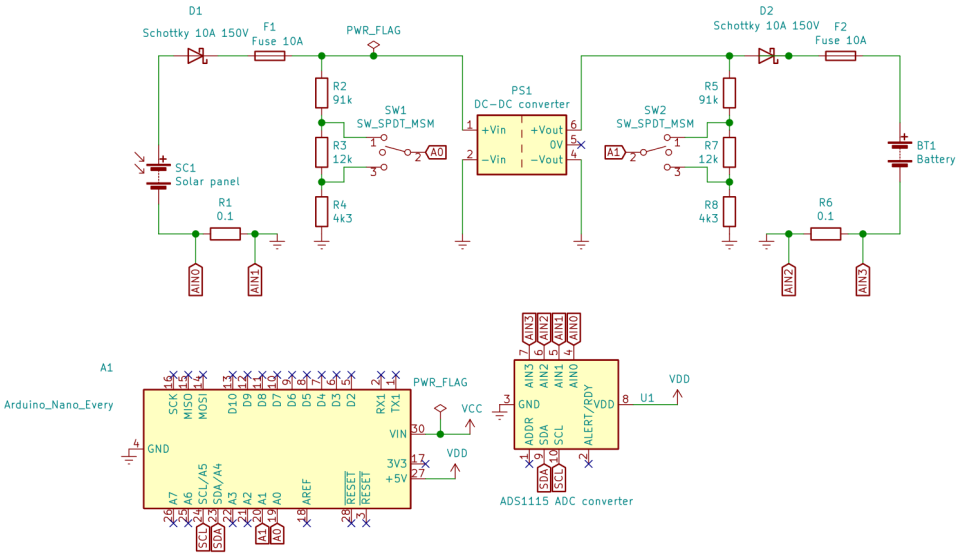

Figure 5.22: Electric scheme of lo side sensing circuit finished

where SW1 and SW2 are single pole, double throw switches used to pick the desired full scale range between 125 V and 33 V, the center in off for added protection.

5.3 Calibration

The calibration phase has been one of the most delicate ones, since all the components in the circuit have a certain degree of precision. The chosen calibration method has been to compare the readings to an instrument with known tolerances (the calibrator available at Politecnico di Torino).

Setting a known voltage and current to the circuit it is possible to compare the readings of Arduino with the input voltage and, with a set of 10 measures make the regression line that can approximate the linear behaviour of the sensor.

Said line is used to understand the starting error of the sensor and to correct it; the equation used id the following.

$$V_{corr} = m \cdot V_{raw} + q \tag{5.6}$$

Where:

- V_{corr} is the corrected voltage, the accurate measure,
- m is the coefficient of the regression line calculated,
- $V_{unranraw}$ is the raw measure, the uncalibrated reading from Arduino,
- q is the intercept of the regression line calculated.

The values of m and q are summed up in the following table

Scale	m	q
PV (120V)	0.9986094	0.1271476
Battery (120V)	1.0024851	0.1672536
PV(30V)	1.0113978	0.0281079
Battery (30V)	0.9988022	0.03653015
Current (10A)	0.9925873	0.0039021

Table 5.1: Coefficients used for the calibration

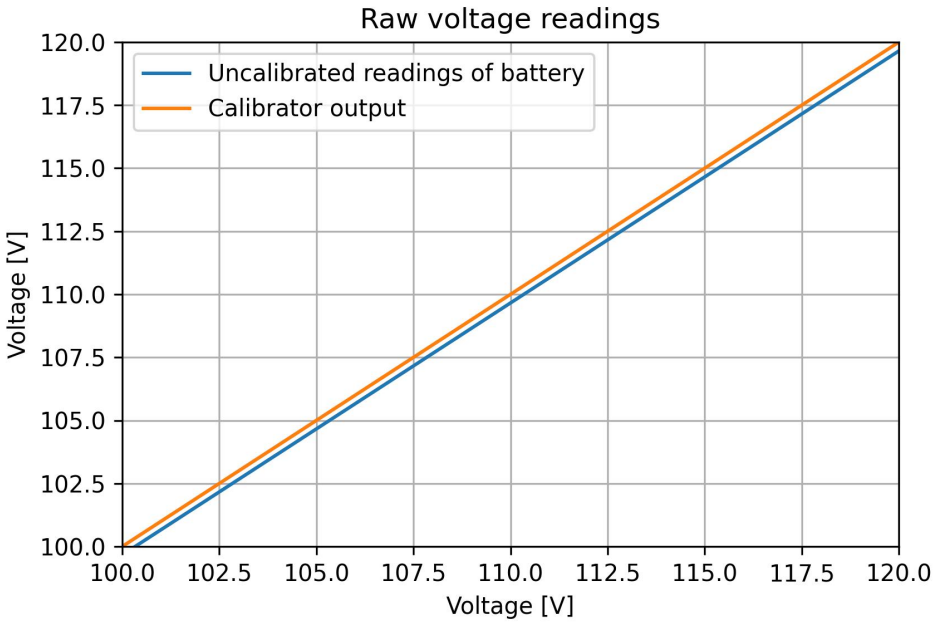

Figure 5.23: Readings of the battery respect to the calibrator

After the calibration the readings improved greatly with a mean deviation going from -4.377061e-02V to 1.339100e-14V.

Below the tables and graphs of the calibration.

Nominal Voltage	V PV	V Battery	deviation PV [V]	deviation Battery[V]
120	120.015557	119.650027	0.015557	-0.349973
110	110.024414	109.658884	0.024414	-0.341116
100	100.033271	99.667742	0.033271	-0.332258
90	90.042128	89.189226	0.042128	-0.810774
80	80.050986	79.685456	0.050986	-0.314544
70	69.938000	69.694313	-0.062000	-0.305687
60	59.946857	59.703170	-0.053143	-0.296830
50	49.955714	49.712028	-0.044286	-0.287972
40	39.842728	39.720885	-0.157272	-0.279115
30	29.851585	29.729742	-0.148415	-0.270258
20	19.860442	19.738599	-0.139558	-0.261401
10	9.869300	9.747456	-0.130700	-0.252544
0	0.000000	0.000000	0.000000	0.000000

Table 5.2: Uncalibrated values referred to the calibrator

Nominal Voltage	V PV	V Battery	deviation PV [V]	deviation Battery[V]
120	119.975807	120.114622	-0.024193	0.114622
110	109.998558	110.098650	-0.001442	0.098650
100	100.021310	100.082678	0.021310	0.082678
90	90.044061	89.578123	0.044061	-0.421877
80	80.066812	80.050735	0.066812	0.050735
70	69.967889	70.034763	-0.032111	0.034763
60	59.990640	60.018792	-0.009360	0.018792
50	50.013392	50.002820	0.013392	0.002820
40	39.914469	39.986848	-0.085531	-0.013152
30	29.937220	29.970877	-0.062780	-0.029123
20	19.959971	19.954905	-0.040029	-0.045095
10	9.982723	9.938933	-0.017277	-0.061067
0	0.127148	0.167254	0.127148	0.167254

Table 5.3: Calibrated values referred to the calibrator

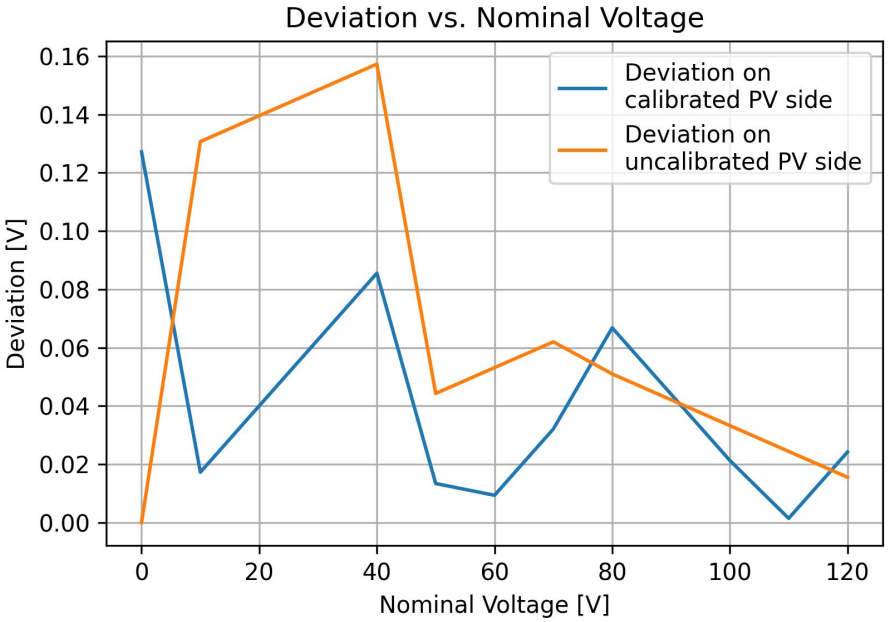

Figure 5.24: Deviation before and after calibration on the panel

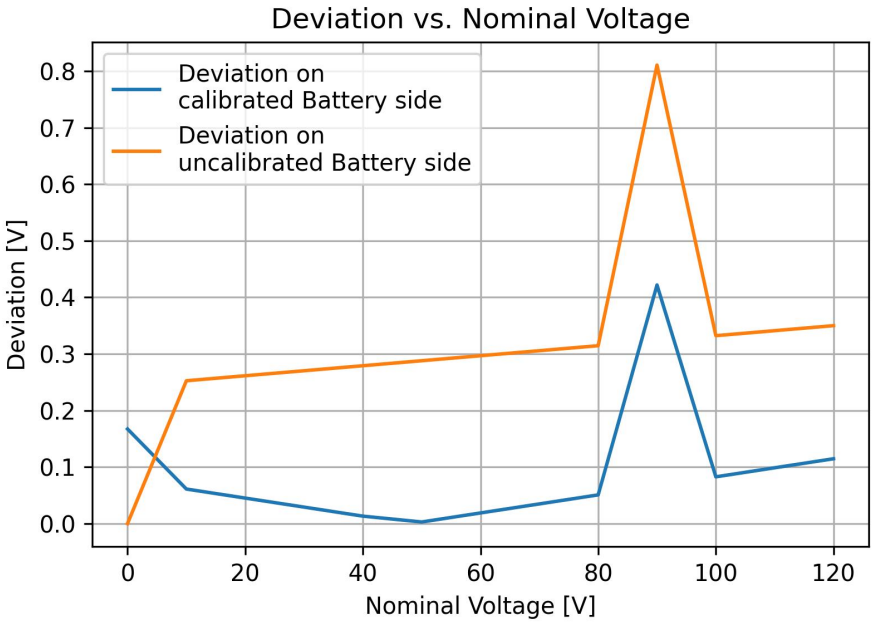

Figure 5.25: Deviation before and after calibration on the battery

Nominal Voltage	V PV	V Battery	deviation PV [V]	deviation Battery[V]
30	30.001446	29.989737	0.001446	-0.010263
27	27.010614	27.004047	0.010614	0.004047
24	23.987273	24.018358	-0.012727	0.018358
21	20.996441	21.000564	-0.003559	0.000564
18	18.005609	18.014875	0.005609	0.014875
15	15.014777	14.997081	0.014777	-0.002919
12	11.991436	11.979288	-0.008564	-0.020712
9	9.000604	8.993598	0.000604	-0.006402
6	5.977263	5.975805	-0.022737	-0.024195
3	2.986431	2.990115	-0.013569	-0.009885
0	0.028108	0.036530	0.028108	0.036530

Table 5.4: Calibrated values referred to the calibrator on 30V scale

Nominal Voltage	V PV	V Battery	deviation PV [V]	deviation Battery[V]
30	29.635556	29.989126	-0.364444	-0.010874
27	26.678429	26.999856	-0.321571	-0.000144
24	23.689160	24.010586	-0.310840	0.010586
21	20.732032	20.989174	-0.267968	-0.010826
18	17.774905	17.999904	-0.225095	-0.000096
15	14.817778	14.978492	-0.182222	-0.021508
12	11.828508	11.957079	-0.171492	-0.042921
9	8.871381	8.967809	-0.128619	-0.032191
6	5.882112	5.946397	-0.117888	-0.053603
3	2.924984	2.957127	-0.075016	-0.042873
0	0.000000	0.000000	0.000000	0.000000

Table 5.5: Uncalibrated values referred to the calibrator on 30V scale

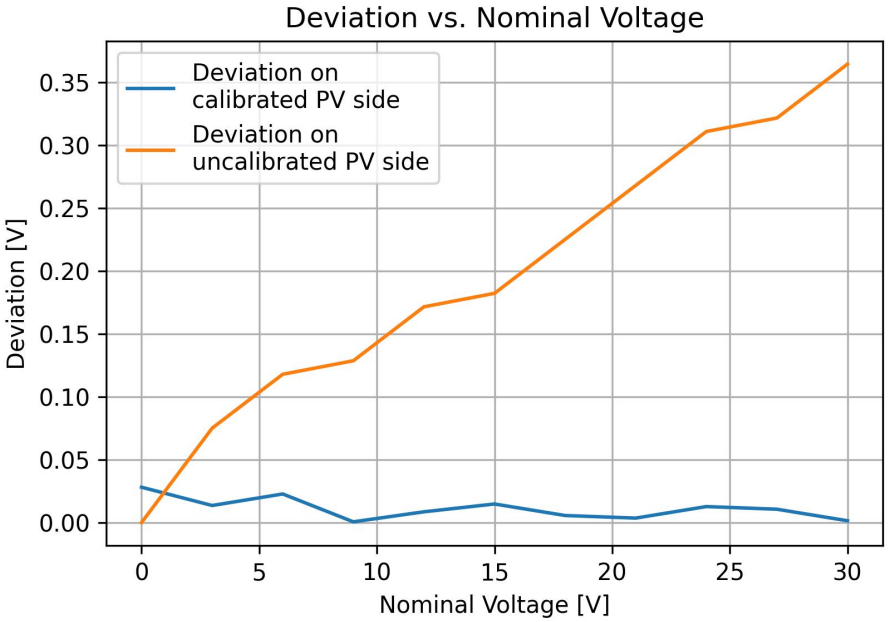

Figure 5.26: Deviation before and after calibration on the PV 30V range

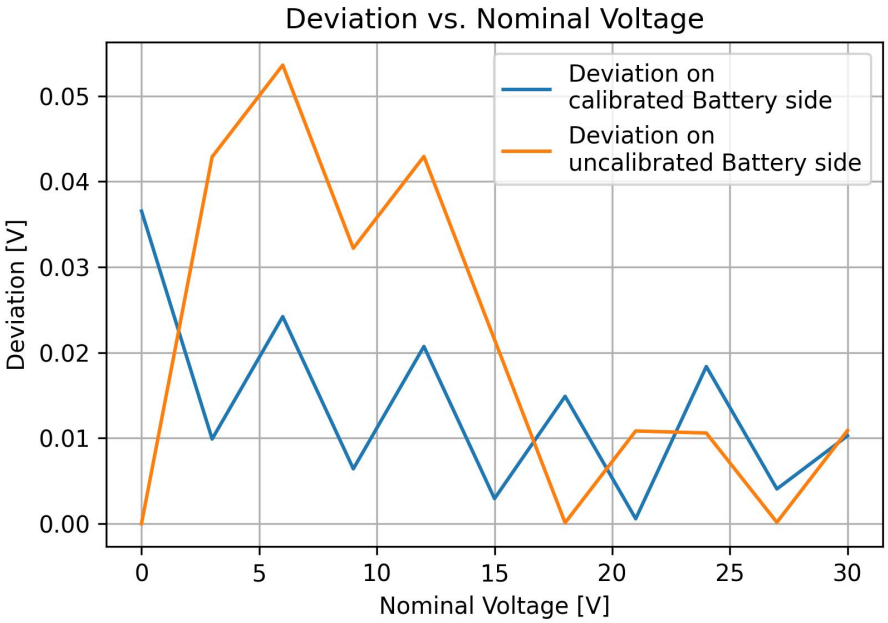

Figure 5.27: Deviation before and after calibration on the battery 30V range

Nom i [A]	i uncal [A]	ϵ uncal [A]	i cal [A]	ϵ current [A]	abs ϵ [A]
10	10.080000	0.080000	10.009182	0.009182	0.009182
9	9.066875	0.066875	9.003567	0.003567	0.003567
8	8.050000	0.050000	7.994230	-0.005770	0.005770
7	7.043125	0.043125	6.994818	-0.005182	0.005182
6	6.039375	0.039375	5.998509	-0.001491	0.001491
5	5.030000	0.030000	4.996616	-0.003384	0.003384
4	4.020625	0.020625	3.994723	-0.005277	0.005277
3	3.019375	0.019375	3.000895	0.000895	0.000895
2	2.010000	0.010000	1.999003	-0.000997	0.000997
1	1.008125	0.008125	1.004554	0.004554	0.004554
0	0.000000	0.000000	0.003902	0.003902	0.003902

Table 5.6: Data from the analysis on the calibrator

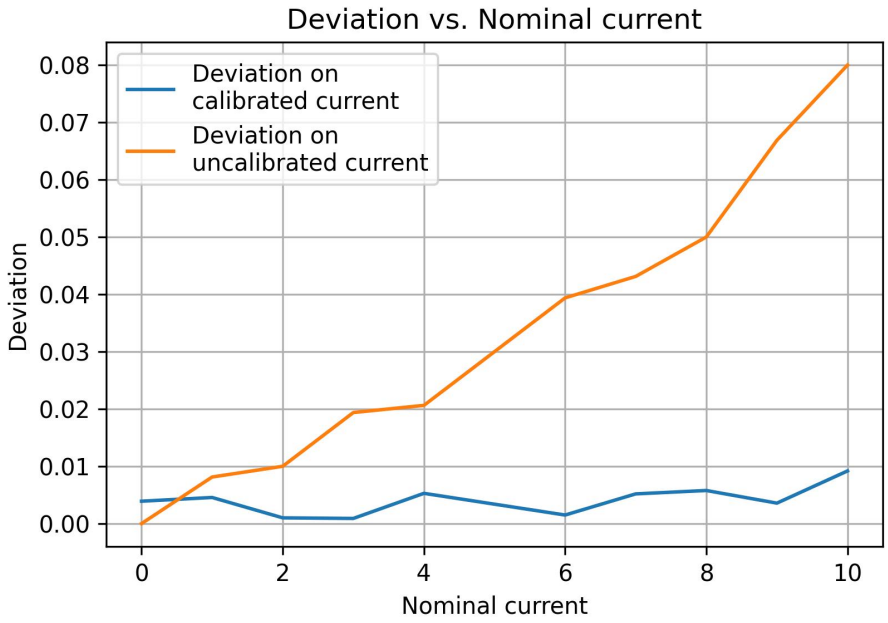

Figure 5.28: Deviation before and after calibration on the current

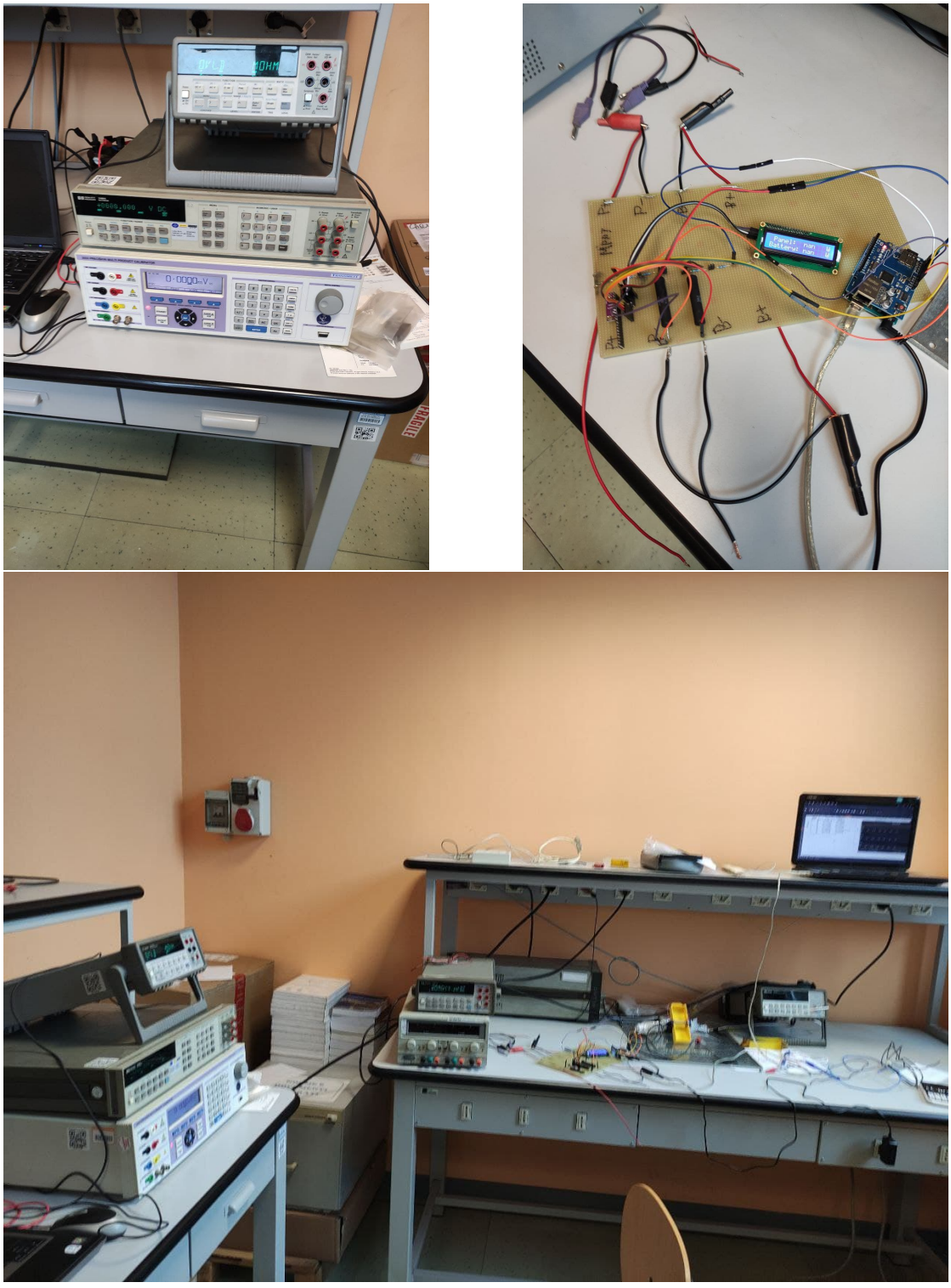

Figure 5.29: Circuit and calibrator at Politecnico di Torino

5.4 Data analysis

In order to collect and visualize the data needed for the project a system made of 2 Solbian SP144 panels connected in series have been used, connected to the DC converter under test and the Arduino power sensor with the SD logging card. The converter is connected to a series of 8 12 V lead car batteries and a load (a 800 W iron) to discharge them.

The system has been left to work for 8 hours in a sunny day, sampling every 2 seconds. After the data collection a script to visualize the data has been written in Python (see the comments in green for details).

```
#import the used libraries for the analysis
import pandas as pd
from matplotlib import pyplot as plt

#load the dataset from the file
log= pd.read_csv('LOG.TXT',delimiter='\t',header=None)

#remove the empty rows/columns
log=log.dropna(axis=1)
log=log.dropna(axis=0)

#label the columns
log.columns=['v_p','v_b','i_p','i_b','p_p','p_b','eta']
log['eta']=pd.to_numeric(log['eta'],errors='coerce')

df=log.reset_index()

#sort values by battery current to have a correct plot
df_sort=df.sort_values(by=['i_b'])

#choose the number of bins you want the plot to be divided into
bins=20

#group in bins by delivered current and average every bin then rename
gruppo=df.groupby(pd.cut(df['i_b'],bins))
medie=gruppo.mean()
medie.rename(columns={'i_b':'i_batt'},inplace=True)

#make the standard deviation of the groups and rename
dev=gruppo.std()
dev.rename(columns={'i_b':'i_batt'},inplace=True)
dev.tail()

#join the average and std dataframe in one and clean the empty values
tot=medie.join(dev,rsuffix='_std')
tot.dropna(axis='index', inplace=True)

#make the string that will appear in the plot
string=f'''{df['eta'].count()} samples
{bins} bins considered
```

```
{int(df['eta'].count()/bins)} samples each bin'''

#make the errorbar plot and configure the plot, save
plt.figure(figsize=(20, 10))
plt.plot(tot['i_batt'],tot['eta'])
plt.errorbar(x=tot['i_batt'],
y=tot['eta'],xerr=tot['i_batt_std'],
yerr=tot['eta_std'],fmt='r ',elinewidth=0.5)
plt.title('Efficiency vs delivered current',
fontdict = {'fontsize' : 25})
plt.ylabel('Efficiency [\%]',fontdict = {'fontsize' : 20})
plt.xlabel('Delivered current [W]',fontdict = {'fontsize' : 20})
plt.minorticks_on()
plt.figtext(0.2,0.2,s=string,fontdict={'fontsize':'xx-large'})
plt.grid(which='major',linewidth=1)
plt.grid(which='minor',linewidth=1, linestyle=':')
plt.savefig('chart.png',dpi=300)
plt.show()
```

The analyzed data produces the table 5.7.

v_p	v_b	i_p	i_b	p_p	p_b	eta	v_p_std	v_b_std	i_p_std	i_b_std	p_p_std	p_b_std	eta_std
38.700	84.661	0.413	0.141	15.823	11.867	74.982	3.332	6.077	0.061	0.015	1.348	1.093	2.075
39.235	81.294	0.520	0.187	20.214	15.217	75.243	2.517	3.644	0.083	0.016	1.820	1.498	1.714
40.879	83.511	0.636	0.243	25.733	20.221	78.481	3.097	7.044	0.101	0.013	2.043	2.041	2.495
38.948	87.321	0.864	0.317	33.222	27.651	83.329	2.797	9.435	0.168	0.018	3.867	2.951	2.266
40.473	87.738	0.998	0.374	39.427	32.722	83.326	3.876	9.691	0.262	0.018	5.959	4.027	2.448
39.667	88.341	1.207	0.440	47.236	38.914	82.457	3.131	9.369	0.240	0.017	5.624	4.335	1.189
39.478	83.877	1.263	0.496	49.797	41.605	83.556	0.986	4.047	0.089	0.017	2.996	2.468	0.858
39.484	84.208	1.406	0.555	55.476	46.695	84.179	1.048	3.409	0.086	0.018	2.973	2.478	0.852
39.094	84.980	1.593	0.616	62.210	52.338	84.166	1.031	3.349	0.105	0.017	3.506	2.575	1.115
38.466	86.297	1.812	0.682	69.624	58.794	84.460	1.043	2.666	0.104	0.017	3.093	2.424	0.854
37.929	87.768	2.028	0.741	76.867	65.049	84.639	0.971	2.311	0.093	0.018	3.037	2.368	0.865
37.739	88.479	2.254	0.806	85.015	71.297	83.890	0.877	2.020	0.100	0.017	3.203	2.213	1.068
37.982	89.284	2.440	0.865	92.652	77.166	83.299	0.999	2.609	0.086	0.017	3.692	2.880	0.892
38.148	90.620	2.657	0.926	101.320	83.881	82.832	0.788	2.540	0.136	0.016	4.711	3.005	1.235
38.233	93.134	2.953	0.987	112.865	91.896	81.501	0.854	4.159	0.202	0.017	7.599	4.898	1.544
38.439	95.027	3.223	1.048	123.824	99.544	80.459	0.828	3.644	0.183	0.018	6.849	4.101	1.554
38.879	98.914	3.544	1.102	137.828	109.020	79.222	0.912	5.404	0.273	0.017	11.719	7.207	1.849
39.895	107.524	4.061	1.169	162.002	125.649	77.679	0.833	6.134	0.295	0.016	12.173	7.138	1.876
40.414	110.205	4.400	1.230	177.811	135.524	76.372	0.781	4.991	0.329	0.017	13.499	7.033	2.233
40.813	112.437	4.675	1.276	190.711	143.475	75.280	0.594	1.857	0.196	0.014	6.541	2.682	1.565

Table 5.7: Analyzed values with mean and standard deviation

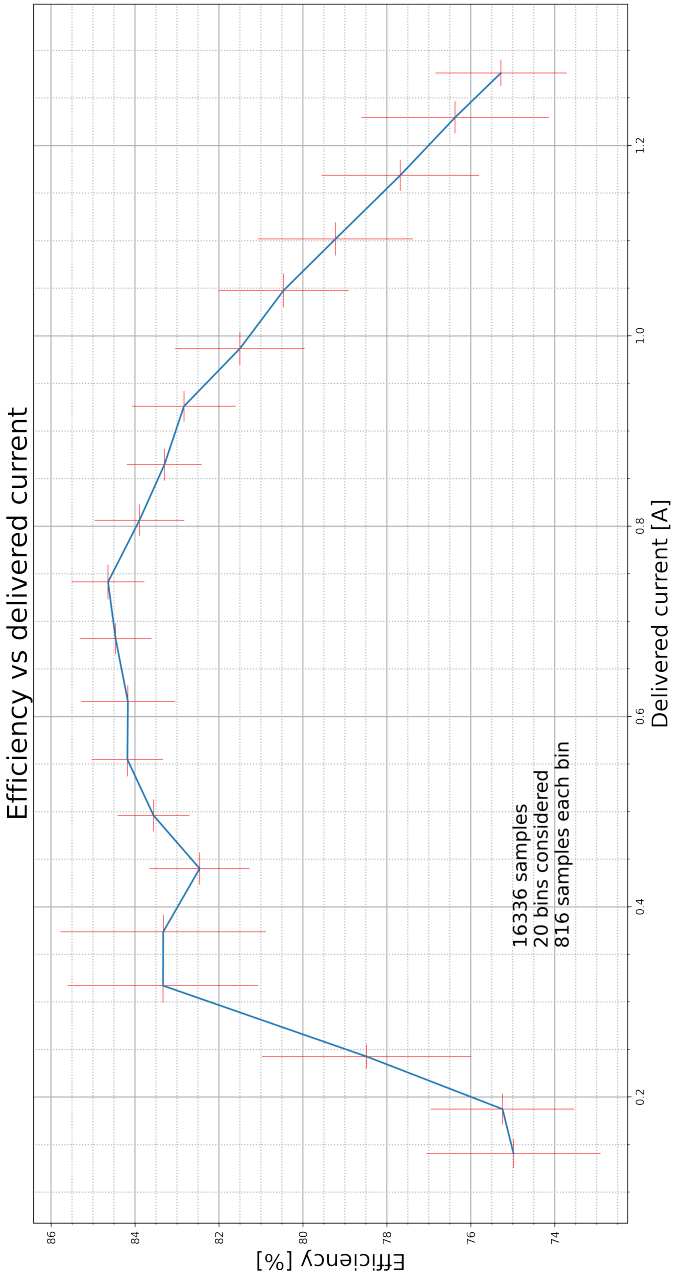

Figure 5.30: The analyzed data

The yielded data can be plotted in a efficiency-current graph 5.30.

As it can be seen the efficiency is lower with respect to a commercial grade DC converter, those can reach values above 95% [33].

Bibliography

[1] International Renewable Energy System Agency IRENA. *Energy transition*. URL: https://www.irena.org/energytransition (cit. on p. 2).

[2] Sammarco G. «La transazione energetica». In: () (cit. on pp. 3, 5).

[3] IEA. *Access to electricity*. URL: https://www.iea.org/reports/sdg7-data-and-projections/access-to-electricity (cit. on p. 4).

[4] IEA. *Access to clean cooking*. URL: https://www.iea.org/reports/sdg7-data-and-projections/access-to-clean-cooking#abstract (cit. on p. 4).

[5] European commission. *'Quadro 2030 per il clima e l'energia*. URL: https://ec.europa.eu/clima/policies/strategies/2030_it#:~:text=Il%5C%20quadro%5C%202030%5C%20per%5C%20il%5C%20clima%5C%20e%5C%20l%5C%27energia,a%5C%20effetto%5C%20serra%5C%20%5C%28rispetto%5C%20ai%5C%20livelli%5C%20del%5C%201990%5C%29 (cit. on p. 5).

[6] IEA. *Italy*. URL: https://www.iea.org/countries/italy (cit. on p. 5).

[7] Elemens. *Gli obiettivi di efficienza energetica ai nastri di partenza*. Sept. 2020. URL: https://www.efficienzaenergetica.edison.it/primo-piano/obiettivi-efficienza-energetica-2030/ (cit. on p. 6).

[8] Wikipedia contributors. *Solar energy — Wikipedia, The Free Encyclopedia*. [Online; accessed 15-September-2021]. 2021. URL: %5Curl%7Bhttps://en.wikipedia.org/w/index.php?title=Solar_energy%5C&oldid=1040691406%7D (cit. on p. 7).

[9] Wikipedia contributors. *Photovoltaic power station — Wikipedia, The Free Encyclopedia*. [Online; accessed 16-September-2021]. 2021. URL: %5Curl%7Bhttps://en.wikipedia.org/w/index.php?title=Photovoltaic_power_station%5C&oldid=1043580303%7D (cit. on p. 7).

[10] Antonio Luque and Steven Hegedus. *Handbook of Photovoltaic Science and Engineering*. eng. New York: John Wiley & Sons, Incorporated, 2011. ISBN: 9780470721698 (cit. on pp. 7, 8, 14, 23, 46).

[11] G.N Tiwari. *Solar Energy*. eng. Nova, 2005. ISBN: 1-59454-614-2 (cit. on p. 8).

[12] John A Duffie. *Solar Engineering of Thermal Processes*. eng. Hoboken: John Wiley & Sons, Incorporated, 2013. ISBN: 0-470-87366-3 (cit. on pp. 11, 13).

[13] Fabio Scaglia. *Studio di fattibilità di un sistema con fotovoltaico, eolico e accumulo, integrato da gruppo elettrogeno, per stazione radio ; rel. Filippo Spertino*. ita. Torino, 2017 (cit. on pp. 13, 23, 46, 59, 62, 69).

[14] Agostino Dematteis. *L'integrazione dei sistemi fotovoltaici negli edifici pubblici : caso studio con flussi energetici e convenienza economica / Agostino Dematteis ; rel. Filippo Spertino, Paolo Di Leo*. ita. Torino, 2016 (cit. on pp. 13, 23, 46, 59, 69).

[15] Alessandro Ciocia. *Sistema fotovoltaico ad alte prestazioni integrato in barriere acustiche / Alessandro Ciocia ; rel. Filippo Spertino, Vittorio Verda*. ita. Torino, 2012 (cit. on pp. 14, 59).

[16] Weidong(Xiao. *Photovoltaic Power System: Modelling, Design and Control*. eng. John Wiley & Sons, Incorporated, 2017. ISBN: 1-119-28034-6 (cit. on pp. 36, 38, 52, 53).

[17] John Wohlgemuth. *IEC 61215: What it is and isn't*. 2012. URL: %5Curl%7Bhttps://www.nrel.gov/docs/fy12osti/54714.pdf%7D (cit. on p. 41).

[18] S.B Kjaer, J.K Pedersen, and F Blaabjerg. «A review of single-phase grid-connected inverters for photovoltaic modules». eng. In: *IEEE transactions on industry applications* 41.5 (2005), pp. 1292–1306. ISSN: 0093-9994 (cit. on p. 52).

[19] Kumaran Saenthan Nathan. *A Novel DC-DC Converter for Photovoltaic Applications*. eng. 2019 (cit. on p. 59).

[20] Marie-Cécile Péra, Daniel Hissel, Hamid Gualous, and Christophe Turpin. «Electrochemical Accumulators». eng. In: *Electrochemical Components*. Hoboken, NJ USA: John Wiley& Sons, Inc, 2013, pp. 253–276. ISBN: 9781848214019 (cit. on pp. 62–64, 68, 69, 72).

[21] Pistoia. *Lithium-Ion Batteries : Advances and Applications*. eng. Elsevier, 2014. ISBN: 0-444-59513-9 (cit. on pp. 63, 72).

[22] Yasser E Abu Eldahab, Naggar H Saad, and Abdalhalim Zekry. «Enhancing the design of battery charging controllers for photovoltaic systems». eng. In: *Renewable & sustainable energy reviews* 58 (2016), pp. 646–655. ISSN: 1364-0321 (cit. on p. 75).

[23] b_e_n. *What is an Arduino?* URL: %5Curl%7Bhttps://learn.sparkfun.com/tutorials/what-is-an-arduino/all%7D (cit. on p. 88).

[24] Gergely Makan, Robert Mingesz, and Zoltan Gingl. «Reliable readings from Arduino voltmeters». eng. In: *Physics education* 56.4 (2021). ISSN: 0031-9120 (cit. on p. 90).

[25] Farnell. *Arduino Uno*. URL: %5Curl%7Bhttps://www.farnell.com/datasheets/1682209.pdf%7D (cit. on p. 90).

[26] Wikipedia contributors. *Voltage divider — Wikipedia, The Free Encyclopedia*. [Online; accessed 1-November-2021]. 2021. URL: %5Curl%7Bhttps://en.wikipedia.org/w/index.php?title=Voltage_divider%5C&oldid=1047836365%7D (cit. on p. 91).

[27] HyperPhysics. *Hall Effect*. URL: %5Curl%7Bhttp://hyperphysics.phy-astr.gsu.edu/hbase/magnetic/Hall.html%7D (cit. on p. 91).

[28] Thariq Ramadhan Muhamad Falih Akbar Ivy Averina. *ACS712 Current Sensor*. 2019. URL: %5Curl%7Bhttps://create.arduino.cc/projecthub/instrumentation-system/acs712-current-sensor-87b4a6%7D (cit. on p. 92).

[29] *The Differential Amplifier*. URL: %5Curl%7Bhttps://www.electronics-tutorials.ws/opamp/opamp_5.html%7D (cit. on p. 97).

[30] Wikipedia contributors. *Multiplexer — Wikipedia, The Free Encyclopedia*. https://en.wikipedia.org/w/index.php?title=Multiplexer&oldid=1045426376. [Online; accessed 1-November-2021]. 2021 (cit. on p. 98).

[31] Wikipedia contributors. *Programmable-gain amplifier — Wikipedia, The Free Encyclopedia*. https://en.wikipedia.org/w/index.php?title=Programmable-gain_amplifier&oldid=992391033. [Online; accessed 1-November-2021]. 2020 (cit. on p. 98).

[32] Texas Instruments. *ADS111x Ultra-Small, Low-Power, I^2C-Compatible, 860-SPS, 16-Bit ADCs With Internal Reference, Oscillator, and Programmable Comparator*. 2018. URL: %5Curl%7Bhttps://www.ti.com/lit/ds/symlink/ads1115.pdf?ts=1635711984205%5C&ref_url=https%5C%253A%5C%252F%5C%252Fwww.ti.com%5C%252Fproduct%5C%252FADS1115%7D (cit. on p. 99).

[33] Texas Instruments. *Genasun product page*. URL: %5Curl%7Bhttps://sunforgellc.com/genasun/#gen_product_row%7D (cit. on p. 115).